Cation substitution in two coccolithophore species

Can coccolithophores be used in material synthesis?

Hanna Elina Melteig

**Master thesis at the Department of Physics/Department of Chemistry,
Faculty of Mathematics and Natural Sciences**

The University of Oslo

60 study points

01.02.2016

Cation substitution in two coccolithophore species

Can coccolithophores be used in material synthesis?

Hanna Elina Melteig

2016

Cation substitution in two coccolithophore species

Hanna Elina Melteig

http://www.duo.uio.no/

Print: University Print Center, University of Oslo

Abstract

Few things would be better than getting rid of CO_2 while producing useful materials. Coccolithophores use CO_2 in their photorespiration, in addition to using CO_2 to produce coccoliths – small platelets made of calcite. Ca is a central cation in this process, and the goal of this project is to investigate to what extent other divalent cations can partially substitute for Ca and become part of the growing coccolith. The long term goal is to enable algae to harvest cations and produce materials for us, such as cathode materials for batteries.

The experiments was performed by controlling the seawater composition with respect to cations like Ca^{2+}, Mg^{2+}, Fe^{2+} and Mn^{2+} for growth of two coccolithophore algae. The resulting biomineralized materials, the coccoliths, were analyzed by SEM and XRD.

It appears that coccolithophores are capable of substituting Ca with Mg, up to a certain, low, level, but we have not found significant signs of inclusion of Mn or Fe. Uptake of Mg has been reported in other calcifying species. Nevertheless, the results from this thesis will need further studies to conclude.

Abbreviations

AAS	Atomic Absorption Spectroscopy
BCM	Biologically Controlled Mineralization
BIM	Biologically Induced Mineralization
EDS	Energy Dispersive Spectroscopy
EH	*Emiliania huxleyi*
EM	Electromagnetic
ESAW	Enriched Seawater Artificial Water
ESNW	Enriched Seawater Natural Water
ETD	Everhart-Thornley Detector
ICP-MS	Inductively Coupled Plasma-Mass Spectrometry
NC	No coccoliths
PC	*Pleurochrysis carterae*
PDF	Powder Diffraction File
PS	Polysaccharide (1 and 2)
SEM	Scanning Electron Microscope
SSD	Solid State Detector
XRD	X-ray Diffraction

Terms and definitions

Aragonite	$CaCO_3$, one of three possible polymorphs for this composition. The space group for aragonite is *Pnma* (62)[1]. The other two polymorphs are calcite and vaterite.
Biomimetics	Imitating structures and systems from nature to enhance modern technology.
Bionanotechnology	Technology that is enabled by biomimetics on a nanoscale or by using biological building blocks. Some also include technology depending on nanotechnology that is used to better understand biotechnology and to improve the methods.
Calcite	Calcium carbonate, $CaCO_3$, one of three possible polymorphs with this composition. This is the most stable of the three, and also the one that is found in coccoliths. The space group for calcite is: *R*-3*c* h (167)[1]. The other polymorphs are vaterite and aragonite.
Coccolith	Calcified scale with species specific fine structure produced by coccolithophores, consisting of calcium carbonate crystals and organic matrices[2, 3].
Coccolithophores	A group of Haptophyte algae in which most species produce calcified scales known as coccoliths[4].
Coccolithosomes	Granular bodies 25 nm in diameter that participate in the calcification process[5].
Coccosphere	Layer of coccoliths forming the outermost covering of the cell[6].
Diploid	A cell that contains a pair of chromosomes is called a diploid cell. This is written as 2N, where N is the number of chromosome pairs.

Dolomite	Carbonate mineral composed of Ca, Mg and carbonate. The space group for dolomite is *R*-3 h (148)[1].
Exocytosis	Transport of material out of a cell by the use of a vesicle.
Frustule	Shells, cell wall, or outer covering in diatoms. Frustules are made of silicon dioxide.
Halite	NaCl, commonly known as rock salt.
Haploid	A cell that contains one of each chromosome (no pairs). These cells are often used for sexual reproduction.
Haptonema	A flagellum-like structure found in Haptophyte algae. It is used for attachment, and for feeding[7].
Heterococcolith	A coccolith consisting of complex crystal units put together[8]. The coccolith is formed inside the cell, before it is secreted to the surface[4]. Heterococcoliths are known to occur in the diploid life stage of coccolithophores[9].
Hermann-Maugin notation	This is a notation for crystals (repeating patterns) that combine space groups, plane groups, and point groups.
Holococcolith	A coccolith usually consisting of small, morphologically simple crystallites[8]. The holococcoliths are formed outside of the cell[4]. Holococcoliths occur in the haploid life stage of some coccolithophores[9].
Magnesite	$MgCO_3$, carbonate mineral composed of Mg and carbonate. The space group for magnesite is *R*-3*c* h[1].
Nannolith	Calcareous structures produced by haptophytes that cannot be categorized as holococcoliths or heterococcoliths[8]. Nannoliths occur in the haploid life stage of some coccolithophores[9].

PDF	Powder Diffraction File, a file that can be found in one of the worlds biggest databases for powder diffraction: The International Centre for Diffraction Data.
Proto-coccolith	Circle of crystals with a specific orientation that grows and become the coccolith.
PS	Polysaccharide (1 and 2), often found in *P. carterae*, and proven to participate in calcification processes inside the cell.
R-unit	Radially oriented crystal in a heterococcolith[10].
Siderite	$FeCO_3$, carbonate mineral with the space group R-3c, the same as for calcite[11].
Unit cell	Smallest non-repetitive unit that contains all the information to draw the whole crystal structure.
Vaterite	$CaCO_3$, one of three possible polymorphs with this composition. The space group for vaterite is $P6_3/mmc$ (194)[1]. The other two are calcite and aragonite.
V-unit	Vertically oriented crystal in a heterococcolith[10].

Preface

This study of possible usage of coccolithophores in material synthesis has been conducted at the University of Oslo as a collaboration between the Department of Chemistry and the Department of Biosciences under the MENA study program. The main supervisor for this project was Ola Nilsen at the Department of Chemistry and Wenche Eikrem was co-supervisor at the Department of Biosciences.

The subject of this thesis is to investigate if cations can substitute Ca in coccoliths. These results can give us a better understanding of biomineralization. The results may also indicate whether we can use calcifying species to harvest elements or to produce materials of interest, as starting materials for synthesis of other functional materials based on the elements they have harvested during their growth. The structures in the coccoliths may be interesting because of their optical properties, or as drug delivery agents because they are small enough to fit into the bloodstream in addition to being non-toxic.

In parallel with the current project I have worked extensively with the iGEM-project (international genetically engineered machine) and with science communication for the faculty. The current project was started at August 2014 and ended with submission February 2016.

I want to thank my supervisors, who made this possible, both because they made a project within the field that I wanted to work in, but also because they have been very understanding when I used some of my time for science communication as well as writing on my thesis.

In the end, I just want to thank all my friends and family who have been a patient audience when I talked about algae and master-related problems. I want to thank Mari, Anne, Julie, Ingunn, Rune, Olav and Lars-Olav who showed up on campus, and last, but not least, I want to thank Vilde, who took a particular interest in reminding me to work hard. I specially want to thank Kristian Lausund, Haakon Liavaag, Jan Erik Thrane and Anders Wold who helped me with equipment and cultures of algae. I also want to thank Ina and Ketil at the office, because they have made sure that taking a master's degree and hanging out in the office was a fun thing to do. I will miss them!

Hanna Elina Melteig, University of Oslo, January 2016

Table of contents

1 Introduction

How do you imagine paradise? Many people picture the Garden of Eden as a beautiful green park where everybody plays around with their loved ones. They all have time. No one is hungry. Nobody works. Is this just a dream, or can it be achieved by advances in technology?

Recent development in the field of bionanotechnology suggests that we may achieve the dream of not having to work. We can use microorganisms to do the work for us. Experiments with viruses show that they can be used to produce batteries[12], and even move and control quantum dots, that are needed for quantum computers[13]. The advantages of using microorganisms are many: They are precise, the can repeat the same procedure over and over, they are small, they are fairly easy to keep, and they are fast.

In this regard, nature is literally a gold mine. There are vast amounts of different organisms, with different assets that we can use to our advantage. In 2006 Gorby et al. showed that *Shewanella oneidensis*, a bacteria species, can be used to produce electrically conductive nanowires[14]. Entirely biological motors have been made out of DNA[15]. For industries that require slightly larger "motors", algae have been turned into small transporters[16]. A large subgroup of algae, diatoms, makes shells, or so called frustules, out of silica. Because of their particular shape and physical properties they have been suggested as gas sensors and possible coatings, among other things[17]. TiO_2 uptake in diatoms has been of particular interest, since this might turn the frustules into possible parts in solar panels[18]. The latter study was the primary source of inspiration in this project.

If one group of algae can use different elements in their shells, then maybe this is true for other organisms. This project seeks to explore whether coccolithophores, a kind of algae which produces coccoliths, i.e. cell coverings, from calcium carbonate ($CaCO_3$) , can use different elements in the place of calcium (Ca). If this is the case, coccolithophores can be used to harvest cations or to make structures that are interesting for material synthesis. This project will then bring us one step closer to hiring microorganisms as part of our workforce. Another aspect of this project is gaining insight into the biomineralization process. This process is by far not fully understood today, and this project may be a small step in gaining deeper insight.

1.1 Project definition

The aim of this thesis is to investigate if coccolithophores can be used in material synthesis or possibly as means of harvesting cations, such as brown algae have been shown to do[19]. Specifically, this project will investigate if divalent cations can take the place of Ca in the $CaCO_3$ materials forming the coccolith structure.

The biomineralization process can vary for different species. This is why two rather different species of coccolithophores were chosen: *Emiliania huxleyi* (*E. huxleyi)* and *Pleurochrysis carterae* (*P. carterae*). These two species have previously been used as model organisms in biological research and are thus well known. In addition, it is shown that the calcification process in these two algae are slightly different[20], which will be explained in more detail in section 1.2.3.

The chosen divalent cations to replace Ca cations were iron (Fe), magnesium (Mg) and manganese (Mn). These were chosen because they are all parts of a normal seawater composition[21], and because they can exist as divalent cations. Mg and Mn are also previously known to replace Ca in $CaCO_3$-types of structures [22] [23]. Siderite is a carbonate containing Fe that also has the same space group (*R*-3*c* h) as calcite[11].

None of these metals are known as toxic to algae at normal concentrations and Mg is often found as a $MgCO_3$ in coralline algae[24]. Mg is also a part of the chlorophyll complex that is important for photosynthesis[4]. Other metals that might have been chosen for this kind of experiment are cadmium (Cd), which is known to take the Ca place in for instance bone structure[25], strontium (Sr)[26], molybdenum (Mo), zinc (Zn), copper (Cu), or cobalt (Co)[21]. All of these elements also exist in natural seawater, and many of them are elements that algae need in small amounts. In order to limit the workload to a manageable amount, only Fe, Mg, and Mn were chosen. If the experiments give positive results with these elements, then this may be a way to use algae to produce more complex materials or partake in making materials by producing a carbonate which in turn can be used in synthesis of the wanted material, such as $CaMnO_3$.

In this project the two coccolithophore species were cultured under constant temperature and dark-light cycles. The seawater was artificially made to reduce the amount of variables and contain controlled amounts of Ca and the added cations. They were cultured until the

population density was stabilized. Then the structure and elemental composition of the coccoliths were analyzed with a Scanning Electron Microscope (SEM) and with X-ray Diffraction (XRD).

1.2 Previous works

This project is inspired by promising similar research on diatoms. It has been shown that diatoms can replace Si^{4+} with Ti^{4+} in their frustules made of SiO_2[18]. There are already several examples of different elements that can replace Ca in living species[25]. In addition, the calcite structure is known to be rather flexible with ionic substitution of Ca with other divalent cations[27]. It has previously been shown that calcifying species can produce $CaCO_3$ with a range of different Mg-compositions[28].

In fact, the mentioned studies are based on prior work on biomineralization and how different organisms use minerals. A general definition of biomineralization, in contrast to mineralization, is that the mineralization process is initiated and sometimes controlled by organisms. Biomineralization often occurs at low temperatures, often fast and controlled, with a very specific result.

Prior studies on this subject were not only done to better understand nature, but also because this field can have large commercial interests. Understanding of biomineralization in general can be used to construct bone tissue [29, 30], make advanced strong and lightweight materials[31], to use plants as mineral miners or extracting heavy metals[32].

The mentioned studies have been conducted on various organisms to understand the mineralization process, and it turns out that there are different strategies for controlling this process. This is great news for everyone who wishes to use this technique industrially, because it means that there are plenty of methods to choose from. It is not great news for those seeking simple understanding of how it works, because the process is not necessarily the same for another species. There are even differences between the two relatively similar species in this study, as you will see in section 1.2.3, where *E. huxleyi* and *P. carterae* are compared.

1.2.1 Biomineralization

Biomineralization processes consist of several fields of science and hold many unanswered questions. What elements can, or cannot, be included in such processes? What are the mechanisms for controlled mineralization? Are there any limits to what structures microorganisms can build? What we know so far is not much and we are far from seeing the complete picture; however, we do know something.

Many organisms require inorganic elements, not only organic molecules, to grow. Some of these have an important impact on the organism, like iron in our blood, calcium in corals and in our bone tissue, or magnesium in photosynthetic organisms. However, some organisms are more creative. One type of bacteria creates magnetic particles of iron oxides, presumingly using them to navigate[33].

Some minerals that are known to occur in different organisms are calcium, magnesium, lead, iron, barium, strontium, potassium, zinc, nickel, silver, arsenic, silicon, copper, sulfur, titanium, manganese, and sodium[34]. Even if this list is quite extensive, it is not complete. We can also add tungsten[35, 36], fluorine[37], vanadium[38], molybdenum[36], tantalum[39], niobium[40], and cobalt[41] to the list. These metals are used by organisms and have a biological function. The list is even longer if we add elements that have a biological function only when a different, but preferred, ion is limited. For instance, cadmium turns out to have a biological function for marine diatoms under zinc deficiency[42]. However, when a replacement occurs, it may not be beneficial, for instance when cadmium replaces calcium in bone tissue[25].

Recently, it was discovered that some bacteria are capable of reducing metals, by eating the electrons. Some bacteria can even reduce uranium and have a high tolerance for radioactivity[43, 44]. The discovery of extremophiles, as such organisms are called, makes it possible to imagine that most, or even all, elements may have a biological function somehow[44]. Thus, we might have to accept that the number of elements that have biological functions and have potentials within biomineralization is quite extensive, and is in fact unknown.

For unicellular organisms there seems to be some general steps in the mineralization processes. In an overview about biomineralization from 2003, the mineralization process is described as three types, in which two of them are biologically controlled mineralization

(BCM), and the third is biologically induced mineralization (BIM)[34]. Of the two kinds of BCM, one type involves crystal formation within the cell (often within the Golgi apparatus) where the crystals are highly organized. In the other type of BCM the crystal formation appears to be carried out within the cell wall or cell mucilage[45]. The general principles of biomineralization seem to be the same for a broad range of organisms.

BIM is usually a process that takes place outside the cell, and where the organisms release substances to initiate the mineralization. BIM can both be an active process or a process that simply influences the precipitation. Several bacteria make a biofilm that can act as a substrate for precipitation[46]. We will focus on BCM since this is the mode where the organism controls the process all the way, and because the heterococcoliths in this project are a result of a BCM-process. BCM is illustrated in Figure 1, where a bacterium is used as an example[33].

The general BCM process simplified in 6 steps (see Figure 1):

1. A specific site on, or in, the cell is sealed off.
2. Ions, in this case the Ca cations, are either actively transported into the cell, or passively.
3. Molecules inside the cell bind the ions.
4. These molecules, or specific transport molecules, move the ions to the compartment.
5. When a state of supersaturation is reached, the controlled nucleation occurs in the compartment, due to stereochemical and electrochemical properties of the ions and ligands. Often biological molecules are involved in this process.
6. The crystals grow in an ordered manner, creating crystals that often have a specific orientation, morphology and size.

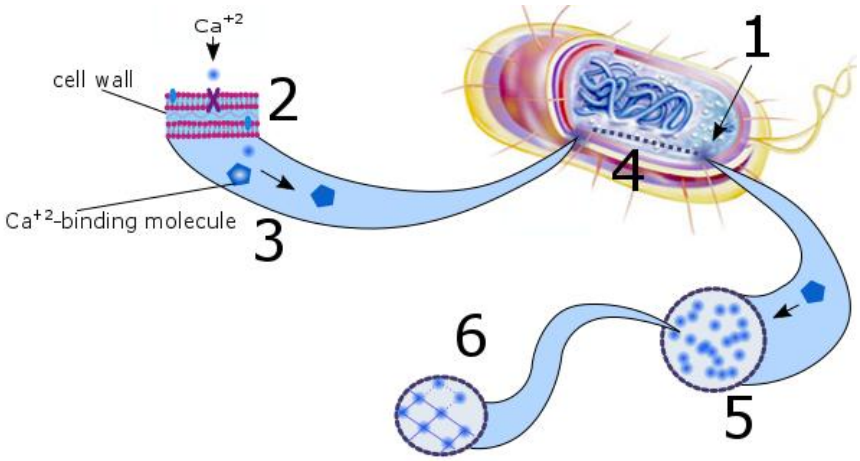

Figure 1: Schematics of the general principles in biologically controlled mineralization (BCM) with a bacterium as example. 1: A specific site in the cell is sealed off. 2: cations are transported into the cell. 3-4: There are usually specific molecules that transport the ions to the sealed compartment. 5: The sealed compartment usually contains a supersaturated solution. 6: Nucleation occurs in a controlled manner. Exactly how the process is controlled is not known, at may vary between organisms. The bacterial cell is modified from McGraw-Hill Global Education Holdings [47].

1.2.2 Cation substitution in marine species

Several calcifying marine species seem to be able to use different cations in their calcite structures. In corals, it has been known for a long time that Mg can substitute Ca in the calcite structure. An extensive study from 1954 suggests that the degree of substitution vary with season and temperature[48]. In 1968 Moberly et al. found that the coralline algae *Porolithon* and *Goniolithon* contained 16 – 30 mol % $MgCO_3$[49]. However, it was later shown by Milliman et al. that coralline algae may contain more Mg than what is possible to see by X-ray diffraction (XRD)[50].

Mg to Ca substitution is actually used as a tool for geologists to find out more about the conditions in prehistoric seas, particularly in relation to temperature[51]. The substitution is affected in particular by the growth, which again is influenced by temperature, light-conditions, and physiological cycles[49]. This is not only the case for coralline algae. Cation substitution seems to be a widespread phenomenon in calcifying marine species, such as mollusks[52], mussels[53], and snails[54], to mention some examples. This capacity has a wide array of applications, from commercial exploitation of new colors in pearls[55], and to scientific investigation of toxicity and pollution[19, 53, 56].

Some studies have been done on cation substitution of coccolithophores. An article from Herfort et al. 2004 shows that both Ca and Mg have an effect on coccolith formation[57]. Too much or too little of either element causes malformations in the coccoliths. Mg levels as high

as 116 mM gave few and malformed coccoliths. When the Mg concentrations were down to 15 and 0 mM, the coccoliths were equally malformed. The malformations were described as incomplete coccoliths.

One of the issues when studying cation substitution in coccolithophores compared to corals, or calcifying animals, is that the coccoliths are hard to clean, and thus it is difficult to analyze the samples. Stoll shows that with Inductively Coupled Plasma-Mass Spectrometry (ICP-MS), and proper cleaning methods, *E. huxleyi* with a normal seawater composition, has low magnesian calcite in the coccoliths, meaning a Mg/Ca-ratio of 0.1 – 0.2 mmol/mol[58]. The same paper found an increase in Mg/Ca-ratio of 6% per 1 ºC increase of temperature. Stoll shows in an article a year later, that temperature and growth rate seem to influence the Sr/Ca-relationship in several coccolithophores[59]. According to the article, Sr/Ca-relationship increases by 1-2% per 1 ºC increase of temperature, but the variation can reach up to 30%, depending on light and temperature conditions.

Mg, in particular, is also known to play a role in the coccolith forming process. Mg is thought to stabilize the unstable amorphous calcium carbonate phase that is believed to occur right before crystallization[60].

1.2.3 Biomineralization in *E. huxleyi* and *P. carterae*

As previously mentioned, *E. huxleyi* and *P. carterae* are model organisms. Nevertheless, we still do not understand their calcification process in detail.

Both *E. huxleyi* and *P. carterae* belong to a group, or phylum, of algae that are known as haptophytes. Note that the names of families and groups may be subject to changes. There is also some dispute about what the haptophyte phylogenetic tree should look like. In Figure 2 there is an overview from 2003 that shows the relationship between *E. huxleyi* and *P. carterae*, among other coccolithophores. Note that this is a simplified overview that focuses on the production of calcified scales, coccoliths, and what type of scale that is produced in different life phases. Both *P. carterae* and *E. huxleyi* produce coccoliths in the diploid phase and organic scales in the haploid phase. They both produce heterococcoliths, which means that the coccoliths are produced within the cell, and then exocytosed. Some coccolithophore species produce holococcoliths or nannoliths, and the process may take place at different locations, perhaps both inside and outside the cell[61].

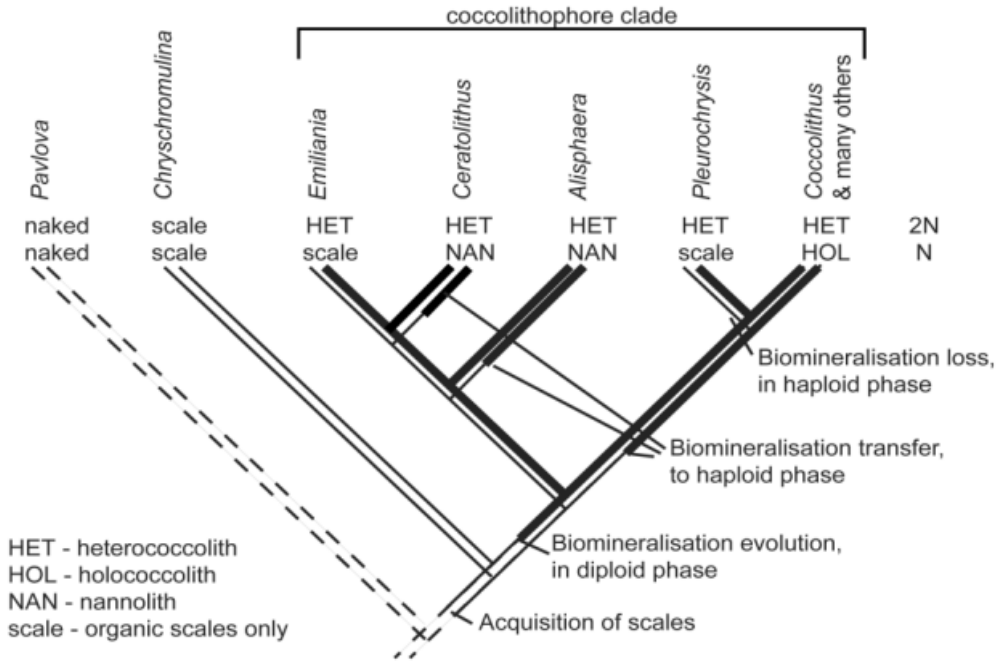

Figure 2: The relationship between the development and life cycle of *Emiliania huxleyi* and *Pleurochrysis carterae*. Contrary to most coccolithophores, *Emiliania huxleyi* does not produce coccoliths in the haploid life stage. *Pleurochrysis carterae* is assumed to have had the ability to produce coccoliths in the haploid phase, but then lost it at a later evolutionary stage. The figure is made by Young, 2003[9].

The characteristic morphological feature of the haptophytes is the haptonema, a structure that looks like a flagella, but has other properties such as coiling and bending. The haptonema is present in many coccolithophores. Coccolithophores have at least one life stage with cells covered by coccoliths. *E. huxleyi* is also known to have a non-calcifying diploid life stage. All of the coccolith-types are based on the calcite crystal structure, but some other algae groups like *Charophyta* and *Phaeophyta* adopt the aragonite structure[45].

Biomineralization in *E. huxleyi*

There are variations in the calcification process for different species, but for *E. huxleyi* there might also be differences between the varieties of *E. huxleyi* [62]. There are also variations in the Ca:C ratio in the coccoliths. There may be a higher carbon content in some coccoliths because of a higher degree of organic molecules covering the coccolith, or trapped between the interlocking crystals. One coccolith estimated to weigh 1.8 pg on average, with C 0.28, O 0.87 and Ca 0.67 pg, or with a distribution of 1.4:3.2:1 in molar ratio[63].

Figure 3 is a schematic drawing of the *E. huxleyi* cell, to show where in the cell the calcification takes place.

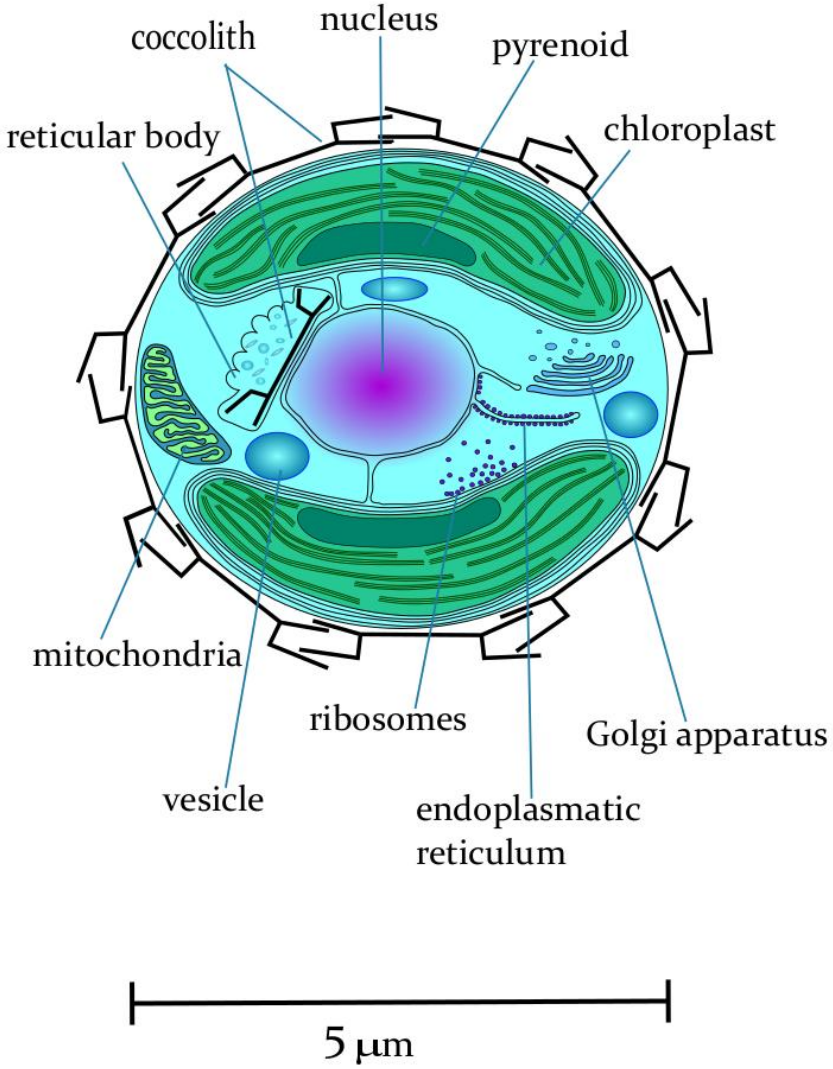

Figure 3: Overview of an *Emiliania huxleyi* cell forming a coccolith. In *Emiliania huxleyi* the coccoliths are formed close to the nucleus, surrounded by a reticular body. The illustrated *Emiliania huxleyi* cell is in the calcifying, diploid, life phase.

All the steps are summarized below, and Figure 3 shows where in the cell the coccolith is made as well as the coccolith vesicle, and the reticular body. The steps are illustrated in Figure 4. The different crystal units (vertical and radial) in the coccoliths are presented in Figure 5.

1. A precursor, a so-called base-plate scale, is formed close to the nucleus inside a so-called coccolith vesicle. The content of the base-plate is not fully determined, but it is likely to contain both polysaccharides and proteins[20]. Ca is transported to the vesicle and the concentration increases. The Ca accumulation is thought to occur either in the Golgi body or in the membrane of the reticular body[64].

2. Nucleation starts around the rim of the precursor inside the vesicle[10]. The reticular body forms on the coccolith vesicle. The reticular body is unique to *E. huxleyi*. When the rim of the precursor is defined by calcite crystals, it is called a proto-coccolith.
3. The crystals of the proto-coccolith are positioned where the elements in the coccolith start growing[3, 10]. The crystallographic axes of these crystals alternate, which means that the nucleation at this stage is highly controlled. The R-units, radially oriented crystal units, will extend parallel to the base-plate. The V-unit, vertically oriented crystal unit, will grow in the vertical direction.
4. The inner part of the tubes (inner part of the R-units) extends inwards. The coccolith and the reticular body grow until the coccolith is complete.
5. The reticular body disappears and the whole coccolith is exocytosed.

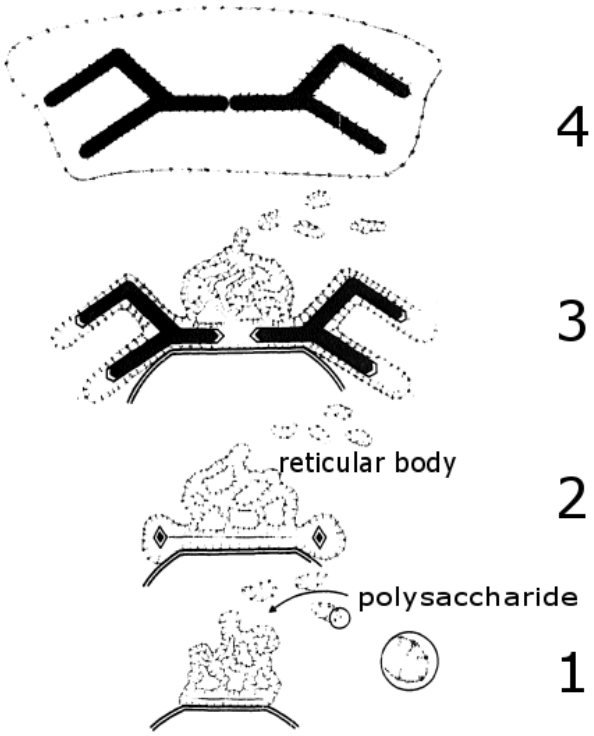

Figure 4: Coccololith production in *Emiliania huxleyi*: 1 A coccolith vesicle is formed near the nucleus. 2: A reticular body is formed and crystal nucleation starts on the edges of a baseplate. 3: The crystal units expand. 4: The coccolith is exocytosed. The figure is made by Westbroek et al. 1993[65].

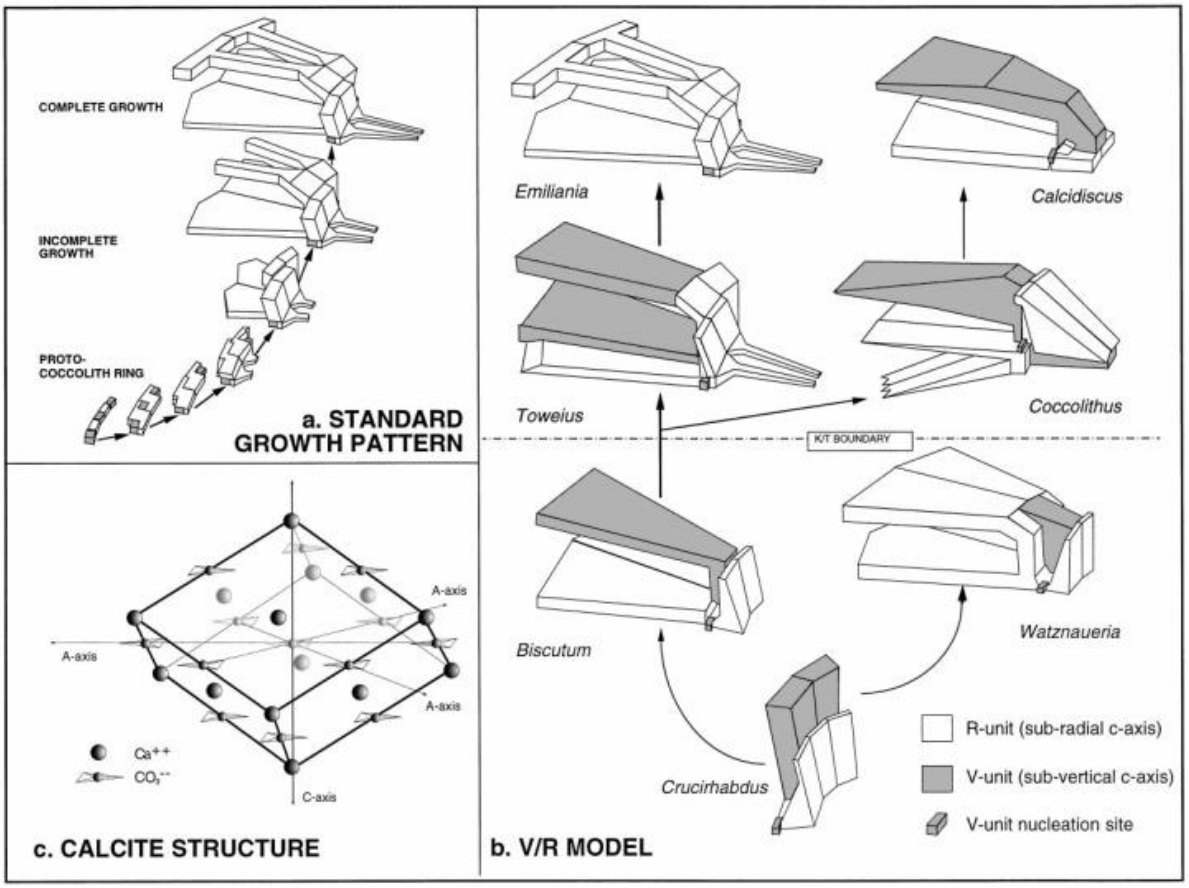

Figure 5: The different elements in a coccolith. a) shows the standard growth pattern in *Emiliania huxleyi* starting with a proto-coccolith. The V-unit is completely overgrown by the R-unit. b) The V/R-model explains the different units in most coccolithophore species. c) The crystal growth in coccolithophores is controlled in two directions, along the a- and the c-axis. The figure is made by Young et al. 1999[8].

Figure 5(a) shows how the V- and R-units form a crystal unit. *E. huxleyi* has a slightly different shape of the R- and V-units, as the V-unit is very small and not visible unless the coccolith is broken[10]. This differs from other coccolithophore species, which often have distinct R- and V-units, as shown in Figure 5(b).

Biomineralization in *P. carterae*

Many of the steps in the calcification process are the same for *P. carterae* as for *E. huxleyi*, but since there are some small variations, coccolith formation in *P. carterae* is explained as well. Figure 6 shows a *P. carterae* cell in the process. The details are found on the page following Figure 6. The steps are illustrated in Figure 7.

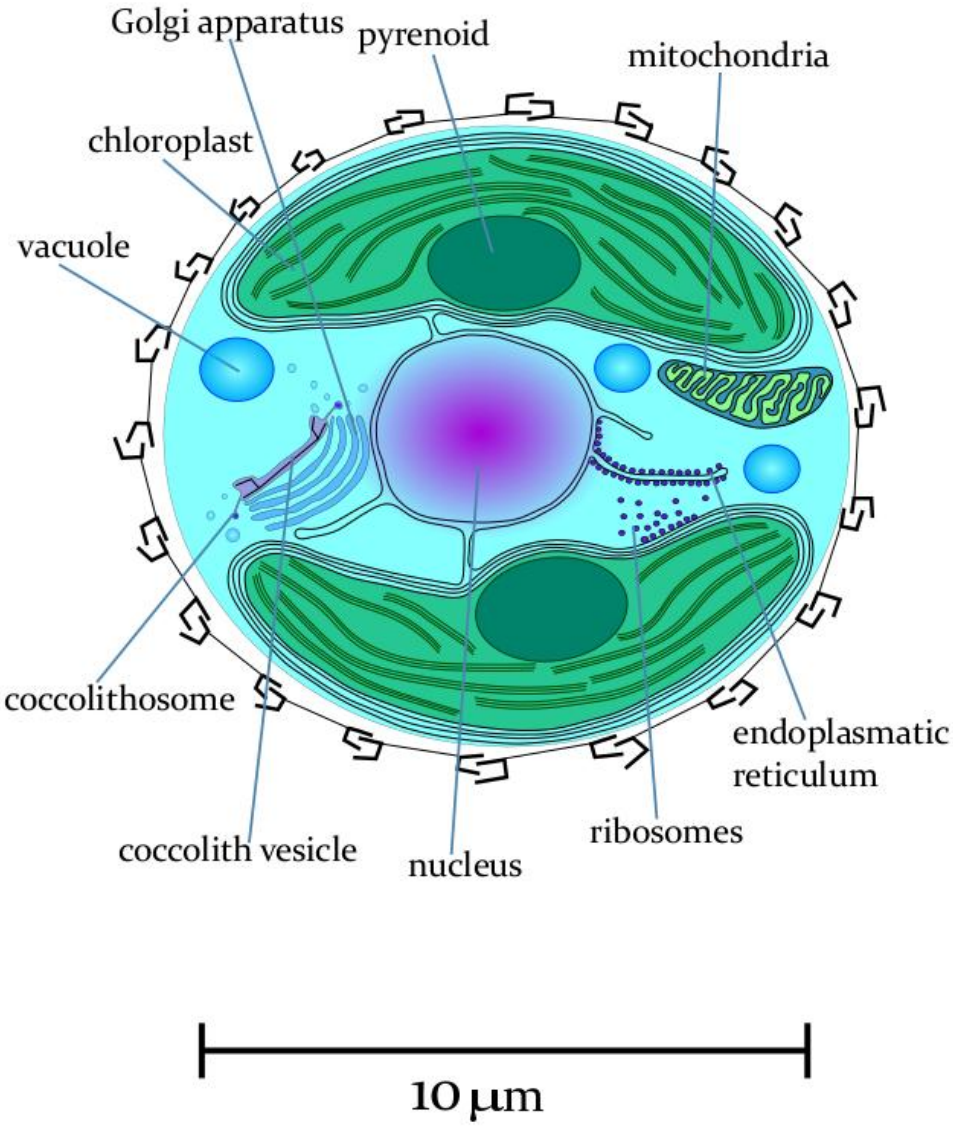

Figure 6: *Pleurochrysis carterae* cell in the coccolith forming process. The coccolith is formed from a Golgi derived vesicle, called a coccolith vesicle Haptonema and flagella have been omitted from the illustration. The *Pleurochrysis carterae* cell in the illustration is in the diploid phase.

An overview of the coccolith forming process is described below. The process is illustrated in Figure 7.

1. A precursor, a base-plate, is formed in a coccolith vesicle that is derived from the Golgi apparatus. The base-plate consists of polysaccharides and has a distinctive microfibrillar structure on the surface[8].
2. Ca is transported to the vesicle, and the concentration increases. Two polysaccharides (PS) are linked to the calcification process in *P. carterae*. These are called PS1 and PS2[66, 67].

3. The vesicle takes on a more complex form with certain extensions containing dense particles called coccolithosomes. The coccolithosomes transport the Ca to the coccolith vesicle.
4. Nucleation starts around the periphery of the base-plate. When the rim of the base-plate is calcified all the way, it is called a proto-coccolith. The majority of the coccoliths have 23-25 units (both V- and R-units). The V- and R-units generally alternate[68]. The crystals grow mostly upwards and outwards (possibly due to the base-plate) and the vesicle gradually expand.
5. When the R- and V-units are complete the vesicle dilates, but the coccolith is still protected by a dense organic coating. In *P. carterae* the R- and V-units are about the same size, but different shape[10]. The coccolith is then exocytosed.

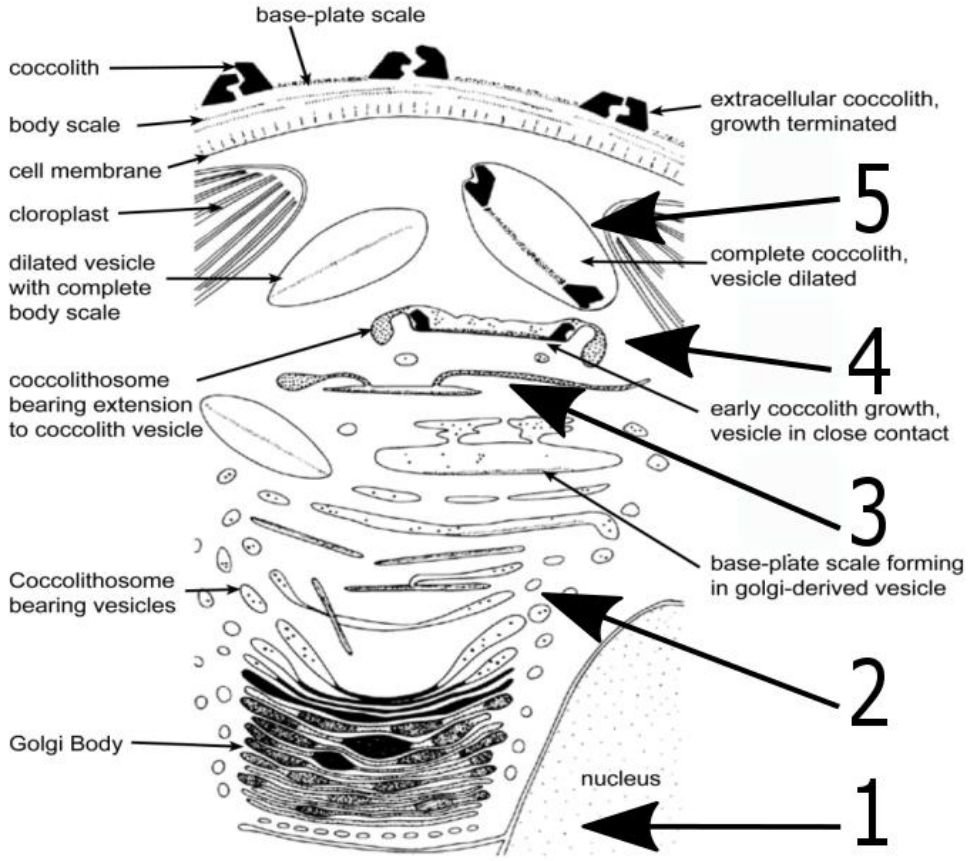

Figure 7: The coccolith forming process in *Pleurochrysis carterae*: 1: A baseplate is formed in the Golgi apparatus (Golgi body)and forms a coccolith vesicle. 2: Polysaccharides transport Ca to the coccolith vesicle. 3: Coccolithosomes containing Ca are formed in the coccolith vesicle. 4: Nucleation starts along the edge of the baseplate. 5: The crystal units expand. When the coccolith has reached its final shape, it is exocytosed with a dense organic cover. The original figure was made by Van der Wal et al. 1983[5].

Differences and similarities between *E. huxleyi* and *P. carterae*

We have seen that there are some differences between *E. huxleyi* and *P. carterae*. These differences are summarized in Table 1, and visualized in Figure 8.

Table 1: Overview of differences in calcification between *Emiliania huxleyi* and *Pleurochrysis carterae*.

	Emiliania huxleyi		*Pleurochrysis carterae*	
Specific molecules involved in coccolith formation	not known, but possibly one Ca binding protein	[62]	PS1 and PS2	[66]
Place of calcification	Reticular body, close to the nucleus	[20]	Coccolith vesicle, derived from the Golgi apparatus	[8]
Baseplate	Made of polysaccharides and protein, but not fully analyzed	[62]	Made of polysaccharides	[20]
Ca accumulation	Possibly in the Golgi body, or in the membrane system of the reticular body	[64]	Ca accumulation and transport is likely helped by the PS1 and PS2-molecules in the coccolithosomes	[67, 68]
Size of R- and V-units	V- unit is comparably small and overgrown by expanding R-unit	[10]	R- and V-units are similar in size, and fit closely together	[10]
Number of crystal units in the rim	No data		20-30 crystals are observed, but the most common is 23-25	[68]

We see that there are differences in the way that these algae accumulate Ca-ions and in the molecules used. This may have an impact on this project. The coccoliths are approximately the same size, but the *P. carterae* cell is larger. The nucleus is bigger than pictured in both species, but here reduced to make space for the process. The purple spheres are thought to be vesicles carrying Ca-ions. In *E. huxleyi*, Ca is believed to be concentrated in the Golgi apparatus or in the membrane of the reticular body. In *P. carterae*, these Ca-carrying vesicles are likely to come from the Golgi apparatus, where Ca is thought to be concentrated by the PS1 and PS2. In step 2, *P. carterae* has coccolithosomes attached to the coccolith vesicle. Coccolithosomes are thought to be Ca-carrying vesicles that are attached to the coccolith vesicle. In the last step the *E. huxleyi* coccolith is likely exocytosed with enzymes that attaches the coccolith to the other coccoliths, while coccoliths in *P. carterae* are exocytosed with an organic cover.

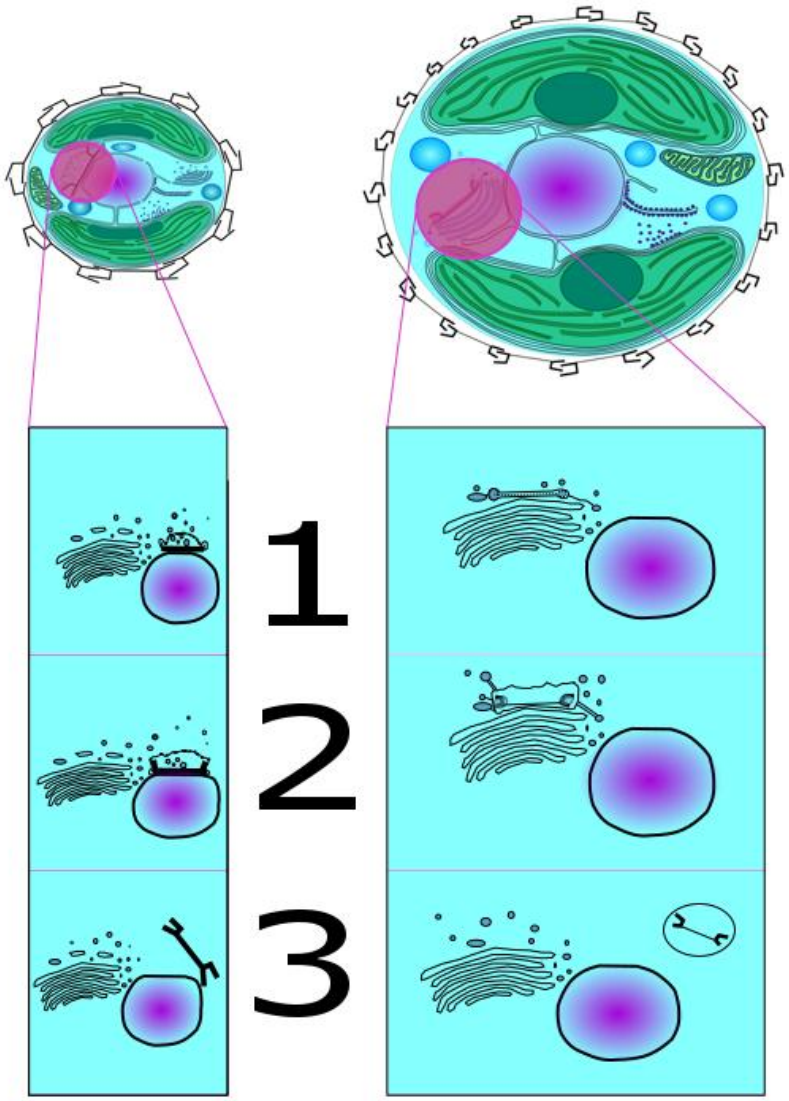

Figure 8: Summary of the calcification process in *Emiliania huxleyi* (left) and *Pleurochrysis carterae* (right). The process is slightly different in the two species. 1: In *Emiliania huxleyi* the coccolith forming process occurs close to the nucleus, whereas the coccolith vesicle is derived from the Golgi apparatus in *Pleurochrysis carterae*. 2: *Emiliania huxleyi* develops a reticular body, whereas *Pleurochrysis carterae* coccolithosomes attached to the coccolith vesicle. 3: In *Emiliania huxleyi* the vesicle/reticular body, dissolves, whereas for *Pleurochrysis carterae* the coccolith vesicle dissolves, but the coccolith keeps a dense organic layer.

1.2.4 Coccolith mineral structure

$CaCO_3$ can exist in three different stable crystalline polymorphs, calcite, aragonite and vaterite. An organism seems to be very specific in the type of polymorph it deposits during growth. Even though there are many organisms that produce $CaCO_3$, they seem to produce either calcite or aragonite. Vaterite is rare in organisms[45]. Structurally, there might be a reason why the organisms are so specific, since aragonite is slightly denser than calcite. Calcite has a density of 2.71 g/cm^3, while aragonite is slightly denser with 2.84 g/cm^3[1].

Below is an illustration that shows how the carbonate anions are stacked in calcite (left) and aragonite (right). By considering the carbonate groups as layers, you can see that the aragonite layers are the same for every second layer, while they are shifted to allow for more space between them for the calcite structure, Figure 9.

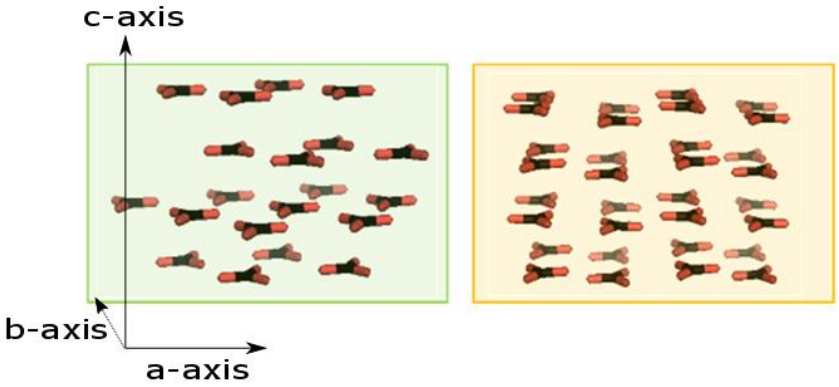

Figure 9: The packing patterns of carbonate anions in two of the polymorphs of CaCO3: Calcite (left) and aragonite (right). Carbonate groups are shown as 'Y' shaped sticks where the carbon is black, and the oxygen is red. The differences are primarily in the way the CO_3^{2-}– molecules are packed. The Ca cations are omitted for clarity. The original figure was published at www.scepticalscience.com[69].

Both *E. huxleyi* and *P. carterae* precipitate coccoliths in the calcite structure with the space group *R*-3*c* h (167). In the case of calcite, the lattice type is rhombohedral, hence the *R*, with a threefold inversion rotation axis (-3). A representation of the crystal structure for calcite and aragonite is given in Figure 10.

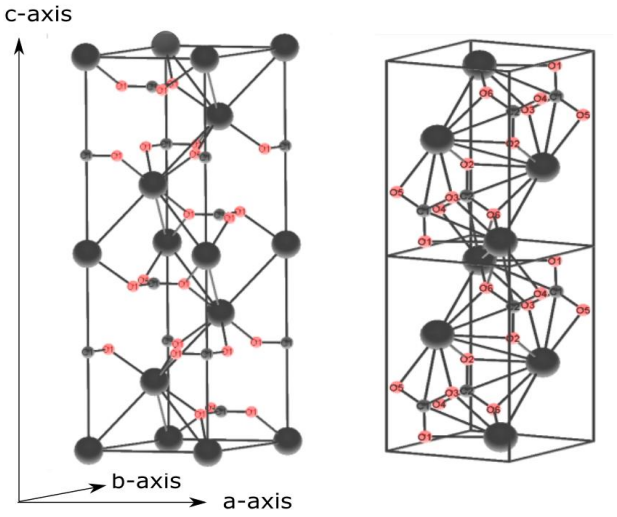

Figure 10: The crystal structure of calcite (left) has a rhombohedral lattice type, whereas aragonite (right) has an orthorhombic structure. The aragonite structure is illustrated by two unit cells to better see the repeating pattern in the carbonate. The calcite structure is illustrated by only one unit cell. The red dots are oxygen, the small, grey dots are carbon, and the bigger black dots are Ca (but in the calcite structure the crystal structure is the same when the cation is Mg, Mn or Fe[70]). The figures are modified from Pearson´s Crystal Data[1].

Two minerals with the same crystal structure will have similar XRD patterns. In Figure 11 and Figure 12, the XRD pattern of pure calcite and magnesite are similar, but somewhat shifted in relation to each other. The highest intensity in calcite is almost ten degrees further up in magnesite.

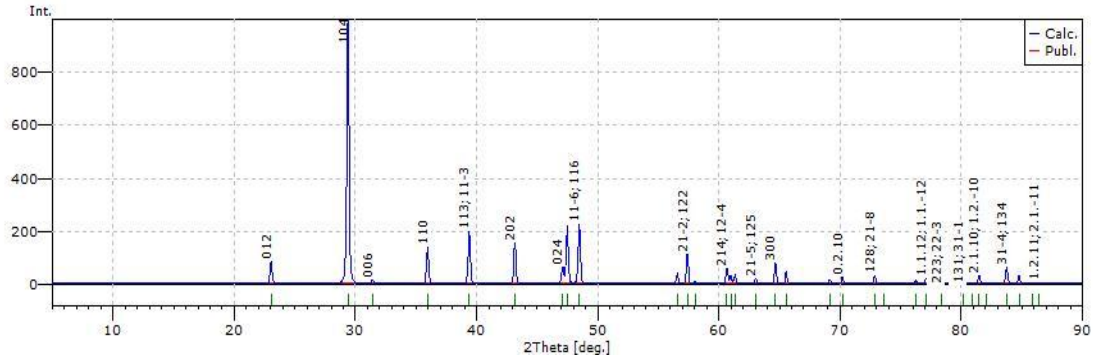

Figure 11: The X-ray Diffractogram of calcite (PDF)[1].

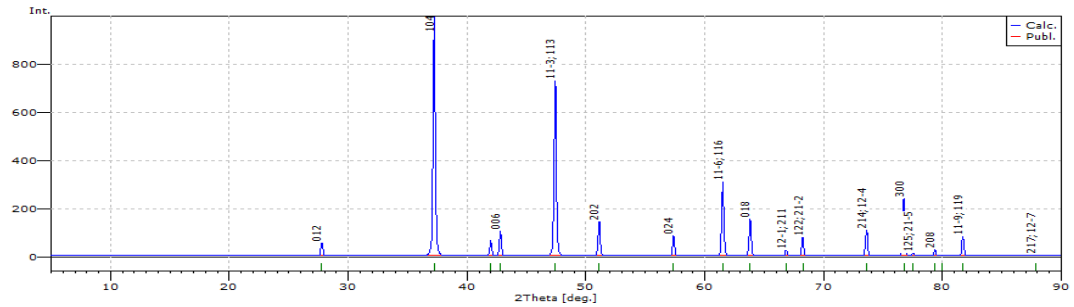

Figure 12: The X-ray Diffractogram of magnesite ($MgCO_3$) (PDF)[1].

In Figure 13, A, the area where the highest intensity reflections (d_{104}) is expected to be found. Another reflection of interest is d_{211} which matches one of the halite reflections. In Figure 13 B, the calcite PDF is shifted to match the reflections better.

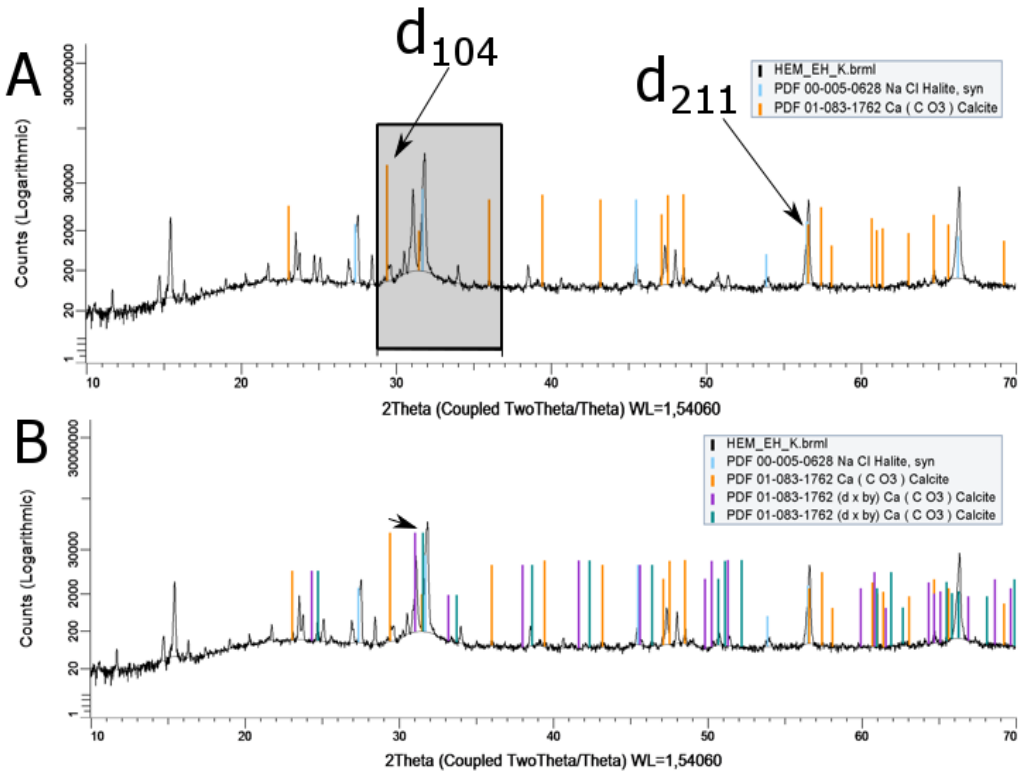

Figure 13: Diffractogram A: The marked area shows where the reflections with the highest intensities of magnesian calcite are expected to be found according to the diffractograms of calcite and magnesite. The highest intensity reflection is called d_{104}. Another reflection that has been used to calculate the Mg-content is d_{211}. Unfortunately this reflection matches one of the reflections of halite. Diffractogram B: When the calcite PDF is shifted towards higher angles (more Mg), the PDF seem to match better with some of the reflections.

The shift in the refractions has been used to calculate the amount of Mg, in relation to Ca, in calcifying species to determine how much Mg they contain[71] using Vegard's law. Vegard's law describes the relationship between lattice parameters and two solids, with the same crystal structure, in a solid solution. Vegard's law:

$$a_{\mathrm{A}_{(1-x)}\mathrm{B}_x} = (1-x)\,a_{\mathrm{A}} + x a_{\mathrm{B}}$$

The lattice parameters for the solid solution are noted as $a_{A(1-x)}b_x$, where x is the percentage of solid B in solid A. The lattice parameters for pure solid A are noted as a_A, and the lattice parameters for pure solid B are noted as a_B.

In a diffractogram all the reflections do not necessarily shift as much. This is why some reflections are better to look at than others. For Ca-Mg relations reflection number 12, or reflection d_{211} (hkl-system), has been used[50]. For calcite, this reflection can be found at 56.560° 2θ, and for magnesite the same reflection is found at 66.860° 2θ (measured with a

wavelength of 0.154060 nm). For a solid state solution with a calcite structure containing both Mg and Ca, d_{211} could be found anywhere between $2\theta = 56.560°$ and 66.860°, and the displacement of the reflection would indicate the amount of Mg in the calcite structure. For dolomite ($Ca_{(1-x)}Mg_xCO_3$), the reflection d_{104} has been used measure the Mg-content[72]. This is the reflection with the highest intensity. For one of the dolomite phases ((1972) 62, 772-783) from Pearson's Chrystal Database where the Mg content is 10%, the d_{104} can be found at $2\theta = 29.740°$.

The chosen elements for this work are all known to form carbonates, and to perform complete or partial substitution solid solubility with Ca in the calcite structure. The sizes of the elements do not vary much, and all are notably smaller than Ca. The table below sums up the differences between these elements and their carbonates:

Table 2: Overview of the different elements in the carbonates of interest and their unit cells.

	Ca	Mg	Fe	Mn
Calculated atomic radius	194 pm[73]	145 pm[74]	156 pm[70]	161 pm[75]
Relative atomic mass	40.078[73]	24.305[74]	55.845[70]	54.938[75]
Chrystal structure as a carbonate	*R*-3*c* h[1] (calcite)	*R*-3*c* h[1] (magnesite)	*R*-3*c* [76] (siderite)	*R*-3*c* h[1] (rhodochrosite)
Unit cell a (carbonate)	0.49898 nm[1]	0.42981 nm[1]	0.46916 nm[76]	0.4772 nm[1]
Unit cell c (carbonate)	1.7062 nm[1]	1.26690 nm[1]	1.53796 nm[76]	1.5637 nm[1]

2 Methods and theory

The methods and theory behind the experiments are presented in this chapter. First, I will present the recipe of artificial seawater, before continuing with the culturing techniques and how to separate the organic material from the coccoliths, and lastly how to analyze the composition of the coccoliths.

2.1 Artificial seawater

There are two main categories of artificial seawater: "Enriched Seawater, Natural Water" (ESNW) and "Enriched Seawater, Artificial Water" (ESAW). ESNW has been used to culture algae for about 100 years[21]. The growth media has been updated many times to optimize the growth conditions for algae, as we understand them better. In this experiment, it was necessary to use ESAW instead of ESNW to control the Ca-amount and also to control some of the metal concentrations. If this is not required, then it is often easier to use ESNW. One of the recipes for ESAW has been shown to give better growth conditions for *E. huxleyi* than ESNW[21]. The recipe is presented in Table 3.

It is important to note that different algae have different requirements for seawater[77]. The variations in concentrations that algae can survive in are also quite wide. Winter summarizes these variations in his book *Coccolithophores*, where he gathers evidence that *E. huxleyi* can tolerate salinities between 11-41 ppt; temperatures between 1–30 ºC; a wide variety in nutrient concentrations; and pressures and light conditions ranging from the surface and down to 200 meters below the surface[78]. The optimal seawater also depends on what you want to achieve, since it has been shown that different temperatures and nutrient concentration can affect calcification[79, 80]. The specifics of ESAW for this thesis are listed in Chapter 3.

Table 3: The recipe that was used as a base for ESAW, based on the recipe made by Berges et al. in 2001[21].

compound	g/L	amount for 11 L
dH2O		11 L
NaCl	21,190000	233,090000
Na2SO4	3,550000	39,050000
KCl	0,599000	6,589000
NaHCO3	0,174000	1,914000
KBr	0,086300	0,949300
H3BO3	0,023000	0,253000
NaF	0,002800	0,030800
Salt solutions		
MgCl2-6H2O	9,592000	105,512000
CaCl2 2H2O	1,344000	14,784000
SrCl2-6H2O	0,021800	0,239800
Major nutrient 1		
NaNO3	46,700000	513,700000
Major nutrient 2		
NaH2PO4 H2O	3,090000	33,990000
Major nutrient 3		
Na2SiO3 9H2O	15,000000	165,000000
Metal stock 1		
FeCl3 6H2O	1,770000	19,470000
Na2EDTA 2H2O	3,090000	33,990000
Metal stock 2		
ZnSO4 7H2O	0,073000	0,803000
CoSO4 7H2O	0,016000	0,176000
MnSO4 4H2O	0,540000	5,940000
Na2MoO4 2H2O	0,001480	0,016280
NaSeO3	0,000173	0,001903
NiCl2 6H2O	0,001490	0,016390
Na2EDTA 2H2O	2,440000	26,840000
Vitamin stock		
Thiamine-HCl	0,100000	1,100000
Biotin	0,002000	0,022000
B12	0,001000	0,011000

2.2 Culturing techniques

Many factors can affect algae other than the nutrients in the saltwater. Since algae are (mostly) photosynthetic, the light conditions are among the most important factors. This includes the strength of the irradiance and the light:dark cycle. Other factors are temperature, CO_2-level in the water, and movement in the water.

In the paper on artificial seawater that was used in this project, Berges et al. used the following conditions: The temperature was kept at 16 ± 1 ºC, and the irradiance was 50 ± 5 µmol quanta $m^{-2}s^{-1}$ at a 14:10 light:dark cycle[21].

2.2.1 Light conditions and temperature

The growth conditions that were used in Berges' experiment, are just one way of setting up the conditions. There can be variations within the species that are adapted to different situations[79]. There are different strains of *E. huxleyi*, and these are adapted to quite different conditions[81]. For instance *E. huxleyi* can tolerate irradiance levels ranging from surface irradiance to less than 1% of the surface levels[4]. However, studies show that the intensity of light influences the coccolith formation, and that some level of irradiance is needed for optimal coccolith production in this species[82]. For *E. huxleyi*, the irradiance is more important than the light:dark cycle[83]. There are also variations in the light:dark cycles, and some species even grow with continuous light. It seems that *E. huxleyi* is one of the species that can do that as long as the intensities of the light is not too high[84]. *E. huxleyi* can also grow under a wide range of temperatures from 1-2 ºC[78, 85] to 30 ºC[86].

For *P. carterae* it seems that 16:8 light:dark cycle with 18 ºC has been used in other experiments[6, 87]. However, in an article by Moheimani et al. *P. carterae* was grown under the following conditions: 25 ºC, with 150-190 µmol quanta $m^{-2}s^{-1}$ provided by white day light in a 12:12 light:dark cycle[88]. *P. carterae* can grow in temperatures ranging from 4 ºC to 28 ºC, but dies after 5 days in 3 ºC [88].

In physics, the wavelength, or the energy, of the photons is often the interesting aspect of the measurement. For algae and plants the interesting aspect is how many photons in the spectre of electromagnetic waves they can use. This is why the irradiance is often given as measurement of quanta of useful photons per square meter per second: µmol quanta*$m^{-2}s^{-1}$. It

is then given that the measurement range is light with a wavelength between 400 -700 nm, which is the visible spectrum of light.

Mol quanta of light can be converted to energy dependent units, such as W/m^2 if the wavelength is known[89].

2.2.2 Growth rates, growth curves and transferring cultures

Growth rate is a measure for how much a population grows on a given time interval. This is important for algal culturing techniques because it affects the population density and thus also the nutrient availability. In a 40 mL flask, you can have an exponential growth rate for a time, but eventually you will reach a maximum population density. The algae will usually live for a while after the exponential growth has stopped.

The population density can be found by counting all algae in a known volume, which can be done both manually and by machine. These techniques are described under analysis methods in section 2.3.6 and 2.3.7. When the population density is measured at regular intervals during the growth period, the data can be plotted as a growth curve. The plotted curve often follows a sigmoid path: Slow growth in the beginning, then exponential growth until the population density stabilizes, as can be seen in Figure 14 below. *E. huxleyi* is known to cause algal blooms, where the population density in culture has been measured to $35*10^6$ L^{-1}[65].

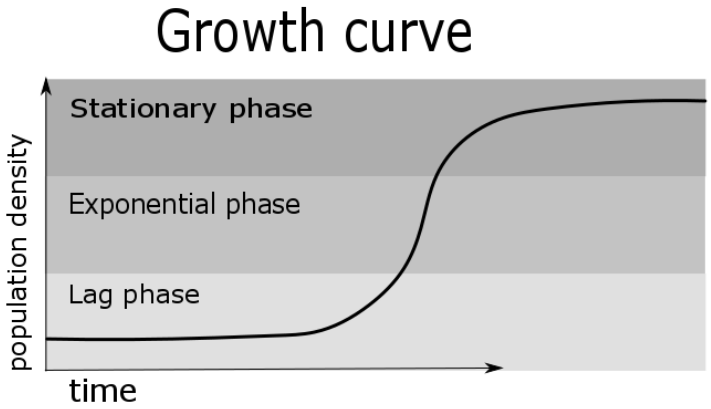

Figure 14: The algal growth curves often follow a sigmoid curve. The population grows exponentially until the population density stabilizes.

Depending on the species, the algae can stay for a while in the stationary phase. When the medium runs out of nutrients, the culture has to be transferred to a new culture vessel with fresh medium.

2.2.3 Coccolith extraction and cleaning methods

Extracting the coccoliths in large amounts is cumbersome. However, some methods for doing this have been developed. In small amounts, the easiest way is to use a pipette to retrieve the coccoliths that have gathered at the bottom, and then apply it to the sample holder or the container that suits further analysis. Although the size of the cells of *P. carterae* and *E. huxleyi* are different, the coccoliths are about the same size. This means that similar methods can be used for these two species. Note that *E. huxleyi* sheds the coccoliths and produce new ones, whereas *P. carterae* coccoliths need to be removed.

In one experiment Takano used sonication treatment and air-bubbling the culture to detach the coccoliths from *P. carterae* [90]. A full 400 mL flat glass bottle containing *P. carterae* was placed in sonication bath for 1 min at 27 kHz. This was repeated at varied intensities every day during batch culture. Thereafter, they used centrifugation to separate cells from calcite particles in suspension. They used a set up where the algae were pumped through a filtering system that allowed coccoliths and old medium to be "rinsed away" throughout the process. A maximum calcite productivity of 18 mg/day in dry weight was obtained in flasks of 400 mL[90].

When methods of coccolith extraction is mentioned in the literature, the most common method for obtaining large amounts of coccoliths seems to be to mechanically (or chemically) remove the coccoliths. Mechanically, this can be done by air-bubbling, sonication, or even shaking the cultures. Acid can be used to remove the coccoliths chemically by dissolving them; however, since the coccoliths are the desired product in this study, this is not a suitable solution.

In a work by Bischoff[71], chlorox and H_2O_2 was used to remove organic material. In these experiments the specimens were larger, so losing parts of the surface of the specimens to be examined was not so crucial.

2.3 Methods of analysis

The methods for obtaining results are presented in this section.

2.3.1 Light microscopy

Light microscopy is a central tool for biologists. Both *E. huxleyi* and *P. carterae* are visible in light microscopes, and it is possible to see the coccoliths.

Light microscopes are optical microscopes and are limited by the wavelength of visible light and the quality of the lens. The smallest object that can be distinguished in an ideal optical microscope is half of the wavelength of visible light. Since visible light is between 400-700 nm, the smallest distinguishable object is 200 nm. Such small structures are possible to see when using an oil droplet and good quality lenses. Bright field microscopy can be useful to have a quick look at the samples, but finer structures (such as haptonema, flagella and coccoliths) are easier to see with phase contrast. The latter microscopy technique delays photons in such a way that the brighter parts are left out, which makes structures with a high refractive index (such as coccoliths) easier to see.

2.3.2 Scanning Electron Microscopy

It is possible to see the coccoliths in a light microscope, but in order to observe the finer structures, it is necessary to have a higher resolution. With a very good Scanning Electron Microscope (SEM), it is possible to "see" atoms[91].

The SEM functions by scanning a sample with a focused beam of electrons. The electrons are focused with a magnetic lens, and scan coils ensure that it is possible to scan the sample with the electron beam. An objective lens focuses the beam on the sample. Figure 15 shows a schematic set up for an SEM.

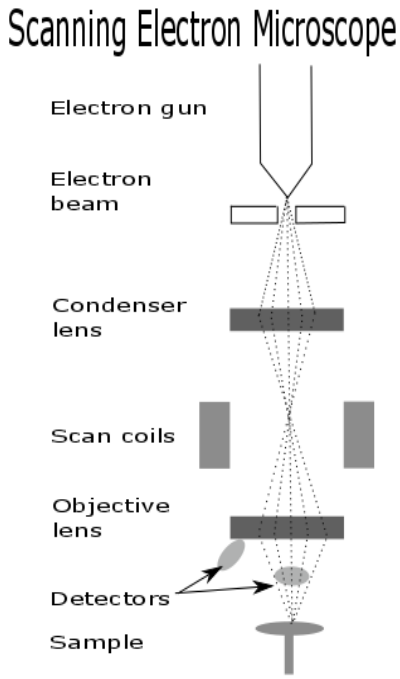

Figure 15: Schematics of an SEM. The electrons are emitted by an electron gun, and pass through a condenser, after which they are steered with the scan coils, and then focused with the final lens, before hitting the sample. The returning electrons (secondary and backscattered) and the X-ray radiation give information about the sample surface and the chemical composition.

The electrons can interact with the sample in different ways. See Figure 16 for an overview of the different signals from the sample. When the electrons hit the sample, they can knock out electrons from the elements. These electrons are called secondary electrons and are detected by an Everhart-Thornely Detector (ETD). The secondary electrons mostly carry information about the surface and the topography of the sample.

Not all electrons from the beam will result in secondary electrons. Some will act elastically with the atoms in the sample, and return with almost as much energy. These are called backscattered electrons. These electrons are detected with a Solid State Detector (SSD), which is placed close to the objective lens. The backscattered electrons give more information of the chemical composition of the sample.

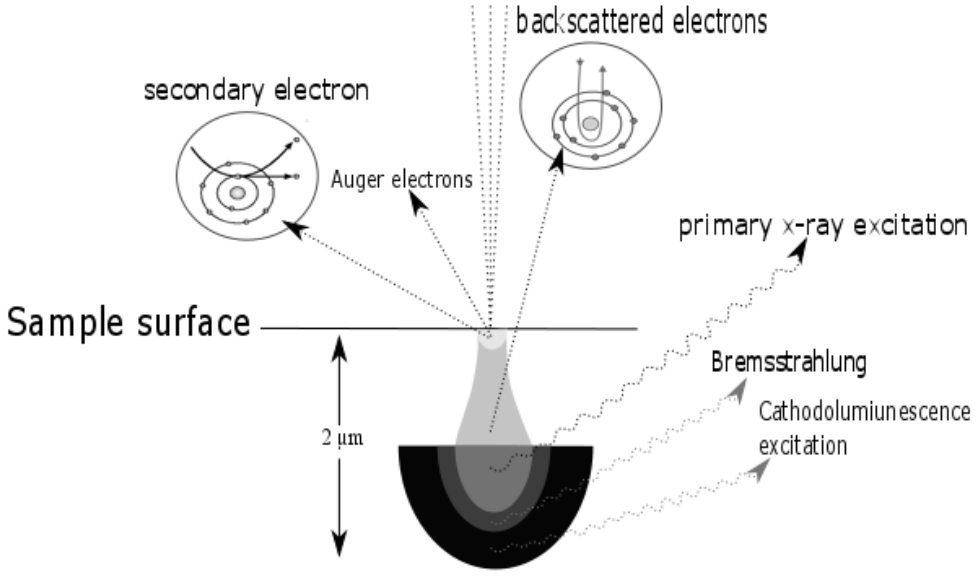

Figure 16: The different sources of information in an SEM. An electron beam scans the sample. This electron beam can knock out electrons in the sample – secondary electrons. Some of the electrons from the beam interact in an elastic way with the atoms in the sample, and return with almost as much energy – backscattered electrons. Electrons that are emitted as a result of excitation are called auger electrons. The electron interaction with the sample can also create radiation. Secondary electrons mostly come from the surface of the sample, and carry information about the topography. Backscattered electrons carry information about the chemistry of the sample.

2.3.3 Energy-dispersive X-ray Spectroscopy

Energy-dispersive X-ray Spectroscopy (EDS) can give you information on the type and amount of elements in your sample. EDS can be done in some SEMs by detecting the X-ray emitted from the sample due to interactions with the electrons from the electron beam. Each element has their specific set of energies for the X-rays they emit. This is called an X-ray emission spectrum. Be aware that shallow samples can show some X-ray emission spectrums from the sample holder and the surroundings. If the sample has a rough surface, this can lead to an even larger deviation in the amount of characteristic X-rays. In addition, several elements may have overlapping signals for multicomponent samples such as biological materials.

A point analysis by EDS requires a sample of at least 2 µm in diameter, which is about the same size as the coccoliths. However, the coccoliths are much thinner. It is important to keep this in mind when considering the EDS analysis of the coccoliths.

There are more accurate methods than EDS for detecting the elemental composition in a sample. For instance, Wavelength Dispersive Spectroscopy (WDS, also a tool for selected SEMs) can detect about 10 times smaller weight percent than the EDS can.

There are several ways to prepare the samples, and many prefer to coat the samples with a thin layer of platinum, gold or carbon to get good pictures and a higher resolution, if imaging is the essential part of the experiment. It is possible to look at coccoliths in the SEM without coating the samples first, but it is then more difficult to capture good images due to charging of the samples, and there is a greater risk of burning the sample with the electron beam.

2.3.4 Atomic Absorption and Mass Spectrometry

Analytical methods that are known to be very precise are Atomic Absorption Spectrometry (AAS) and Mass Spectrometry (MS).

In AAS the sample is heated to a gaseous state. When electrons are excited and fall back to the normal state, they emit visible light. The transition from a higher state to the normal state is specific for each element. This method can be used to find the element composition of a sample, as well as concentration of those elements.

There are different forms of MS, but Inductively Coupled Plasma Mass Spectrometry (ICP-MS) is presented here as it has been used to look at coccoliths before[58]. ICP-MS works by ionizing the sample with inductively coupled plasma, then use a mass spectrometer to separate and quantify the ions.

None of these methods can be used to determine crystal structure. These two methods have not been used in this thesis.

2.3.5 X-ray Diffraction

X-ray Diffraction (XRD) is a method to analyze the structure of a material through finding the spacing between the atoms. XRD –methods described here apply for crystalline, powdered samples.

In powder XRD a monochromated X-ray with a known wavelength, λ, is directed at the sample at a known angle. In addition, the sample is partly rotated to cover all atom spacing – given that the crystals in the powdered sample are randomly oriented. An X-ray will travel through the sample until it hits an atom, then the X-ray is diffracted. The atoms behave as scattering centers. When some of the X-rays are diffracted further down in the crystal structure, they have had to travel a longer way than the X-rays that are diffracted at the

surface. This brings the X-rays out of phase, which means that they will cancel each other out. When the X-rays hit the detector, they create a pattern that shows the spacing between the atoms in the crystal unit. Figure 17 below shows an illustration of the X-rays being refracted by atoms.

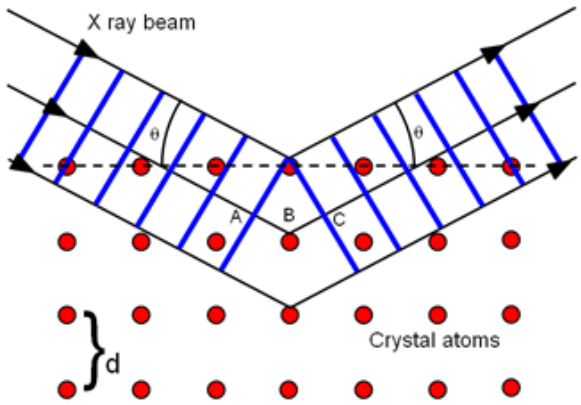

Figure 17: The X-ray beam hits the atoms in the crystal. When the beam is refracted it creates a pattern that is specific to each type of crystal. The illustration was published at the www.iop.org[92].

The diffraction follows Bragg's law: $2d \sin\theta = n\lambda$, where d is the spacing between the atoms (or diffracting planes), θ is the incident angle, n is an integer, and λ is the wavelength of the beam.

Attention should also be given to instrumental effects such as height correction of the sample, fluorescence from the X-ray source such as when analyzing samples containing notable amounts of iron or cobalt, preferred orientation of the sample leading to altered intensity profile. The method is most suited for single phase materials and will have challenges in detecting presence of phases less than 2 vol%.

2.3.6 Hemocytometer

The hemocytometer was created to count cells, and consist of a glass plate over a plastic well. The glass plate is divided into 16 sections to make it easier to keep track of the counted cells. The exact volume under the 16 sections is known. The cells that are within the marked area are to be counted manually by visual inspection. As the volume is known, this count gives you an indication of the population density (cells/mL). Figure 18 illustrates the grid and the set up. Cells that are situated halfway on the inside of the counting area should be counted

half of the time. A rule of thumb is to count the cells to the left and above, and not to the right and below.

An advantage with manual counting in a hemocytometer is that you can see if you have both cells and debris in your culture. An automatic cell counter cannot distinguish between the cells of interest and those that are not. If there is a cluster of cells, the number of cells has to be estimated. It is also possible that cells are not evenly distributed in the medium, and thus your estimation can deviate from the correct cell count. The more samples you take, the more accurate your estimate will be. The only inconvenience using this technique is that it is a very time-consuming process.

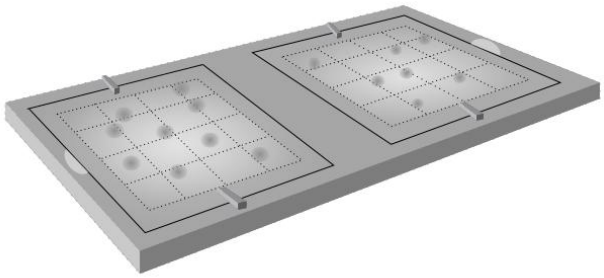

Figure 18: Illustration of a simplified hemocytometer: The grey dots illustrate cells. The volume of cell culture to be counted is beneath the grid.

2.3.7 Counting algae (CASY®)

Cell counting can also be done automatically with an automated cell counter. The counting principle is simple: Living cells are insulators as their membrane have a high resistance. Dead cells do not have an intact membrane and will conduct electricity. The nuclei of the cells also have a membrane that is insulating. For dead cells, this means that the nuclei can possibly be counted, but as it is much smaller than the entire cell, this is a way of distinguishing dead cells from the living.

The diluted cell medium is sucked in to the cell-counting machine and into a funnel made of a synthetic precious stone with a given funnel size. An electric pulse is sent through the crystal, and through funnel containting cells. Depending on the resistance, the amount of cells and the concentration can be counted. Because of the structure of this crystal we can also measure the size of the cells.

The cell culture is diluted in a specific electrolyte. As the cells pass through the crystal, the volume of the cells replaces a given volume of the electrolyte, which again represents a given resistance that can be measured[93].

This system gives an idea of the number of cells in the culture, but there are some uncertainties. This system will count anything in the diluted cell medium that has a higher resistance than the medium. If the culture is contaminated by bacteria this might affect the cell count – especially if the cells are about the same size as the bacteria. The sizes to be counted can be adjusted, so if the cells are at a given size you can exclude other particles. It is also important to know that some kinds of cells have a tendency to cluster – this tendency is shared by *P. carterae*. The cells may be considered as one larger particle and therefore be excluded from the count. The cells also may not be evenly distributed in the medium, which can lead to a wrong estimation of the population density. The more samples you examine, the more correct your estimate will be. The problem of clustering also occurs for the manual cell counting.

The procedure for counting the cells is to start with a given volume of the cell culture. The counter needs 10 mL to operate. The volume from the cell culture is diluted with Casy Ton®[94], which is a solution with given conducting capacities. When the cells are counted you have to take the dilution into consideration.

2.4 Health, Environment, Safety and Ethics

The health, environment and security measures performed before beginning with this study are listed in the Appendix A. Neither the chemicals used, nor the exposure of the saltwater solution is, considered harmful in the doses used. Although some algae have died and also possibly suffered during these experiments, it does not fall under any ethical regulations that require license or permission to conduct the experiments.

3 Experiments

This chapter presents the specifics of the experiments in this project. The chapter is divided into three subchapters: Production of ESAW, experiment, and analysis (counting, pH, SEM and XRD).

3.1 Production of ESAW

The recipe presented in chapter 2 was used as a basis for the ESAW of this experiment. Three main stock solutions of ESAW were made: 100% ESAW, 10% of the Ca ESAW and 5% of the Ca ESAW. In addition, different cations were added, and all the different ESAW are presented in Table 4. $CaCl_2*2H_2O$ was added in various amounts (100%, 10% and 5% of the amount in the recipe). The cations were added by making particular stock solutions. All major nutrients and stock solutions are added as 1 mL /L final medium. When dH_2O is listed, it is distilled water, produced by the Department of Chemistry at the University of Oslo.

In the first generation of the first experiment, the 25-fold concentration of the added cations was only added to the Ca normal. In the last experiment, the 40-fold concentrations were added since the algae seemed to be able to handle the 35-fold concentration.

Table 4: Overview of the different saltwater compositions. The grey-scaled ones were only added for the last experiment. In the last experiment there were 36 different saltwater solutions in addition to the controls.

	Ca 100%				Ca 10%				Ca 5%			
Fe-concentration	25	30	35	40	25	30	35	40	25	30	35	40
Mg-concentration	2.5	3.0	3.5	4.0	2.5	3.0	3.5	4.0	2.5	3.0	3.5	4.0
Mn-concentration	25	30	35	40	25	30	35	40	25	30	35	40

Apart from the elements listed above, no other changes were made to the seawater composition.

The extra elements were added in separate stock solutions directly to the 40 mL culturing flasks. The stock solutions are listed in Table 5.

Table 5: The recipe for the different stock solutions for the added cations. These compounds were added to the ESAW solution that did not contain Ca.

Cation stock solution	g/ 2 dL stock solution
Fe stock solution	
Na2EDTA 2H2O	0,51358
FeSO4*(NH4)2SO4+6H2O	0,488
Mg stock solution	
MgCl2-6H2O	9,592
Mn stock solution	
MnSO4 4H2O	0,0409
Na2EDTA 2H2O	0,0406

The amounts added of the stock solution to give 25-, 30-, 35-, and 40-fold concentrations are given in Table 6. An exception is Mg, which was added with 2.5-, 3.0-, 3.5-, and 4.0-fold concentrations since there is already much Mg in the ESAW receipt. The Mg-stock solutions were made so that the same volumes of the stock solution could be added to 40 mL culturing flasks.

Table 6: The stock solutions were made in such a way that the added amount of stock solution would give the right concentration in 40 mL flasks.

	Stock solution added to 40 mL flasks
25 x	1,00
30 x	1,20
35 x	1,40
40 x	1,60

Below is a list of all the chemicals that were used in the experiment with their CAS-number, batch number and product number. This list also includes Lugol's solution that was used to prepare algae samples for counting.

Table 7: Overview of all the compounds used in the experiment, the provider, purity, CAS-number, product number, and the batch number.

Name of compound	Chemical composition	provider	purity	CAS	Batchnumber	Product number
MilliQ (dH2O) water	H2O	Department of Chemistry		7732-18-5		produced at the dep.
Sodium chloride	NaCl	BDH Laboratory Supplies	≥99.5%	7647-14-5	K27736133 020	RC-093
Sodium sulfate	Na2O4S	Sigma-Aldrich	≥99.0	7757-82-6	SLBK5317V	HYPE60108-759
Potassium chloride	ClK	Sigma-Aldrich	≥99.5	7447-40-7	BCBN7909V	1.01203.0500
Sodium bicarbonate	CHNaO3	Sigma-Aldrich	99.5	144-55-8	SLBK7385V	L1703
Potassium Bromide	BrK	Sigma-Aldrich	≥99	7758 - 02-3	SZBE1130V	VARIHARRICK-KBR100
Boric acid	H3BO3	Sigma-Aldrich	≥99.5	10043-35-3	BCBM0702V	1.70307.0100
Sodium Fluoride	NaF	Sigma-Aldrich	99.99%	7681-49-4		1.06450.0025
Magnesium chloride hexahydrate	Cl2Mg*6H2O	Sigma-Aldrich	≥99.0	7791-18-6	BCBM9269V	25108.260
Calcium chloride hexahydrate	CaCl2*6H2O	Sigma-Aldrich	≥99.0	7774-34-7	BCBM9173V	1.02382.0250
Strontium chloride hexahydrate	SrCl2*6H2O	Hopkin & Williams LTD		10025-70-4	2834/6	1.07865.0250
Sodium nitrate	NNaO3	Sigma-Aldrich	≥99.0	7631-99-4	BCBP1318V	1.06537.1000
Sodium phosphate monobasic monohydrate	H2NaO4P*H2O	Sigma-Aldrich	≥99.5	1049-21-5	BCBN4588V	1.06346.1000
Silicic acid, disodium salt, pentahydrate	Na2SO3Si*5H2O	Sigma-Aldrich	≥95.0	10213-79-3	BCBN7471V	CA11021-334
Ferric chloride	Cl3Fe*6H2O	Sigma-Aldrich	98.0	10025-77-1	BCBM2247V	1.03943.0250
Ferro-Ammonium sulfuricum	FeSO4*(NH4)2SO4+6H2O	Merck's Reagenzien		10045-89-3	53146	3792
Zinc sulfate heptahydrate	ZnSO4 7H2O	J.T. Baker Chemicals		7446-20-0	402264	1.08883.0500
Cobaltous sulfate heptahydrate	CoSO4 7H2O	Merck	≥99%	10026-24-1	409K2796046	CAJT1696-4
Manganese sulfate	MnO4S*H2O	Sigma-Aldrich	≥99	10034-96-5	SLBK6840V	ICN225099, CA97061-880
Dinatriummolybdat	Na2MoO4 *2H2O	Merck	≥99.5%	7631-95-0	1116754	CA97061-880
Natriumselenit	NaSeO3*5H2O	Merck	≥99%	10102-18-8	1153740	CAAA12585-22
Nickel chloride hexahydrate	NiCl2 6H2O	Merck	≥98%	7791-20-0	4154091	CAAA53131-18
Na2EDTA 2H2O	C10H14N2Na2O8 * 2H2O	Sigma-Aldrich	98.5	6381-92-6	SLBF8074V	34549
Na2EDTa 2H2O	C10H14N2Na2O8 * 2H2O	Sigma-Aldrich	98.5	6381-92-6	SLBF8074V	34549
Thimanine hydrocloride	C12H17ClN4OS*HCl	Sigma-Aldrich	≥99	67-03-8	SLBK9699V	47858
Biotin	C10H16N2O3S	Sigma-Aldrich	≥99%	58-85-5	SLBK4624V	B4501
B12	C63H88CoN14O14P	Sigma-Aldrich	≥98%	68-19-9	MKBR6786V	V2876
Lugol's solution	I3K	Department of Biology		12298-68-9		Produced at the dep.

3.2 Algae experiments

All the algae cultures were grown at the Department of Biosciences, University of Oslo. The cultures were grown in a culture room set to operating at 19 ºC, with a light:dark cycle of 12:12. The cultures were shaken regularly (once a day to every second day). The irradiance was 36.85 µmol quanta*$m^{-2}s^{-1}$.

The strains of *P. carterae* and *E. huxleyi* that were used for the experiment were:

Table 8: The species that were used in the experiment, and their origin.

Species	origin	Date	Provider	Number in collection
Pleurochrysis carterae	Moroccan coast	01.09.1983	Roscoff Culture Collection	RCC1402
Emiliania huxleyi	Elle, Oslo Fjord	March 2015	Haakon Liavaag	------

E. huxleyi was obtained at an excursion to the Oslo Fjord made by Haakon Liavaag, a master student at the University of Oslo. The *P. carterae* strain that was used came from Roscoff Culture Collection[95].

3.2.1 Generational experiment

The first experiment consisted of three generations of *P. carterae* and two generations of *E. huxleyi*. The first generation of *P. carterae* was used to check that the cations were not toxic to the algae. The cation concentrations were the same as listed in Table 4, except that the 25-fold concentration was added only to the water with normal Ca-concentration. The cultures were grown for 4 weeks in 40 mL cell culture flasks and *P. carterae* was inspected in light microscope to see that the cells were able to survive. The microscope was set to 40x magnification, and both Bright field and Phase contrast were used.

The second generation of *P. carterae* was grown by transferring 1 mL of culture to the new generations. The first generation of *E. huxleyi* was transferred from normal culture media, 1 mL pr. 40 mL cell culture flask. All the cultures were grown for 4 weeks. The cultures were inspected in light microscope during the experiments. The cultures were counted after three weeks.

The third generation of *P. carterae* and the second generation of *E. huxleyi* were transferred to new flasks, 1 mL pr. 40 mL flask. The cultures were grown for 4 weeks. Samples of the cultures for counting were taken after three weeks.

3.2.2 Manual cell counting

In the first experiment a hemocytometer was used to count algae. 3 mL of culture was taken from the middle of the culture, after shaking it well, and transferred to small 8 mL glasses. 10 µL of Lugol's iodine was added to kill the algae. A pipette was used to insert the algae culture into the counting chambers of the hemocytometer. Cells that were on the edge of the counting chambers were counted when they were to the left and front, but not to the right and below. The volume for the hemocytometer in this experiment was 3.2 µL. In order to find the population density for the entire cell culture (cells/mL) the the counted cells must be multiplied with (1000/3.2).

3.2.3 The repeated experiment

The second experiment was performed in slightly different manner. Instead of running generations of algae, the experiment was set up once, with doubles. In addition, a higher concentration (40-fold) of the cations was added. The species were acclimated to the new environment by growing cultures in a cation concentration with 25 times the normal levels of Ca for three weeks. All the cultures were transferred from these initial acclimation cultures. To get a more accurate idea of how the algae populations would react to the different ESAW, the transfer volume was calculated so that each culture would start with approximately 100 000 cells each.

During this experiment, the cultures were counted every 3rd or 4th day using CASY®. The cultures were grown for three weeks.

pH was measured before the experiment started, and after three weeks.

3.2.4 Cell counting by CASY®

The cultures to be counted were prepared by shaking the culture, then extracting a small volume from the middle of the culture. The higher the expected population density would be, the smaller volume of the cell culture would be needed. To get enough volume to run through the cell counter, the culture was diluted with CASY Ton so that the counting volume was always 5 mL. 400 µL from each of the prepared cultures were counted 3 times to get the average.

For *E. huxleyi* cells between 2-10 µm were counted. For *P. carterae* cells between 10-30 µm were counted. This means that cells outside of this size range would not be counted.

3.2.5 Extracting the coccoliths

Preparation of the SEM samples was done differently in the first and the second experiment. In the generational experiment, all of the culture medium was centrifuged at 15 000 rpm (rounds per minute) for 2 – 3.5 minutes. This resulted in a white pellet in the Eppendorf tubes. The leftover water was removed with a pipette, and water (pH 8.3) was added. This procedure was repeated until the salt concentration was measured to 0 by a refractometer. The salt concentration was measured to be 25-30 ppm before rinsing. The samples were stored in water with a pH of 8.3, with some drops of ethanol to prevent possible bacterial growth.

Due to the lack of coccoliths in the samples from the first experiment, this method was not repeated the second time. The debris on the bottom of the flasks was sucked up by using a pipette, and directly put onto the holder for the SEM or XRD analysis, and then left to dry.

3.2.6 Scanning Electron Microscope

The samples were prepared by pipetting debris (or part of the pellet) onto carbon tape and left to dry. The samples were not coated or sputtered with anything. In the SEM, EDS analysis was taken from two or more coccoliths from each sample by point analysis. Figure 19 shows where on the coccoliths the points were placed. Point analysis was also run outside the coccolith to find the background. The EDS was acquired until the graphs stopped moving, usually between 20 and 30 seconds.

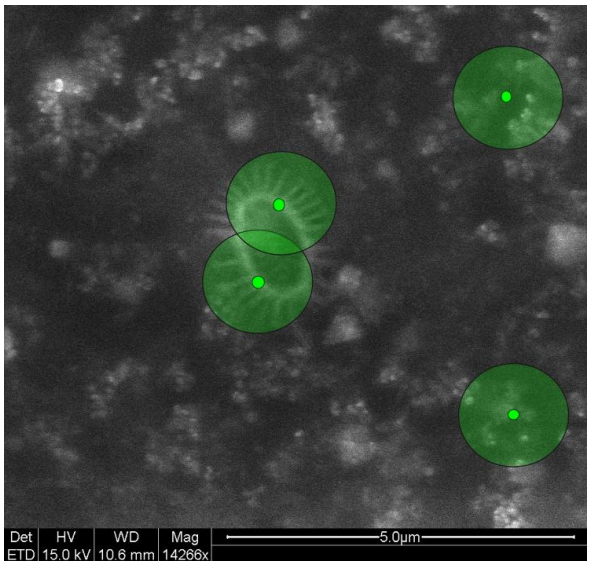

Figure 19: This photo shows approximately how the point analysis was taken at several places on one coccolith. The green circles indicate the sampling area of about 2 µm.

3.2.7 X-ray Diffraction

In addition to the EDS, an XRD analysis was run for the samples of interest. From the first experiment the pellets were pipetted on the sample holder and dried before running the XRD. In samples from the second experiment, the debris on the bottom of the 40 mL cell culturing flasks was pipetted on the sample holder and dried before running the XRD.

The instrument that was used was an D8 Discover, with a Kα1 radiation selected by a Ge (111) Johansen Monochromator with a Lynxeye detector and a 90-position sample changer. Powder X-ray Diffraction data were collected in a 2θ range of 10-70 degree with a count time of 0.7 seconds/step and a step size of 0.02 degree, with a wavelength λ 1.54060.

The program EVA 4.0 was used for the analysis with phase identification from the Powder Diffraction File 2 (PDF2) and Crystallography Open Database (COD).

The samples were compared to a standard of pure calcite in Table 9:

Table 9: CAS-number, provider, purity, and product number of the calcite that was used as a reference for the XRD measurements.

Compound name	Chemical formula	provider	purity	CAS number	Batch number	Product number
calcite	$CaCO_3$	Fluka	≥ 99%	13397-26-7	379884	F21060

3.3 Equipment used for the experiment

Equipment used throughout the project is listed in Table 10, and analytical tools are listed in Table 11.

Table 10: Equipment used throughout both the experiments, with provider and product number.

Equipment	Provider	Product number
Plastic can for storing ESAW	The Department of Chemistry	
Glass bottles	The Department of Chemistry	
pipettes	Saarstedt	86.1171
Erlenmeyer flasks (glass)	The Department of Chemistry	
40 mL flasks for cell culturing	Thermo Scientific	Nunclon delta surface: 156367
40 mL flasks for cell culturing	Saarstedt	TC Flask T25 Standard
Specimen mounts in aluminum	Ted Pella Inc.	16111
Carbon adhesive tabs	Agar Scientific	G3347N
Carbon adhesive tabs	Chemi-Teknin AS	77825-09
XRD sample holders	The Department of Chemistry	

Table 11: A list of all the analytical tools used in the project with provider and product number.

Instrument	Provider	Product number or model
Weight 1	Metler Toledo	AT261 DeltaRange®
Weight 2	Sartorius AG	CP423S
pH-meter	Radiometer Copenhagen	phm 92 Lab pH meter
CASY® Cell Counter	Roche Innovatis AG	Model TT
Hemocytometer	Fuchs Rosenthal	Assistent
Refractometer	Atago	S/Mill
Light microscope 1	Nicon Eclipse	TS100
Light microscope 2	Leica Microsystems	Leica DMLS: 11 020 518 102
SEM	FEI	FEI Quanta 200 FEG-ESEM
XRD	Bruker	D8 Discover
Sentrifuge	Eppendorf	Centrifuge 5424R
Light datalogger	LI-COR	LI-1000

4 Results

The results from the experiment are presented in this chapter. The first part of the chapter will present the data from the algae cultures, before moving on to the results from the analysis from SEM and XRD.

4.1 Cell culturing

In the first experiment, described in section 3.2.1, the first generation of *P. carterae* was inspected in light microscope to see if the different ESAW compositions were affecting the cells. The visible differences are given in Table 12. After 21 days, the following observations given in Table 13, were made for the same cultures.

Table 12: Observations of *Pleurochrysis carterae* after 4 days in culture, generational experiment.

	Observation for *Pleurochrysis carterae* after 4 days
Control	All cultures lived and seemed to be doing well.
Fe	Living cells in all cultures, but also a lot of bacteria.
Mg	Culture with the lowest level of Mg were doing good, the remaining cultures contained a lot of bacteria. The cultures with Ca 5%-Mg3.5 contained cells with some deformations.
Mn	All cells lived and seemed to be doing well.

Table 13: Observations of *Pleurochrysis carterae* after 21 days in culture, first experiment.

	Observations of *Pleurochrysis carterae* after 21 days
Control	All cultures lived and seemed to be doing well.
Fe	The higher the concentration of Fe, the more dead cells and bacteria was observed. Some of the cells in the highest Fe concentrations and lower Ca concentrations seem to be clumped together. However, there were living cells in all of the cultures.
Mg	The cultures with normal Ca concentrations were doing well, regardless of amount of Mg. The lower the Ca concentrations the more the cells seem to be clumped together. There were also some bacteria, but not as much as in the Fe-containing cultures. All cultures contained living cells.
Mn	The cultures with normal Ca concentrations were doing well, but the lower the Ca concentration the more the cells clumped together. All cultures contained living cells.

These observations indicate that the ESAW affected the coccolithophores, but it did not kill them. Therefore, the coccolithophores were counted in order to get a better overview. The method is described in 3.2.2. The results of counting the first generation cultures after two weeks for *P. carterae*, are presented in Table 14, and three weeks for the first generation *E. huxleyi*, are presented in Table 15. The variations between the different ESAW are worth noticing. *P. carterae*-cultures with low-Ca seem to struggle. The cultures with a higher content of Mn seem to be doing better. For *E. huxleyi* it seems that the ESAW with the highest added cation concentrations are struggling, except for the Fe-enriched cultures.

Table 14: The results from counting the first cultures of *Pleurochrysis carterae* after 15 days. The numbers represent the cells counted, not the entire population in the culture. The culture population can be found by the following formula = (counted cells/3.2)*1000. The samples of most interest were counted.

	Ca 100%	Ca 10%	Ca 5%
Control	337		
Fe 25	182	135	39
Fe 30		48	55
Fe 35		36	70
Mg 2.5	319	74	82
Mg 3.0		14	14
Mg 3.5		39	11
Mn 25	472	282	190
Mn 30		274	148
Mn 35		305	114

Table 15: The results from counting *Emiliania huxleyi* after 21 days in culture. The numbers represent the cells counted, not the entire population in the culture. The culture population can be found by the following formula = (counted cells/3.2)*1000. The samples of most interest were counted.

	Ca 100%	Ca 10%	Ca 5%
Control	517		
Fe 25	994	646	2032
Fe 30		897	688
Fe 35		1572	541
Mg 2.5	728	736	674
Mg 3.0		1030	980
Mg 3.5		92	36
Mn 25	549	363	468
Mn 30		260	477
Mn 35		323	398

All the cultures of the generational experiment were counted, but because the population density was not accounted for when the cultures were transferred, the cell counts for the following generations are not reliable. They are therefore not taken into consideration. It seems, however, that the two species were able to cope with the different ESAW compositions. All the cultures were rinsed according to the method described in 3.2.5.

All the cultures from the generational experiment were examined in an SEM. Very few coccoliths were found, even though many coccoliths had been observed in light microscope,

indicating that something was wrong with the preparation. In order to check that it was not the ESAW in itself, the pH in the water was measured before repeating the experiment. The pH was measured both before starting the experiment, and after 21 days. Figure 20 shows the evolution in the pH after 21 days for both *E. huxleyi* and *P. carterae* with all the different ESAW with Ca 100%. The ESAW with Ca 10% and 5% have similar results, and can be found in Appendix B.

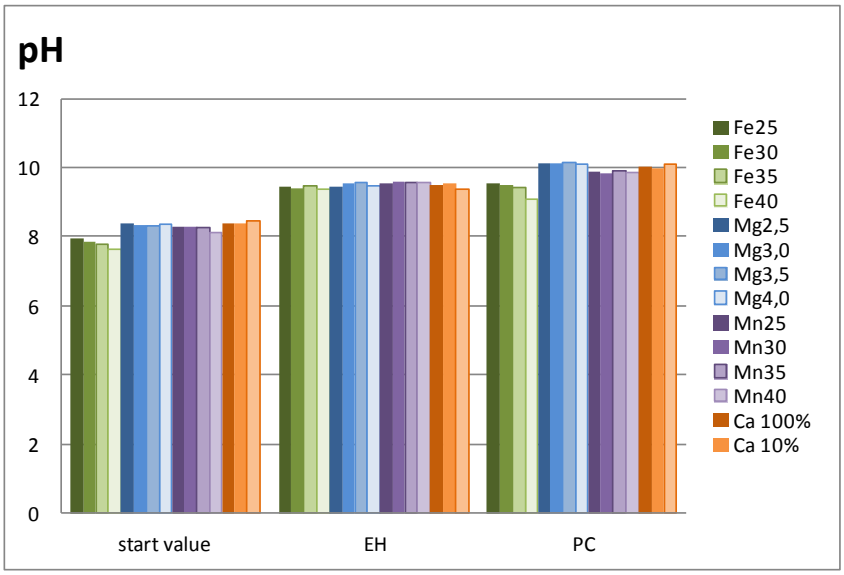

Figure 20: pH-evolution in *Emiliania huxleyi* (EH) and *Pleurochrysis carterae* (PC) with Ca 100%. The pH was measured before adding cells, and after 21 days in culture.

To keep a closer look at how the ESAW could affect the algae, the cultures were counted during the growth period. An automatic cell counter was used in order to have time to count all the cultures. Two examples of growth curves are given on the following page, where both are from *P. carterae* cultures. They show a typical evolution that follows a sigmoid path.

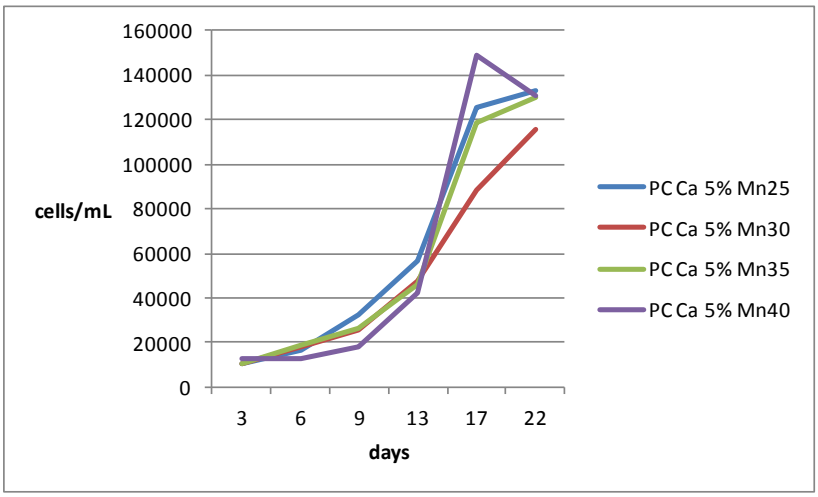

Figure 21: *Pleurochrysis carterae* (PC) growth from the last experiment, 21 days. These graphs follow the sigmoid growth curves that are often expected. ESAW contains Ca 5% and, Mn varies from 25x to 40x.

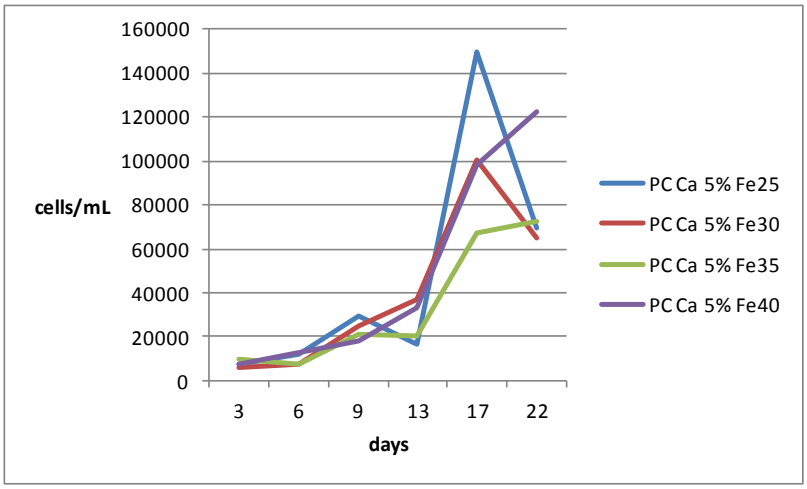

Figure 22: *Pleurochrysis carterae* (PC) growth curve from the last experiment, 21 days. The graph illustrates what the growth curve often looked like in the experiment. ESAW contains Ca 5% and Fe varies from 25x to 40x.

In Figure 22, one of the curves has a drop in the population density before it grows exponentially and drops at the end of the experiment. The population density can vary a bit, so some of this can be explained by natural variation. These variations are discussed in Chapter 5. Although the population follows the same growth curve, the resulting population densities varied greatly as shown in Figure 23 and Figure 24.

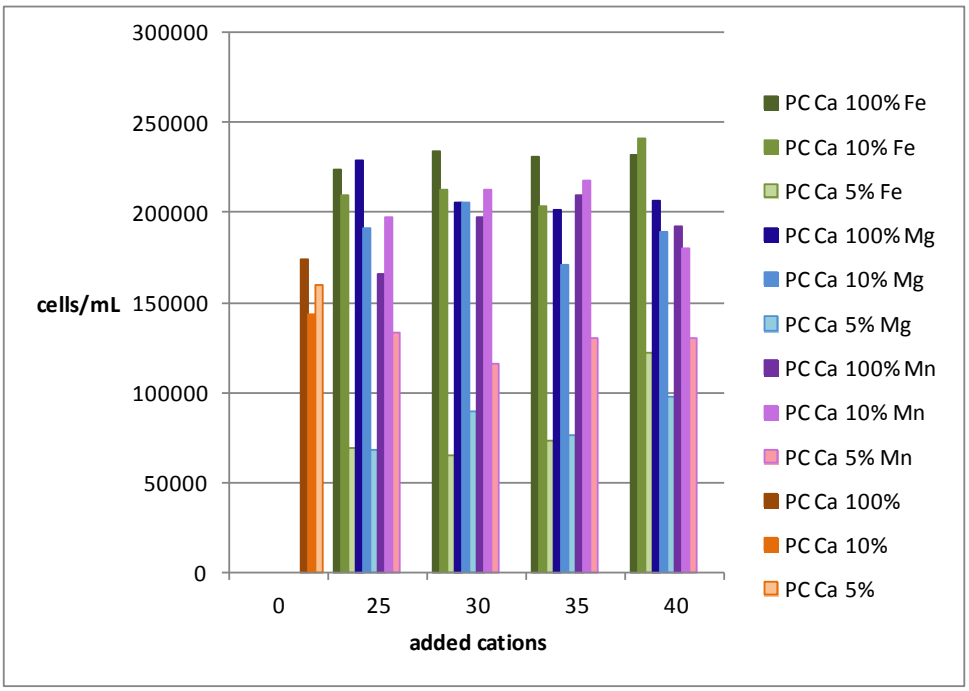

Figure 23: *Pleurochrysis carterae* (PC) growth after 21 days, last experiment. Note that the different ESAW has an impact. All the cultures started with the same number of cells/mL. The numbers displayed are number of cells/mL, and not the entire culture. Along the x-axis are the concentrations of the added cations. Mg is only added as 2.5, 3.0, 3.5 and 4.0 times as the normal concentrations, but is displayed here as 25, 30, 35, and 40 to make it easier to compare. The 0-columns are the controls with different Ca-concentrations.

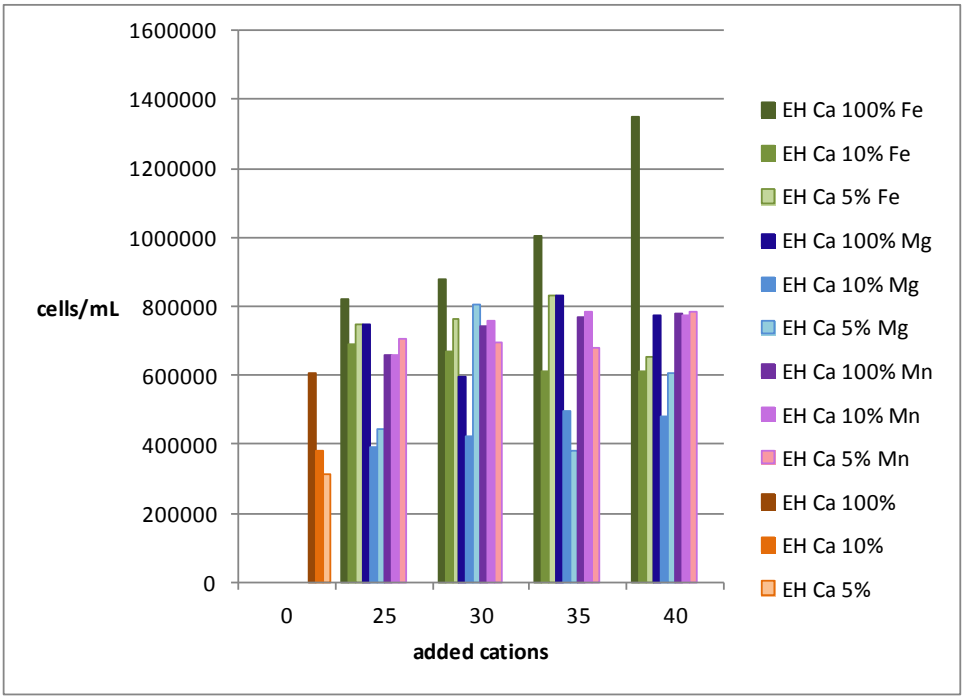

Figure 24: *Emiliania huxleyi* (EH) growth after 21 days, last experiment. Note that the different ESAW has an impact. All the cultures started with the same number of cells/mL. The numbers displayed are cells/mL, and not the entire culture. Along the x-axis are the concentrations of the added cations. Mg is only added as 2.5, 3.0, 3.5 and 4.0 times as the normal concentrations, but is displayed here as 25, 30, 35, and 40 to make it easier to compare. The 0-columns are the controls with different Ca-concentrations.

CASY® also gives the average cell size, and it is worth noticing that this varies according to different ESAW composition. The variations for *P. carterae* are given in Figure 25 and Figure 26, and the variations for *E. huxleyi* are given in Figure 27 and Figure 28.

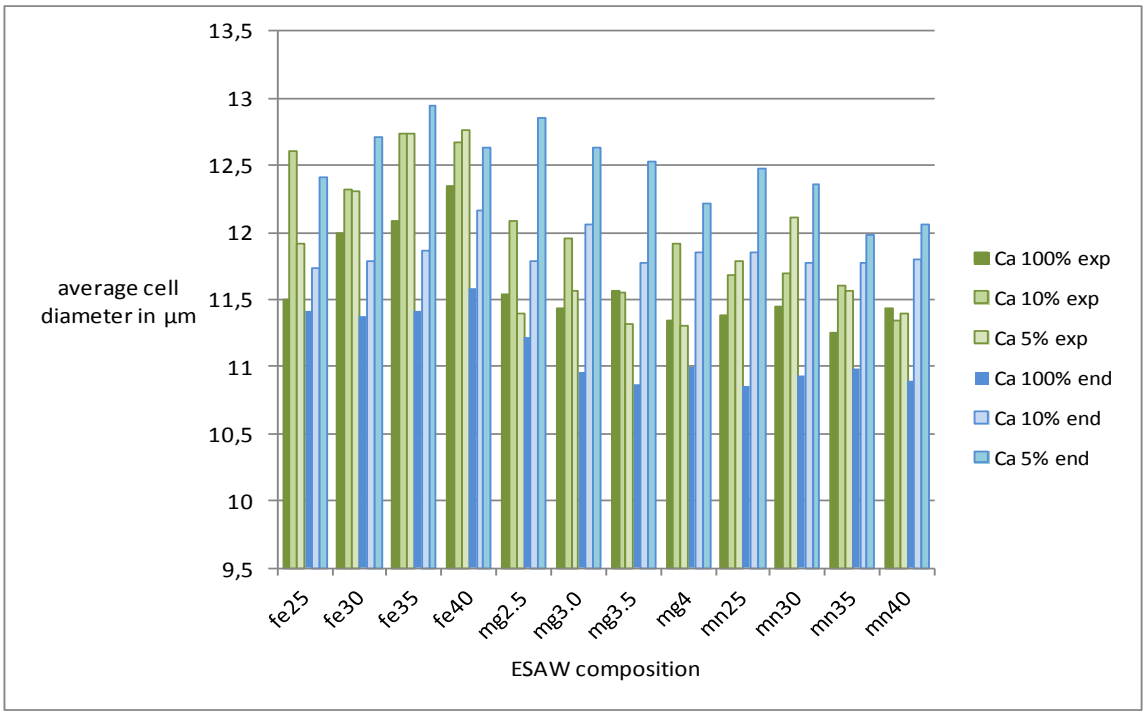

Figure 25: *Pleurochrysis carterae* average cell size in the exponential growth phase (exp, 17 days) and in the end of the experiment (21 days). The cell sizes vary considerably, but they seem to be the largest after 21 days. It also seems that the cells are larger the less Ca the water contains.

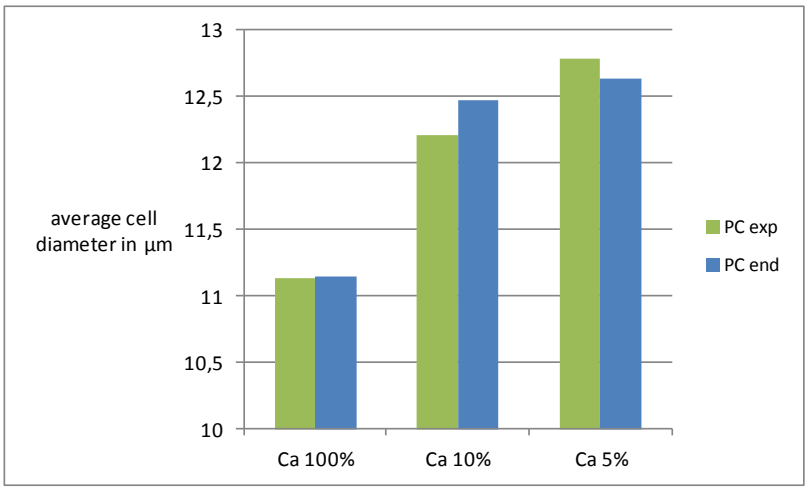

Figure 26: *Pleurochrysis carterae* (PC) average cell size in the controls in the exponential growth (17 days) and in the end of the experiment (21 days). It seems that the cells are larger with less Ca.

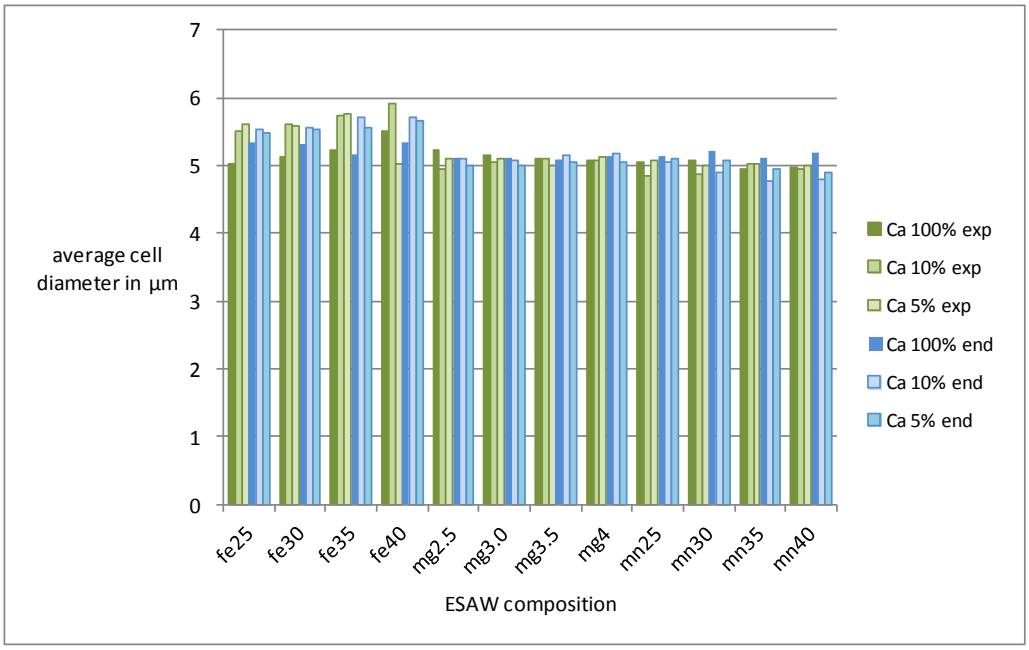

Figure 27: *Emiliania huxleyi* average cell size for all ESAW in the exponential growth phase (17 days) and in the end of the experiment (21) days. It seems that Fe-enriched ESAW has the largest effect on the cell size on *Emiliania huxleyi.*

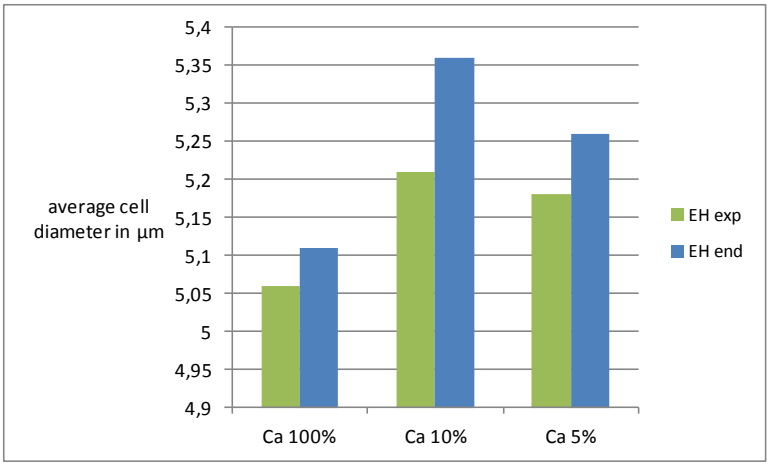

Figure 28: *Emiliania huxleyi* (EH) average cell size in the controls in the exponential growth phase (17 days) and in the end of the experiment (21 days). It seems that less Ca tend to give larger cells.

It seems that the ESAW composition affect both how fast the population grows and the cell size. In *P. carterae* it seems like the population growth is affected by the lowest Ca-concentrations. Both low Ca-concentrations and Fe-enriched ESAW seems to make the cells larger. In *E. huxleyi* the low Ca-concentrations affect the population growth in the controls, but do not seem to affect the other ESAW compositions as much. *E. huxleyi* has the highest population in the Fe-enriched ESAW. The Fe-enriched ESAW also seems to make the *E. huxleyi* cells larger. In the cation enriched ESAW compositions *E. huxleyi* cells are larger with the high-Ca, but in the controls it is the opposite.

4.2 The results from the SEM

After performing the growth cycles, samples were prepared for SEM analysis showing formation of coccoliths in most of the experiments. Table 16 and Table 17 below show which cultures where coccoliths were present in the SEM analysis.

Table 16: Overview of the *Emiliania huxleyi* where coccoliths were found in the SEM, repeated experiment. C: coccoliths, NC: No coccoliths.

	Ca 100%	Ca 10%	Ca 5%
Fe 25	NC	NC	NC
Fe 30	NC	NC	NC
Fe 35	NC	NC	NC
Fe 40	NC	NC	NC
Mg 2,5	a lot of C	few C	few C, deformed
Mg 3,0	a lot of C	few C	few C, deformed
Mg 3,5	a lot of C	few C	few C
Mg 4,0	a lot of C	few C	few C, deformed
Mn 25	few C	few C	NC
Mn 30	few C	few C	NC
Mn 35	few C	few C	NC
Mn 40	some C	few C	NC

Table 17: Overview of the *Pleurochrysis carterae* where coccoliths were found in the SEM, repeated experiment. C: coccoliths, NC: No coccoliths.

	Ca 100%	Ca 10%	Ca 5%
Fe 25	a lot of C	some C	NC
Fe 30	a lot of C	NC	NC
Fe 35	a lot of C	NC	NC
Fe 40	a lot of C	NC	NC
Mg 2,5	some C	some C	some C
Mg 3,0	some C	some C	few C, deformed
Mg 3,5	some C	a lot of C	few C
Mg 4,0	some C	a lot of C	few C
Mn 25	a lot of C	some C	some C
Mn 30	some C	few C	some C
Mn 35	some C	some C	few C
Mn 40	some C	some C	few C

For all the samples where coccoliths were found, a full frame EDS-analysis was taken in addition to two (or more) point analyses of the coccoliths and two (or more) point analyses outside the coccolith.

How the coccoliths were appeatred varied throughout the samples. Observation of only few coccoliths mostly meant that they were somehow damaged. To illustrate the difference a nicely shaped and a damaged coccolith, from both species are presented below. It is possible to see the calcified outer rim in the well shaped *E. huxleyi* coccolith in Figure 29. In comparison, the coccolith in Figure 30, looks misshaped and seems to lack the outer rim.

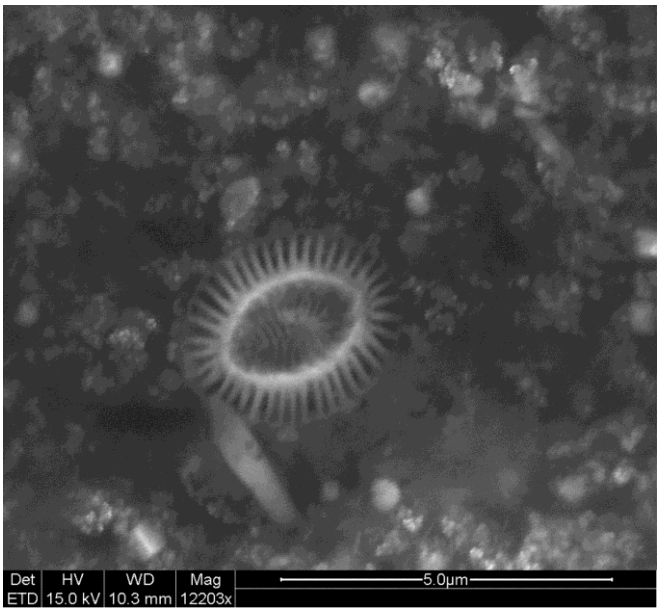

Figure 29: Full coccolith of *Emiliania huxleyi*, repeated experiment. This coccolith is from the ESAW Ca 100%-Mg 3.0.

Figure 30: Example of a damaged coccolith from *Emiliania huxleyi*, repeated experiment. The coccolith is from the ESAW Ca 10%-Mg2.5.

An example of well shaped coccoliths in *P. carterae* can be seen in Figure 31. In comparison, the *P. carterae* coccoliths in Figure 32 seem fragile and damaged.

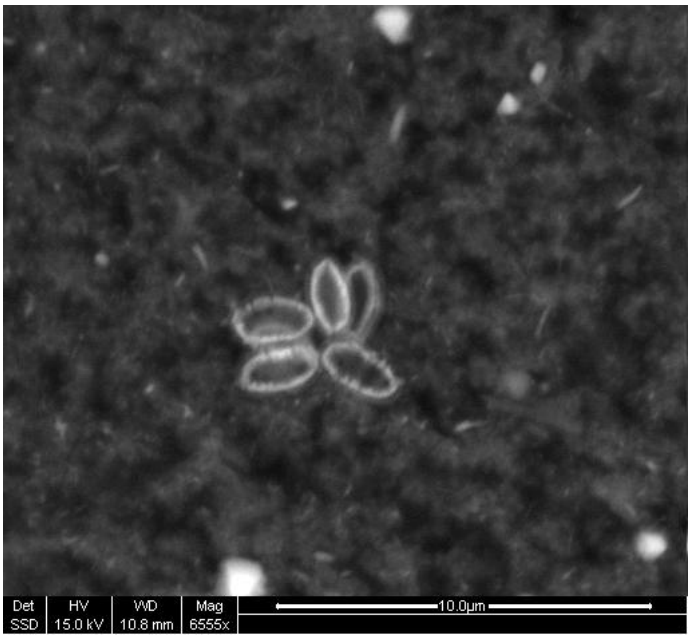

Figure 31: Full coccoliths of *Pleurochrysis carterae*, last experiment. This coccolith is from ESAW Ca control (no added cations). NB! The scale bar on this picture is 10 µm, whereas most of the others are 5 µm.

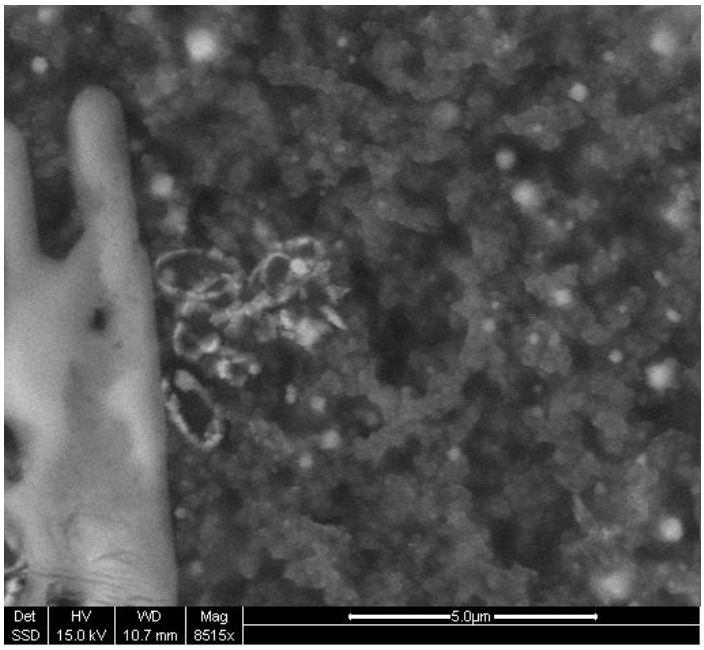

Figure 32: Example of damaged coccoliths from *Pleurochrysis carterae*, last experiment. The coccoliths are from the ESAW Ca 5% (no added cations).

At first glance the last experiments gave a lot of coccoliths to be investigated. The EDS analysis of these samples also seemeed promissing. Table 18 below displays the percentages of Mg in coccoliths from different ESAW, compared to Ca. This percentage is in atomic weigth. The cultures that were chosen for further study in XRD were chosen because of high Mg-content, longer reading time (more reliable data), and many coccoliths.

Table 18: Overview of the percentage of Mg found in point analysis of coccoliths in relation to Ca. These numbers are based on the point analysis with the longest running time, but for some of the coccoliths the number of counts was too low. It is surprisingly high percentage of Mg in the coccoliths, even from ESAW solutions that have normal Mg concentrations. The numbers vary considerably, and there does not seem to be a trend. When two (or more) coccoliths could be found, then two analyses were made, if there were more than two the two highest Mg-percentages were chosen. Finding more than two spots with coccoliths was not always possible, thus some cultures only have one measurement. *Emiliania huxleyi* (EH) and *Pleurochrysis carterae* (PC) both seem to struggle with Fe.

	Ca control		Ca 10%		Ca 5%	
Ca norm	EH	PC	EH	PC	EH	PC
Fe 25		23,4 %				
		43,6 %				
Fe 30		41,7 %				
		37,0 %				
Fe 35		12,2 %				
Fe 40						
Mg 2,5	32,1 %	35,1 %	18,1 %	15,9 %	25,9 %	41,0 %
	16,9 %		10,2 %	33,2 %	23,7 %	42,6 %
Mg 3,0	18,2 %	19,3 %	41,8 %	19,0 %	29,4 %	56,4 %
			13,0 %	10,2 %	23,6 %	13,4 %
Mg 3,5	25,5 %	41,7 %	22,6 %	13,2 %	22,1 %	12,4 %
		13,7 %	54,1 %	30,3 %	19,6 %	18,9 %
Mg 4,0	12,8 %	21,6 %	19,2 %	51,9 %	37,9 %	33,5 %
		31,0 %	13,9 %		52,7 %	44,6 %
Mn 25	11,7 %			26,1 %	23,4 %	14,8 %
	9,3 %	29,4 %		39,4 %	43,6 %	
Mn 30	24,0 %	25,4 %		28,8 %	41,7 %	62,2 %
	50,9 %	17,1 %		23,4 %	37,0 %	
Mn 35	22,0 %	12,5 %		17,9 %	12,2 %	23,5 %
	23,0 %	13,7 %		9,2 %		
Mn 40	61,5 %	33,7 %		13,6 %	47,9 %	10,9 %
	40,1 %				57,2 %	

These results seem promising, however, when we look at the EDS analysis, the elements Na and Mg are very close. This is demonstrated in Figure 33. Knowing that there is a lot of NaCl in seawater, it is to be expected to find these elements in the sample. In Figure 34, there appears to be a lot of Cl in the sample, but no sign of Na. Instead, there is rather much Mg, more than Ca. The EDS can have counted Na as Mg.

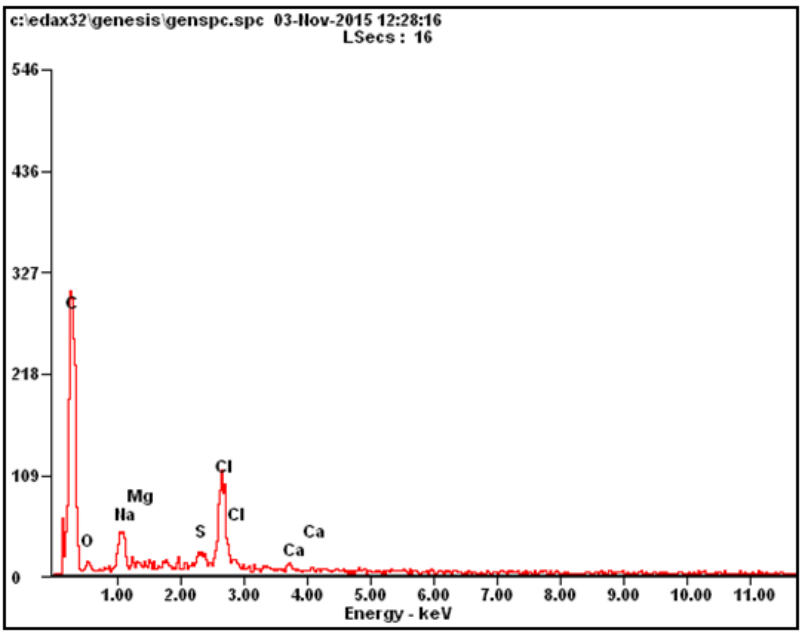

Figure 33: Example of measurement with insufficient count rate and overlap between Na and Mg. This point analysis was kept very short, and is therefore not part of the dataset, but is just shown here as an example.

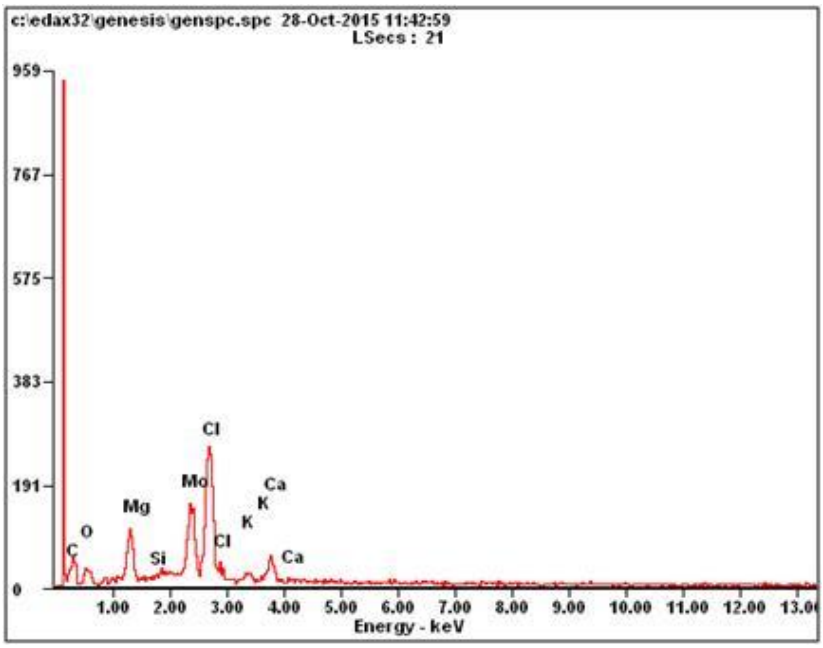

Figure 34: Point analysis of coccolith from *Pleurochrysis carterae*, last experiment. ESAW had Ca 10% (no added cations). In this sample there is no Na displayed, but still a lot of Cl. It is not likely that this sample does not contain Na, so this figure illustrates how the EDS may count elements.

4.3 Results from X-ray Diffraction

The samples that had a high content of Mg from the EDS analysis were chosen for further analysis with the XRD. In addition, samples with high Mg, low Ca from the generational experiment, and Mg-samples from the second experiment, were analyzed.

An empty, clean, sample holder, was analyzed as a reference. The result can be found in Appendix D. A list with an overview of all the reflections for all the samples that have been analyzed can be found in Appendix D. ESAW and pure calcite were also analyzed for comparison with the sample.

Some reflections deserve a closer look. The highest intensity reflections (d_{104} and d_{113}), and selected reflections at higher angles (such as d_{211}) are of particular interest. All the indicated reflections have been listed in Table 19 and Table 20, in the end of the chapter with the calculated Mg-content, given by Vegard'slaw.

The XRD analysis can provide many different types of results, starting with the $CaCO_3$ control and the ESAW (Ca10%). The pure calcite, Figure 35, was compared to the PDF of calcite, vaterite, magnesian calcite, and aragonite in order to safely compare this diffractogram to the results from the coccoliths.

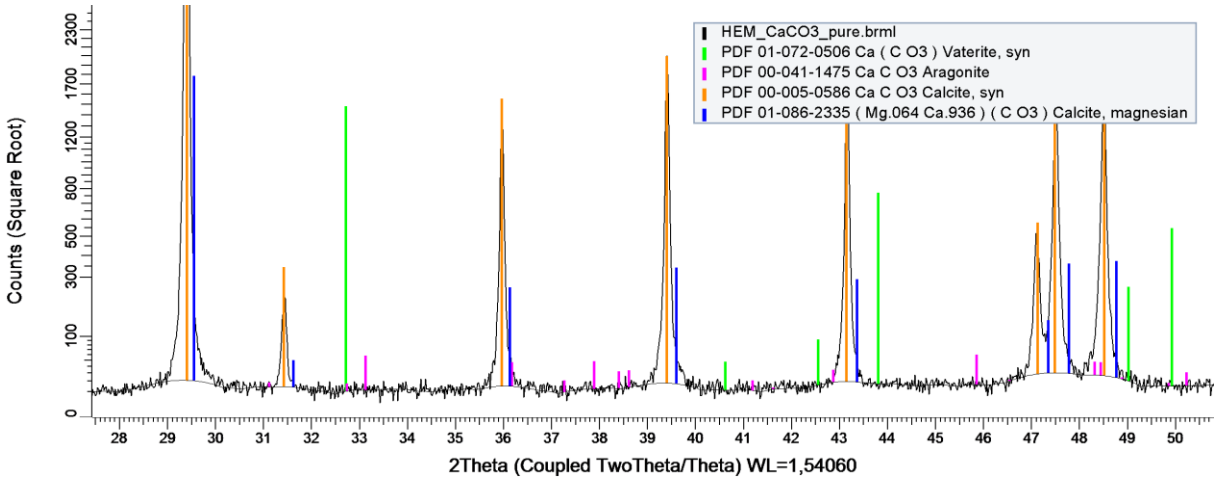

Figure 35: XRD analysis of pure (synthetic) calcite (orange). The phases of the calcite match the reflections in the PDF. In comparison aragonite (pink), vaterite (green) do not match particularly well. Magnesian calcite (blue) has the same reflections, since it adopts the same structure, but is shifted due to the magnesium content.

The control of pure $CaCO_3$ matches the indexed reflection of calcite from the PDF (calcite: PDF-01-083-1762), found in The International Centre for Diffraction Data .

For magnesian calcite, the reflections are shifted slightly to higher angles due to the content of magnesium. The XRD analysis provides results from all individual crystallites in focus, and multiple peaks or broad reflections are expected if the composition of Mg is not evenly distributed throughout the sample. Several phases of magnisan calcite may occur.

The diffractogram for ESAW (Ca10%) is given in Figure 36. It is compared to the calcite (orange) PDF. Notice that there does not seem to be any crystalization without coccolithophores. The most intense reflections are from halite (NaCl), which also matches reflections in PDF (halite PDF-00-005-0628).

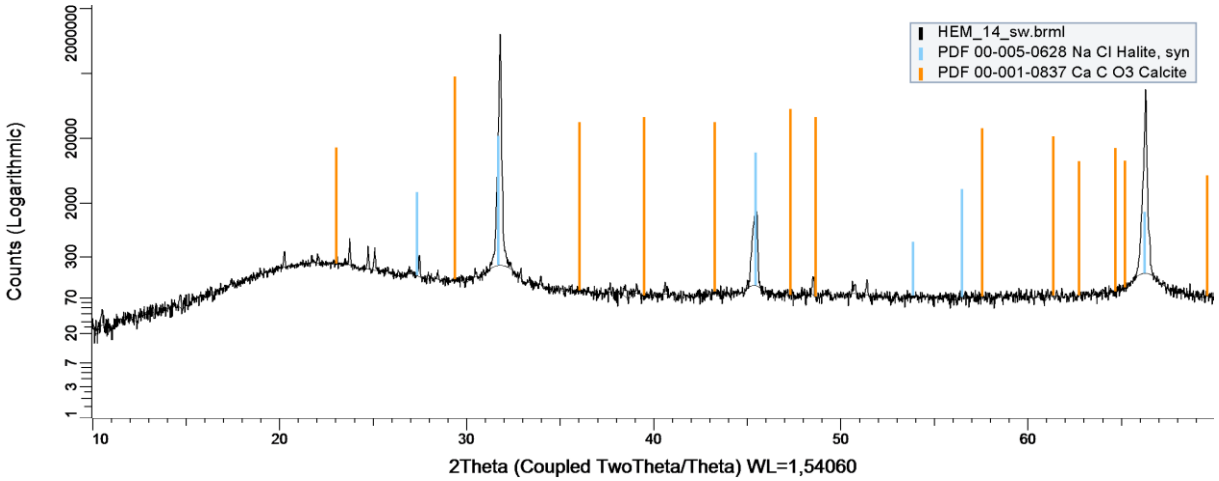

Figure 36: XRD analysis of the ESAW that was used, the Ca concentration was 10% of the normal amount. This analysis helps to rule out which reflections is part of the ESAW. The calcite (orange) structure does not present any strong reflections, neither does magnesian calcite – which lies close to calcite. Halite (light blue) has strong reflections which are useful to know about.

Most of the reflections for ESAW(Ca10%) were identified and can be found in Appendix D.

We can assume that all the reflections that can be found in the ESAW(Ca10%) sample are not relevant since they are not made by coccolithophores. These reflections are therefore considered further in order to focus on the calcite/magnesian calcite reflections. To be sure that the magnesian calcite does not crystalize without the help of coccolithophores, a high Mg ESAW has also been analyzed. The results are given in Figure 37.

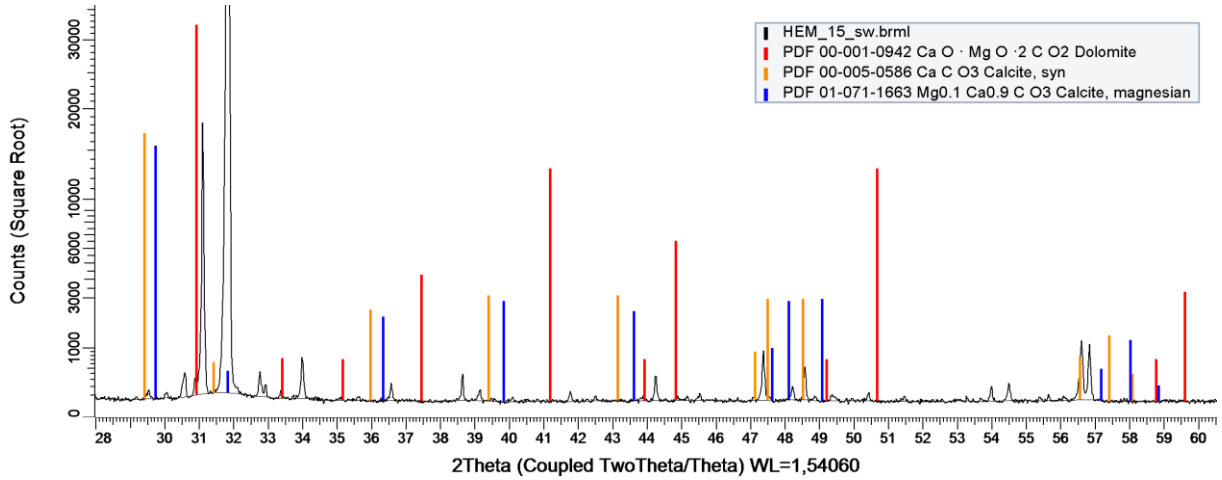

Figure 37: XRD of ESAW with Ca 10%-Mg 3.0. There is some indication of calcite reflections, but also magnesian calcite. One of the most interesting reflections is the dolomite reflection.

There are some reflections in the area where the highest intensity reflections of calcite and magnesian calcite are expected to be. A closer look at the same figure reveals 5 small reflections, Figure 38.

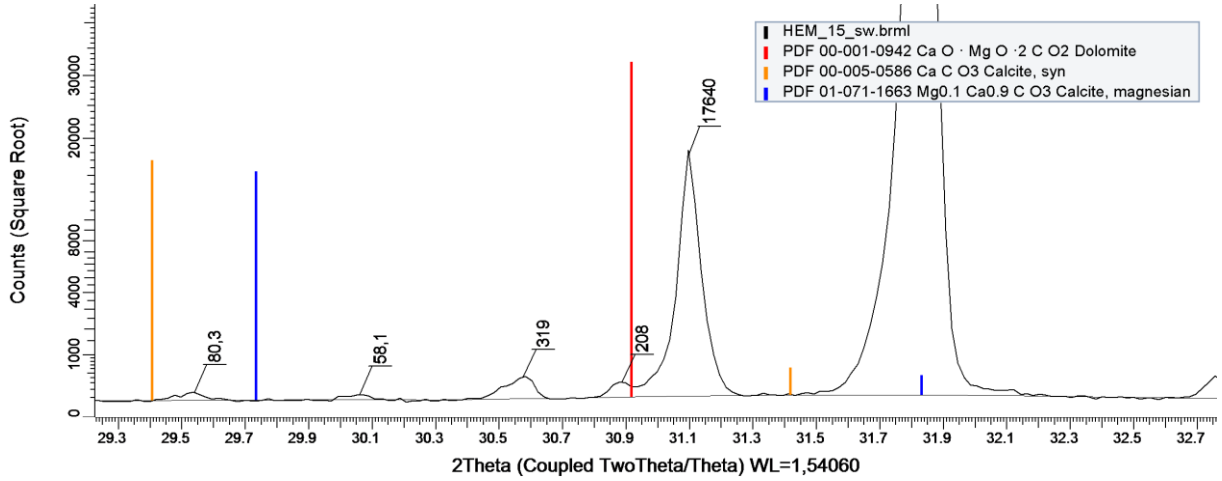

Figure 38: XRD of ESAW with Ca10%, Mg3x. There are reflections in the area 29.4-31.5 where the most intense magnesian calcite reflections are expected to be.

By using the program EVA it is possible to make a shift in the PDF to see if it matches the reflections better. Different shifts of the calcite, magnesian calcite (PDF-01-086-2335), and dolomite (PDF-00-005-0622) are shown in Figure 39.

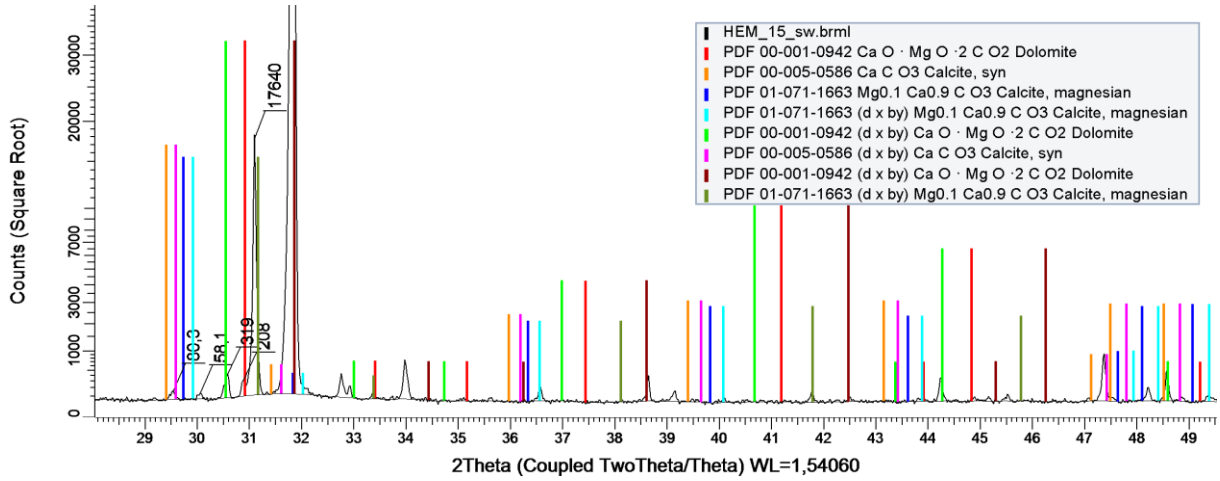

Figure 39: Using EVA to shift the PDF reflections of calcite, magnesian calcite, and dolomite, it is possible to see that that many of the reflections in the ESAW are likely to be shifted reflections of the same phases of these three crystal structures.

XRD analysis of the generational experiment where all the samples were rinsed and centrifuged show sign of calcite and possibly dolomite. The reflections from the calcite phases are slightly shifted towards higher angles. If this shift is due to Mg substitution in the calcite structure, it represents a composition of ca. 0.9% Mg in $CaCO_3$ for the reflections at 2θ = 29.4º, and 27.1% Mg for the reflections at 2θ = 31.2º. The diffractogram is shown in Figure 40, below.

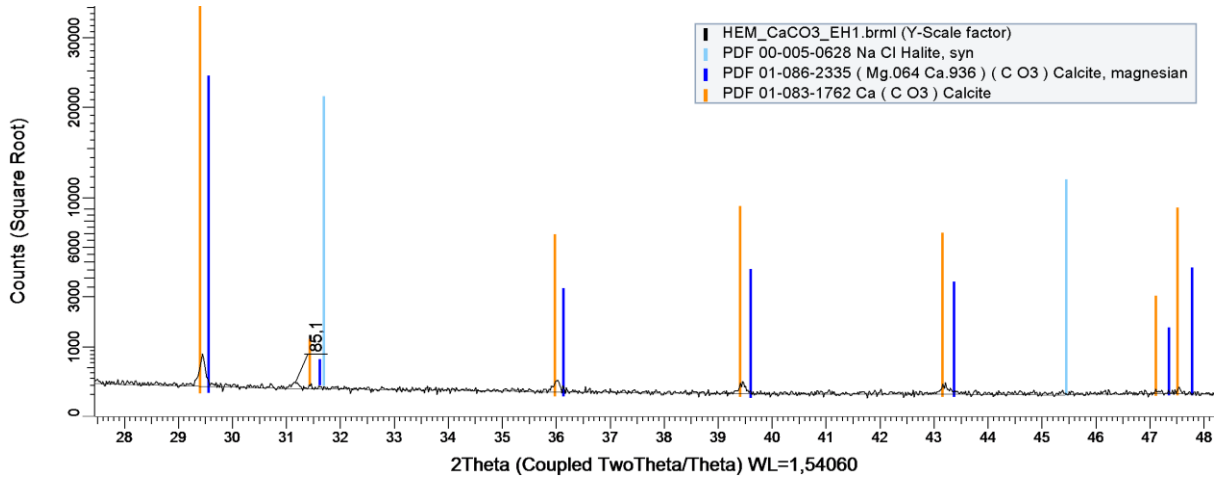

Figure 40: *Emiliania huxleyi* control, generational experiment. The sample has been rinsed and centrifuged. There are signs of calcite (orange), possibly magnesian calcite (blue), but none from halite (NaCl).

Just as for the *E. huxleyi* control, the *P. carterae* control seems to contain calcite, but the reflection at 2θ= 29.4 º seem slightly more shifted indicating a composition of 1.5% Mg in the calcite, see Figure 41.

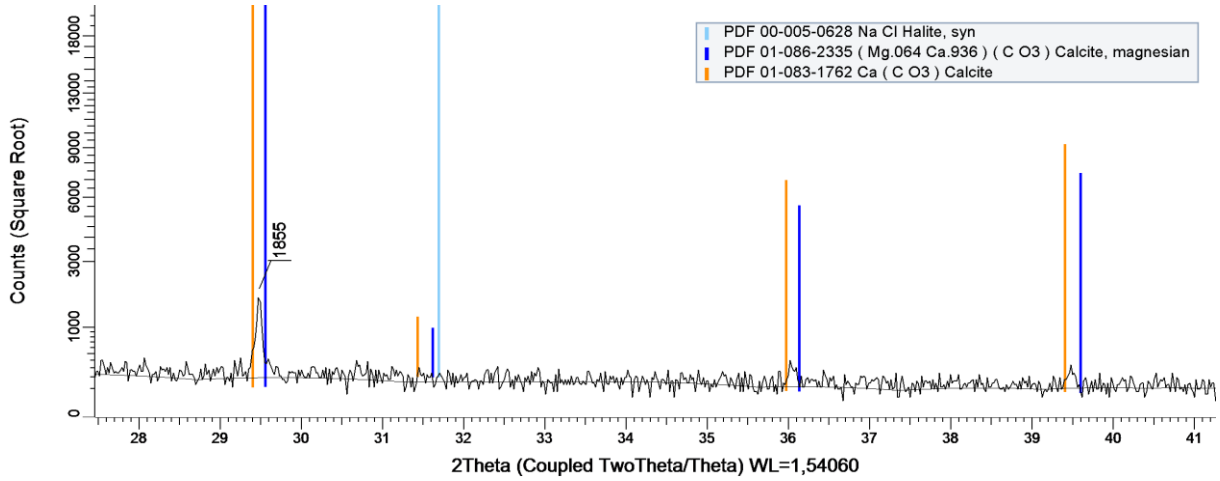

Figure 41: *Pleurochrysis carterae* control, generational experiment, rinsed and centrifuged. Clear calcite (orange) or magnesian calcite (blue) reflections, but no sign of halite (NaCl, light blue). Using Vergard's law the shift in the most intense calcite reflection gives the Mg content of 1.5% in the calcite.

In the repeated experiment, the *E. huxleyi* control has some interesting reflections, Figure 42. The indicated reflections would, according to Vegard's law have a Mg-content of 3.9%, 17.3%, and 25.8%.

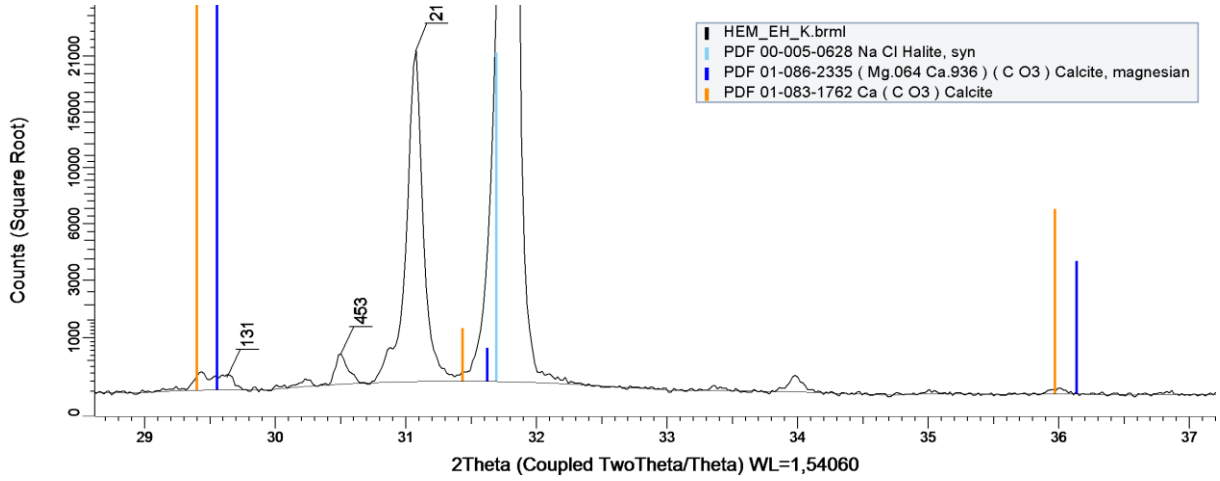

Figure 42: *Emiliania huxleyi* control, repeated experiment. There are several reflections in the area where the high intensity reflections are expected. However, these reflections also match the high Mg-ESAW reflections. Calcite (orange), magnesian calcite (dark blue), and halite (light blue).

Just like for *E. huxleyi*, the calcite reflection for *P. carterae* seems to be shifted towards higher angles, indicating a composition of 1.8 and 26.0% Mg for the indicated reflections, Figure 43.

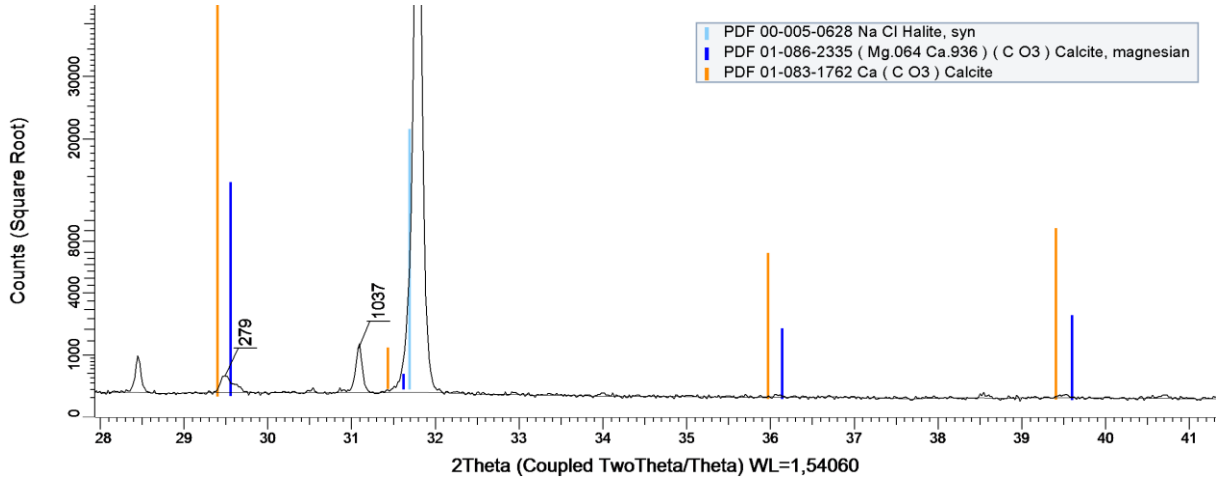

Figure 43: *Pleurochrysis carterae*, control, repeated experiment. Calcite (orange), magnesian calcite (dark blue), and halite (Light blue). The Mg-content in the indicated reflections is 1.8 and 26.0%, according to Vergard's law.

The following figures are from *E. huxleyi* and *P. carterae*, repeated experiment, with changes in the Ca-content. They seem to have the same reflections as the controls. In Figure 44, for *E. huxleyi*, four reflections are indicated. Using Vegard's law the Mg-content in these would be: 3.8, 13.1, 17.5, and 25.6% Mg.

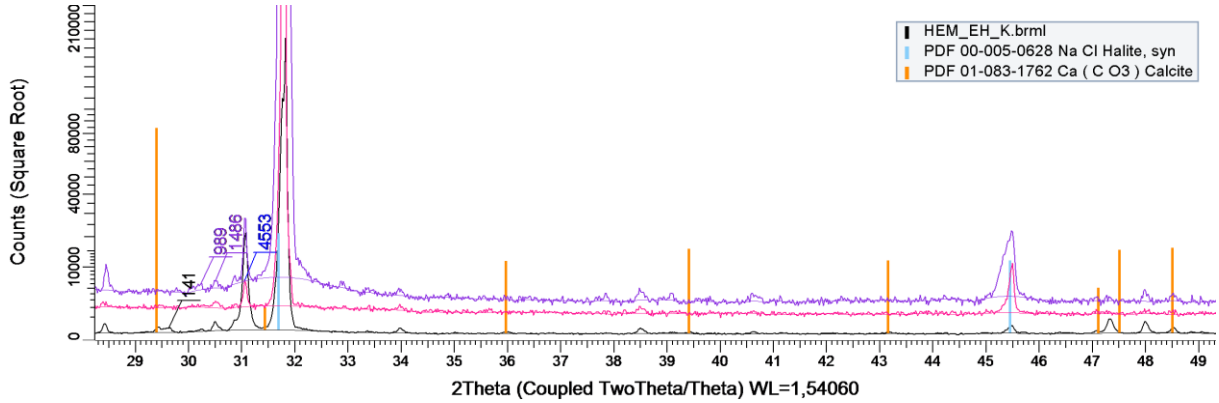

Figure 44: *Emiliania huxleyi*, repeated experiment, control (black), Ca 10% (pink) and Ca 5% (purple). The PDF for calcite (orange), and halite (light blue), are indicated. The reflections that are indicated can possibly be high Mg-reflections and contain the following amount of Mg (from left to right): 3.8, 13.1, 17.5, and 25.6% Mg.

A similar investigation of the same tendensies of *P. carterae* give similar results, see Figure 45.

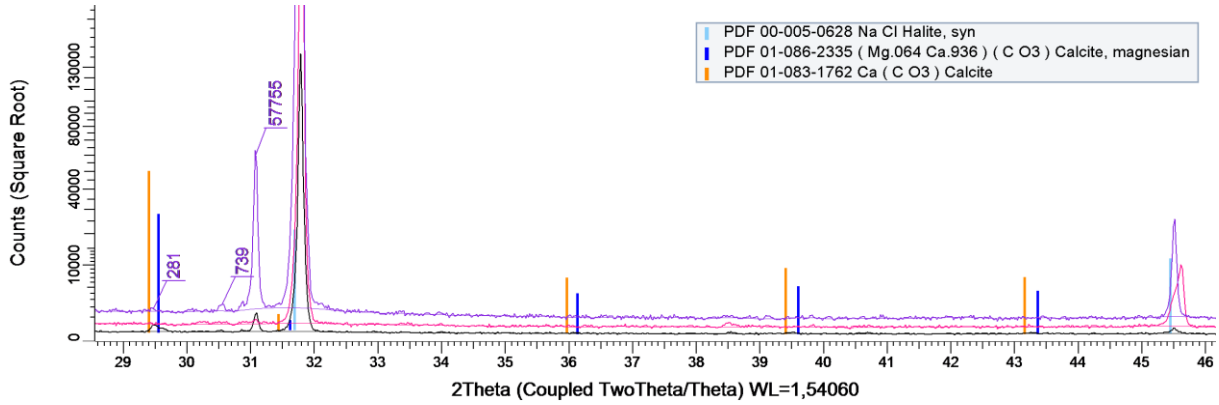

Figure 45: *Pleurochrysis carterae*, repeated experiment, control (black), Ca10% (pink), and Ca5% (purple). Reflections of interest are indicated. Using Vegard's law the Mg content are 1.4, 18.1, and 25.8% (from left to right). The PDF for calcite (orange), magnesian calcite (dark blue), and halite (light blue).

It seems like the middle value (*P. carterae*, Ca 10%) has no reflection in the expected area. The *P. carterae* Ca 5% has no reflections where the largest calcite reflection should be, but has a high reflecion at a higher degree.

The following samples were chosen for XRD analysis because the SEM analysis showed seemingly high content of Mg.

Figure 46 shows the refractions of *E. huxleyi*- samples in the following order: control (black), EH Ca100% -Mn30 (pink), EH Ca100%-Mn40 (purple), EH Ca5%-Mn25 (red), EH Ca5%-Mn40 (salmon).

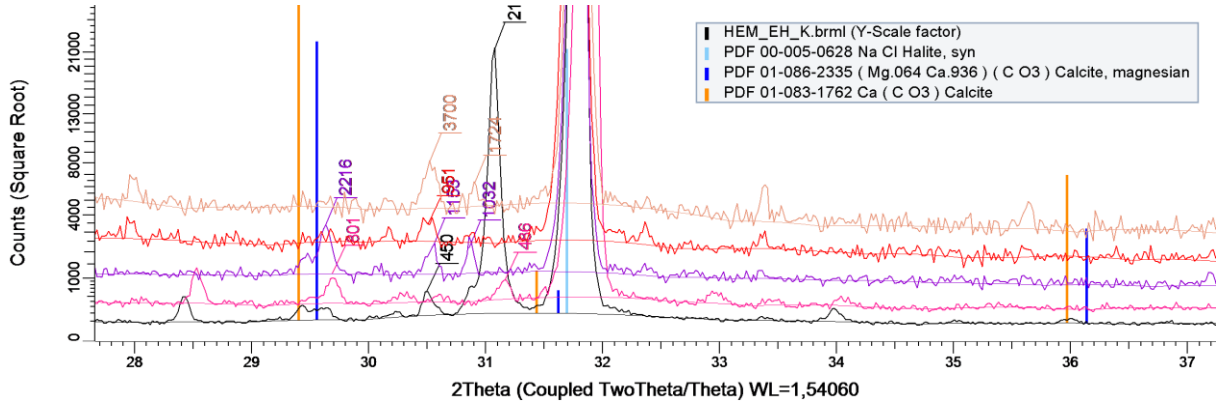

Figure 46: *Emiliania huxleyi*, repeated experiment, control (black), Ca 100% -Mn30 (pink), Ca100%-Mn40 (purple), Ca5%-Mn25 (red), Ca5%-Mn40 (salmon). PDF: Calcite (orange), magnesian calcite (dark blue) and halite (light blue).

The Mg-content for these reflections, is listed in Table 19 and Table 20 in the end of the chapter.

The following Figure shows some *E. huxleyi* ESAW that is Mg-enriched. Note that the reflections are quite similar to those found in Mg-enrciched ESAW, Figure 47.

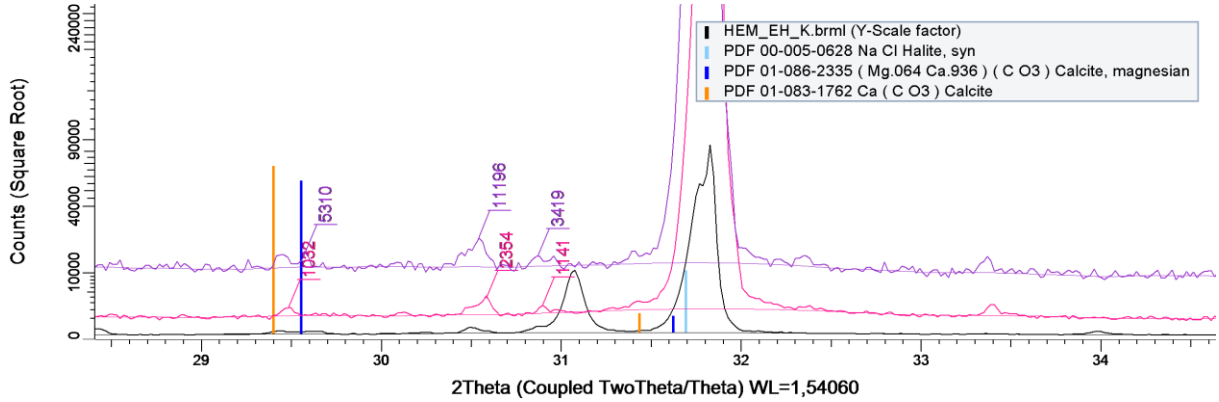

Figure 47: *Emiliania huxleyi*, repeated experiment, control (black), Ca 10%-Mg3.5 (pink), Ca 5%-Mg4.0 (purple). PDF: calcite (orange), magnesian calcite (dark blue), and halite (light blue).

To compare, the cultures with high Mg/low Ca-ESAW from the generational experiment were investigated, and the diffractogram can be seen in Figure 48.

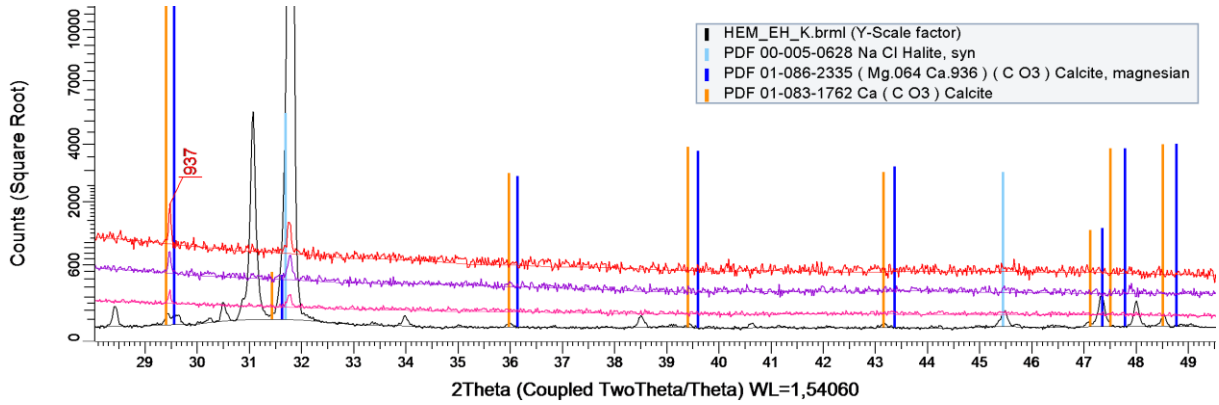

Figure 48: *Emiliania huxleyi*, generational experiment: control (from repeated experiment, black), Ca 5%-Mg2.5 (pink), Ca 5%-Mg3.0 (purple), and Ca 5%-Mg3.5 (red). PDF: calcite (orange), magnesian calcite (blue), and halite (light blue). The small shift in the calcite reflection can indicate an Mg-content of 1.49%.

Note that when the ESAW has been rinsed, there seem to be fewer of the magnesian calcite reflections, especially when compared to the control from the repeated experiment.

The high Mg/Ca 10% from the repeated experiment is presented in Figure 49.

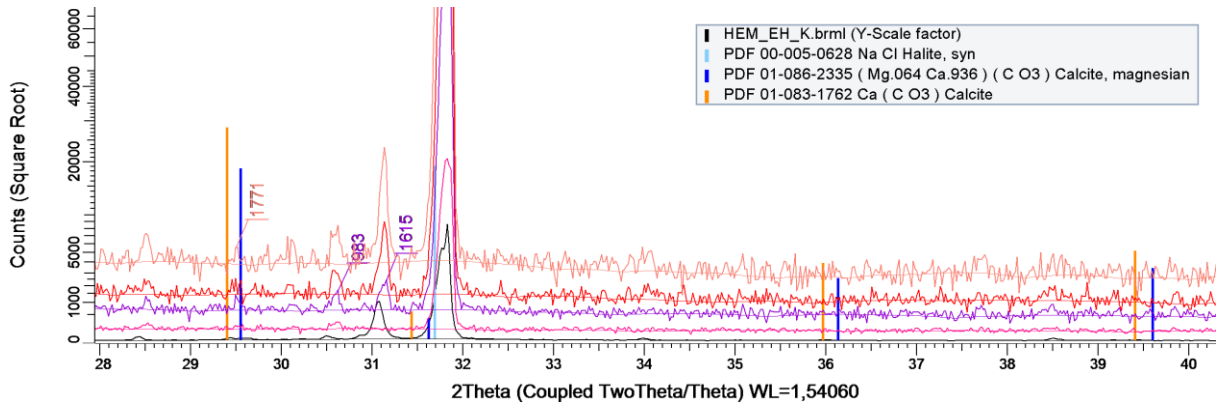

Figure 49: *Emiliania huxleyi*, repeated experiment, Ca 10%: control (black), Mg2.5 (pink), Mg3.0 (purple), Mg3.5 (red), and Mg4.0 (salmon). The indicated refractions are listed in the table in the end of the chapter to find the Mg content. PDF: calcite (orange), magnesian calcite (dark blue), halite (light blue).

The high Mg/normal Ca ESAW is presented in Figure 50.

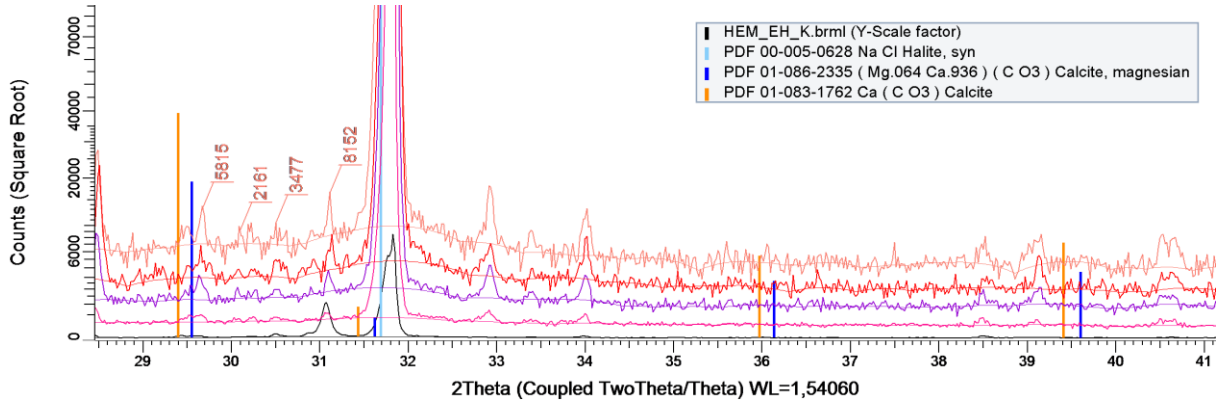

Figure 50: *Emiliania huxleyi*, repeated experiment, Ca 100%: control (black), Mg2.5 (pink), Mg3.0 (purple), Mg3.5 (red), Mg4.0 (salmon). The given reflections can be found in the table in the end of the chapter, to find the Mg content. The calcite phase seems to be shift shifted, but the reflections are not very intense. PDF: calcite (orange), magnesian calcite (dark blue), halite (light blue).

That was all the *E. huxleyi* samples that were analyzed with XRD.The same analysis were done for *P. carterae*. The following three figures shows cultures that had higher Mg-values in the SEM. The Mg-value for the indicated reflections can be found in Table 20 at the end of the chapter. Figure 51 shows Fe-ESAW, Figure 52 shows Mn-ESAW, and Figure 53 shows Mg-ESAW.

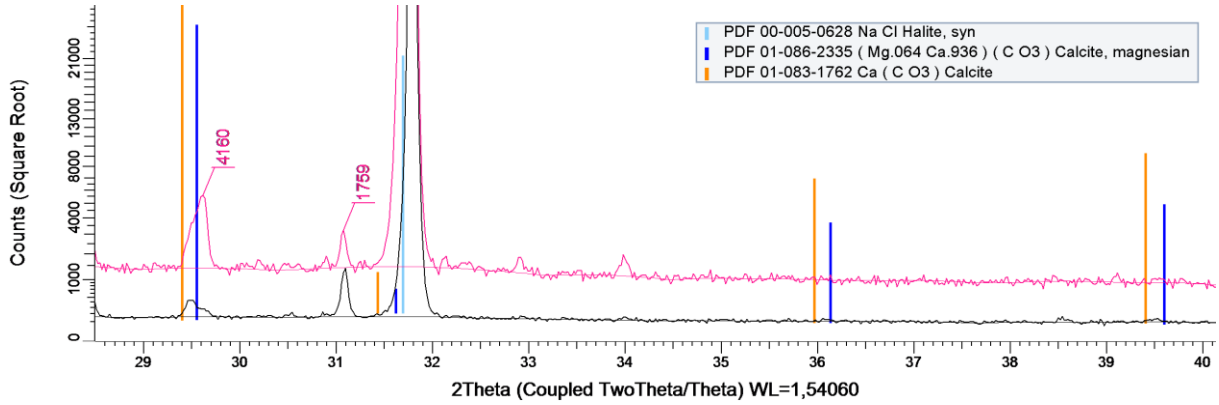

Figure 51: *Pleurochrysis carterae*, repeated experiment, control (black), Ca 100%-Fe25 (pink). The indicated reflections can be found in the table in the end of the chapter. PDF: calcite (orange), magnesian calcite (dark blue), halite (light blue).

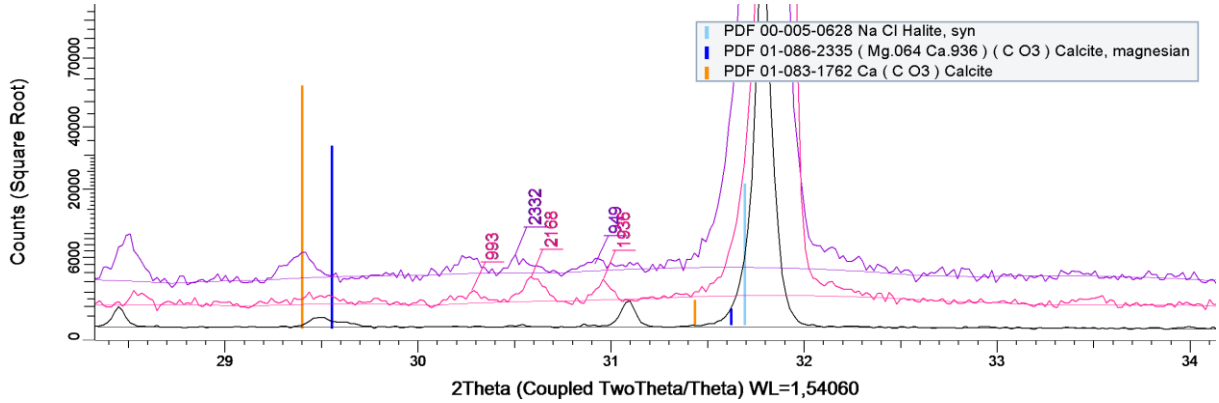

Figure 52: *Pleurochrysis carterae*, repeated experiment, control (black), Ca 5%-Mn25 (pink), Ca 5%-Mn30 (purple). The indicated reflections can be found in the table in the end of the chapter. PDF: calcite (orange), magnesian calcite (dark blue), halite (light blue).

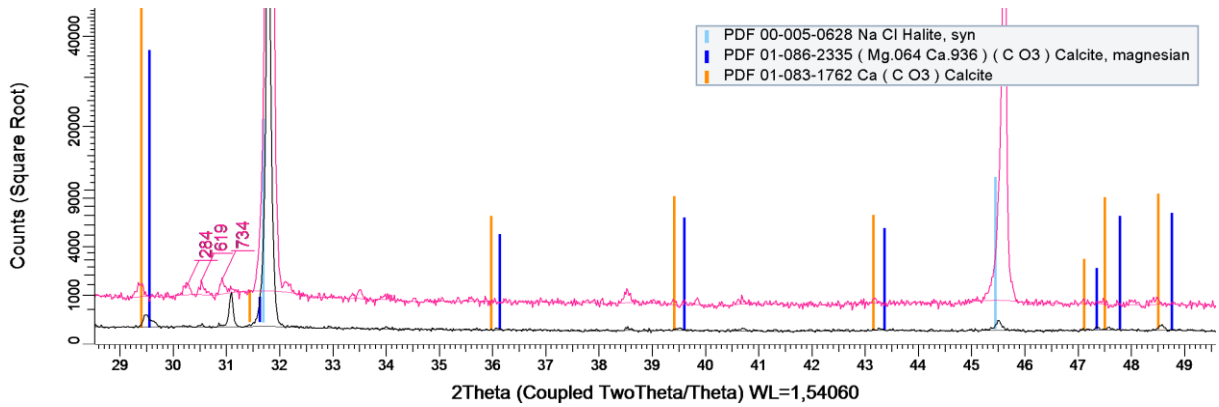

Figure 53: *Pleurochrysis carterae*, repeated experiment, control (black), and Ca 5%-Mg3.0 (pink). The indicated reflections can be found in the table in the end of the chapter. PDF: calcite (orange), dolomite (dark blue), and halite (light blue).

To see if there may be any trends, the high Mg/low Ca ESAW from the generational experiment was analyzed, Figure 54.

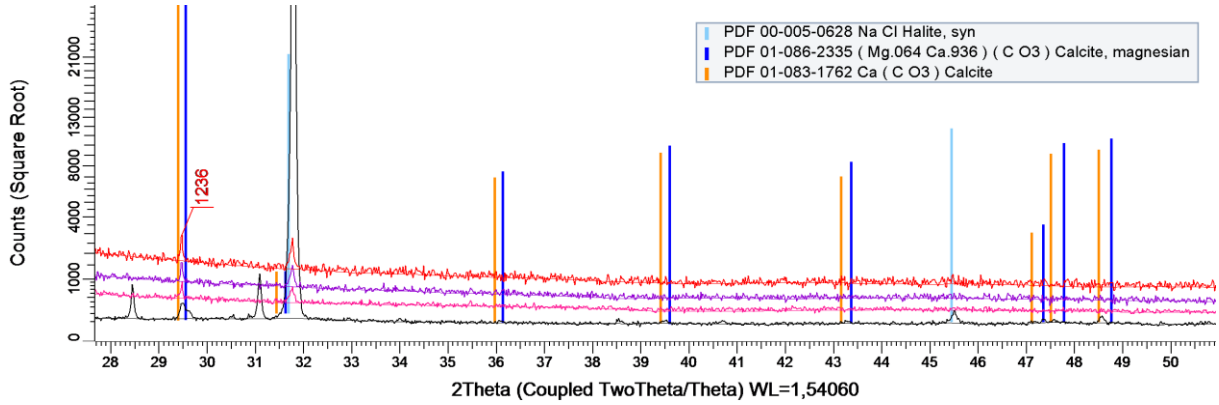

Figure 54: *Pleurochrysis carterae*, generational experiment, control (from last exp., black), Ca 5%-Mg2.5 (pink), Ca 5%-Mg3.0 (purple), and Ca 5%-Mg3.5 (red). PDF: calcite (orange), dolomite (dark blue), and halite (light blue). The shift in the indicated reflection corresponds to an Mg-content of 1.41%.

For *P. carterae* with normal Ca-values, the following diffreactogram shows that there is a slight replacement towards the magnesian calcite. Figure 55, below, shows the diffreactogram for high Mg/Ca 10%.

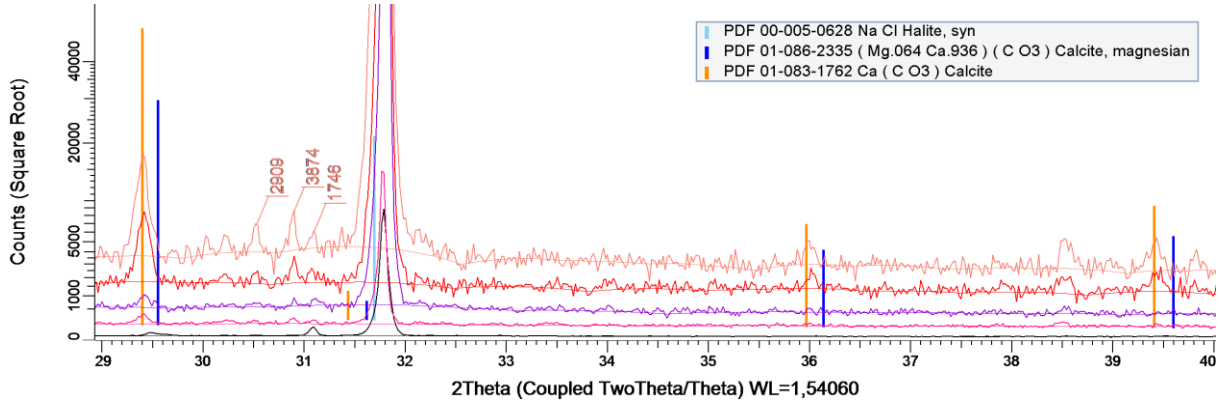

Figure 55: *Pleurochrysis carterae*, repeated experiment, Ca 10%: control (black), Mg2.5 (pink), Mg3.0 (purple), Mg3.5 (red), Mg4.0 (salmon). PDF: calcite (orange), magnesian calcite (dark blue), halite (light blue). The Mg content for all the indicated reflections can be found in the table in the end of the chapter. The reflections for Mg4.0 (salmon) and Mg3.5 (red), are at the same degree, thus only Mg4.0-reflections are indicated.

The last sample is the high Mg/Ca 100% ESAW for *P. carterae*, Figure 56.

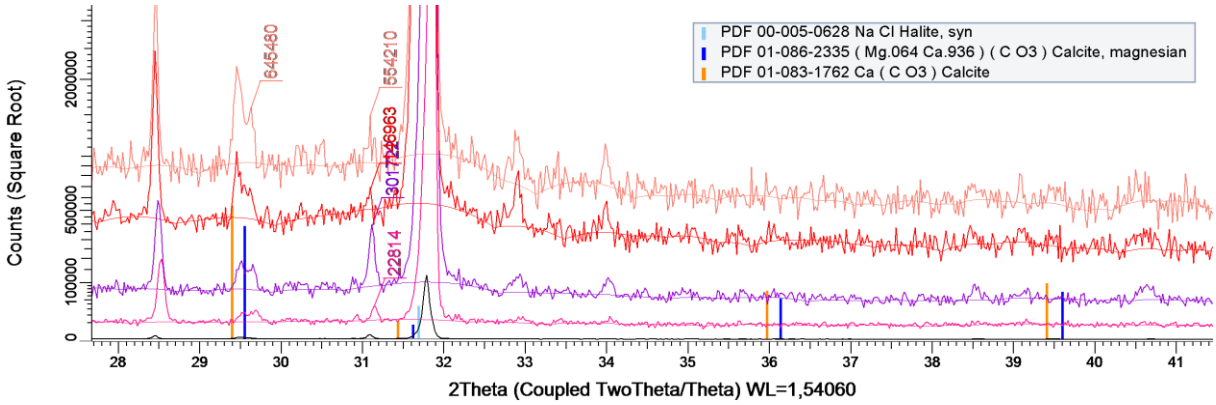

Figure 56: *Pleurochrysis carterae*, Repeated experiment, Ca 100%: control (black), Mg2.5 (pink), Mg3.0 (purple), Mg3.5 (red), Mg4.0 (salmon). PDF: calcite (orange), magnesian calcite (dark blue), and halite (light blue). The Mg content of the indicated reflections is given in the table in the end of the chapter. The indicated reflections are in the same positions, which make it difficult to see the exact numbers. This is not important since the reflections are noted by the degree in the table in the end of the chapter.

Mg content – Vegard's law

Vegard's law was used to calculate approximate Mg-content in different phases of magnesian calcite. The refraction d_{104} was used. The calculations are listed in the following two tables.

Table 19: List of d_{104} positions and the corresponding Mg-content for *Emiliania huxleyi.*

Sample	d104	d-spacing	X	Mg content %
EH_L_Ca100%_control	29,6	3,01	0,04	4
EH_L_Ca100%_control	30,5	2,93	0,17	17
EH_L_Ca100%_control	31,1	2,88	0,26	26
EH_L_Ca10%_control	29,6	3,01	0,04	4
EH_L_Ca10%_control	30,2	2,96	0,13	13
EH_L_Ca10%_control	30,5	2,93	0,17	17
EH_L_Ca10%_control	31,1	2,88	0,26	26
EH_L_Ca5%_control	31,1	2,88	0,26	26
EH_F_Ca100%_control	29,4	3,03	0,01	1
EH_F_Ca100%_control	31,2	2,87	0,27	27
EH_F_Ca5%_Mg2.5/3.0/3.5	29,5	3,03	0,01	1
EH_L_Ca100%_Mg2.5/3.0/3.5/4.0	29,7	3,01	0,04	4
EH_L_Ca100%_Mg2.5/3.0/3.5/4.0	30,1	2,97	0,11	11
EH_L_Ca100%_Mg2.5/3.0/3.5/4.0	30,5	2,93	0,17	17
EH_L_Ca100%_Mg2.5/3.0/3.5/4.0	31,1	2,87	0,26	26
EH_L_Ca10%_Mg2.5/3.0/3.5/4.0	29,5	3,03	0,02	2
EH_L_Ca10%_Mg2.5/3.0/3.5/4.0	30,6	2,92	0,19	19
EH_L_Ca10%_Mg2.5/3.0/3.5/4.0	30,9	2,89	0,23	23
EH_L_Ca5%_Mg4.0	29,6	3,02	0,03	3
EH_L_Ca5%_Mg4.0	30,5	2,92	0,18	18
EH_L_Ca5%_Mg4.0	30,9	2,89	0,23	23
EH_L_Ca10%_Mg3.5	29,5	3,03	0,02	2
EH_L_Ca10%_Mg3.5	30,6	2,92	0,19	19
EH_L_Ca10%_Mg3.5	30,9	2,89	0,23	23
EH_L_Ca100%_Mn30	29,7	3,01	0,05	5
EH_L_Ca100%_Mn30	31,2	2,87	0,27	27
EH_L_Ca100%_Mn40	29,6	3,01	0,04	4
EH_L_Ca100%_Mn40	30,6	2,92	0,18	18
EH_L_Ca100%_Mn40	30,9	2,90	0,23	23
EH_L_Ca5%_Mn25	30,5	2,93	0,17	17
EH_L_Ca5%_Mn40	30,5	2,93	0,18	18
EH_L_Ca5%_Mn40	30,9	2,89	0,23	23

Table 20: List of d_{104} positions and the corresponding Mg-content for *Pleurochrysis carterae*.

Sample	d104	d-spacing	X	Mg-content %
PC_L_Ca100%_control	29,5	3,03	0,02	2
PC_L_Ca100%_control	31,1	2,87	0,26	26
PC_L_Ca10%_control	----			0
PC_L_Ca5%_control	29,5	3,03	0,01	1
PC_L_Ca5%_control	30,6	2,92	0,18	18
PC_L_Ca5%_control	31,1	2,88	0,26	26
PC_F_Ca100%_control	29,5	3,03	0,02	2
PC_F_Ca5%_Mg2.5/3.0/3.5	29,5	3,03	0,01	1
PC_L_Ca100%_Mg2.5/3.0/3.5/4.0	29,6	3,01	0,04	4
PC_L_Ca100%_Mg2.5	31,1	2,87	0,27	27
PC_L_Ca100%_Mg3.0	31,1	2,87	0,26	26
PC_L_Ca100%_Mg3.5	31,1	2,87	0,26	26
PC_L_Ca100%_Mg4.0	31,1	2,87	0,26	26
PC_L_Ca10%_Mg2.5/3.0	---			0
PC_L_Ca10%_Mg3.5/4.0	30,5	2,93	0,18	18
PC_L_Ca10%_Mg3.5/4.0	30,9	2,89	0,23	23
PC_L_Ca10%_Mg3.5/4.0	31,1	2,87	0,26	26
PC_L_Ca10%_Mg2.5	30,3	2,95	0,14	14
PC_L_Ca5%_Mg3.0	30,2	2,95	0,13	13
PC_L_Ca5%_Mg3.0	30,5	2,93	0,18	18
PC_L_Ca5%_Mg3.0	30,9	2,89	0,24	24
PC_L_Ca5%_Mn25	30,3	2,95	0,14	14
PC_L_Ca5%_Mn25	30,6	2,92	0,19	19
PC_L_Ca5%_Mn25	31,0	2,89	0,24	24
PC_L_Ca5%_Mn30	30,3	2,95	0,14	14
PC_L_Ca5%_Mn30	30,5	2,93	0,17	17
PC_L_Ca5%_Mn30	30,9	2,89	0,24	24
PC_L_Ca100%_Fe25	29,6	3,01	0,04	4
PC_L_Ca100%_Fe25	31,1	2,88	0,26	26

The last two tables give the Mg-content of the magnesian calcite phases, given that all the reflections are present. These numbers are not very accurate, but gives an indication of the Mg-content. The Mg-content seems to vary a great deal, but does not seem to follow a trend.

5 Discussion

This chapter will first discuss the how the coccolithophores are affected by the different ESAW compositions, before moving on to discussing the results of the SEM and XRD analysis. In the end of the chapter, the discussion will focus on the substitution of cations and the overview of the thesis.

Growth under different seawater conditions

The growth curves and the observations from the first experiment show that *E. huxleyi* and *P. carterae* can grow under altered seawater conditions. It seems that the cells have reacted in some manner to the change in environment, but also that they become acclimated to these conditions.

Some bacterial growth was seen for a selection of the cultures, paricultarly the Fe-enriched ESAW. It is difficult to know if the alterations of the growth curves are due to the extra bacteria that were observed, or if the bacterial growth was triggered by a change in the media. As the cultures came from the same source, it is likely that they contained the same bacteria. The bacteria source could also be from contamination sources on the outside, but the first scenario is most likely as the problem was persistent for two of the elements, Fe and Mg. When the bacterial growth was reduced, the algae also seemed to be doing better, but this also meant that they had more time to be acclimated. It is thus difficult to determine which of these factors, or both, were the source for algal distress in the first generations. It is clear from the cell counting of the first generations that the cultures with low Ca-contents were not doing well.

When the cultures were transferred, the population density was not taken into consideration. If the transfer volume had been changed according to population density, these cell counts would have given a good indication of how these cultures were doing over time. However, the fact that they did survive over time also tell us that these amounts of cations in the water can at least not be considered acute toxic to coccolithophores. The fact that there is a difference in the cell count between Fe and the two other elements may simply be because Fe is known to trigger algal blooms, and was likely to cause increased population growth in the first place.

When the results from the first three generations of *P. carterae* and the first two generations of *E. huxleyi* were examined in the SEM, few coccoliths were found. Since coccliths were seen with a light microscope, it is likely that something was wrong with the claening method. The problem might be that the coccoliths were covered by organic material and could not be seen in the SEM. Another posibility is that the coccoliths were dissolved in the seawater.

When the experiment was repated, the pH-was measured to see that the different ESAW were not dissolving the coccoliths. The pH in the ESAW after three weeks of growth was higher than in the beginning, but the coccolithophores seemed to be doing fine. According to these measurements *P. carterae* can grow in a pH-range from 7.15 – 10.23. *E. huxleyi* can grow in a pH-range from 7.15 – 9.63.It looks like the *P. carterae* cultures were stabilized at a higher pH than *E. huxleyi*, in these studies. The ESAW started with a pH close to pH 7. One question that arises is weather 7.15 (which was the lowest) is enough to dissolve calcite.

In order to verify this hypothesis, calcite crystals were placed in the same seawater conditions for a month under the same conditions. There were no visible changes to these crystals.

Because the coccoliths are thinner, we cannot rule out that they can have been dissolved in the initial stages of the growth process. This should not, however, be the reason why we had so few coccoliths as the ending pH was quite high. Since the algae use CO_2 and also use some of the minerals, the ESAW ends up being alkaline. The pH-measurements only show that the pH change and that it changes differently according to species. This can probably be related to differences between the species in calcification and photosynthesis.

The growth curves followed a typical sigmoid curve. Some of the curves showed a drop in the middle of the growth curve and at the end. Some of these differences can be due to natural variations, but it also might be due to the CASY® cell counter. The counting number can be affected by debris blocking the funnel, or debris with the same insulating properties and size as the cells. If all the nutriens in the water are used, it is possible that the drop in the population density is because the cells are dying. The growth curves were quite similar for all the ESAW compositions. However, when looking at the population densities, it is quite clear, but not surprising that Fe-enriched ESAW results in dense cultures both in *E. huxleyi* and *P. carterae.* The *E. huxleyi* cells were very small, and allthough the average size of the counted cells were reasonable, this does not outrule that some of the cells that were counted for *E. huxleyi* may have been bacteria.

E. huxleyi has much smaller cells and for one culture the populaion density reached more than 1.3 million cells/mL (The culture with Ca 100%-Fe40), whereas some of the highest densites in *P. carterae* cultures were close to 250 000 cells/mL (Ca 100%-Fe30/35/40). It seems that the ESAW with Ca 5%, regardless of the cations, was the factor that gave smallest populations in *P. carterae*. ESAW with Ca 10% did not seem to affect the *P. carterae* population densities much. The *E. huxleyi* populations were also affected by low Ca, but in the ESAW with Mn-enriched water, there were no difference in the population densities. This may indicate that Mn can be substituted for Ca to some extent, allthough this was not seen in the SEM and XRD results.

When the cells were counted with CASY®, the average cell size was also measured. The cell sizes varied according to ESAW composition and time of measurement. These observations do not seem to be related to whether the algae can substitute cations or not, but is an interesting observation. It seems that lower Ca-concentrations give larger *P. carterae* cells, regardless of added cations. It also seems that the *P. carterae* cells were larger after 21 days than 17 days (exponential growth phase).

The cells were slightly larger at the end of the growth period than in the exponential phase. Less Ca seems to give larger cells in *E. huxleyi*. It seems from the figure that the Fe-concentrations were the factor that affected the cell size the most.

For *P. carterae*, the cell sizes seem to vary to a much larger extent than *E. huxleyi*. *P. carterae* had a change in diameter of about 2 µm. It means that there is about a 40% difference in cell volume (average). For *E. huxleyi* the difference in cell diameter is about 1 µm, but nevertheless, the difference in volume is about 46%. These numbers are just meant to illustrate the point that this might be interesting to pursue further although it is not a part of this thesis.

Sample preparation techniques

The results from the first experiment in the SEM gave very few coccoliths. It is possible that centrifuging and cleaning the samples may have been part of the problem. Firstly, the samples were rinsed with water (pH 8.4) to remove the salt, and thus obtain a sample that would be easier to analyze. One challenge was that calcite dissolves in clean water. This is why water

with a higher pH was used. It would be plausible, otherwise, that the water itself could have dissolved the coccoliths, but that is not likely as the pH was as high as in the culture medium. This water was not analyzed, and is a source of contamination.

Another possibility is that the centrifuging destroyed the coccoliths. This is a possibility even though the routine is reported used in the literature. It is also possible that centrifuging the samples is the reason for the coccoliths being covered in organic debris. The centrifuging was done at 15 000 rpm (rounds per minute) for 2-3.5 min.

In the second experiment, the batches were not centrifuged, nor rinsed. This led to more NaCl in the samples, but also more coccoliths. The coccoliths were gathered from the bottom of the flasks.

Scanning Electron Microscope and Energy Dispersive X-ray Spectroscopy

In the second experiment, the samples were prepared differently, and this seems to have given better SEM results. Coccoliths were not observed in the samples containing higher Fe-levels. One can only speculate, but one possible option can be that the Fe boosted the population growth so much that Ca was a limited resource. For *E. huxleyi* the lowest Ca-concentrations gave no coccoliths in the Mn-enriched ESAW, and only few and deformed coccoliths in the Mg-enriched ESAW.

All of the other cultures contained coccoliths, although some had noticeably few. Some cultures also had clearly damaged coccoliths. Damaged coccoliths seem to particularly affect the Ca-limited cultures. Apart from the visual results, EDS analysis was performed on all samples to gain insight about the element-composition.

An aspect of the EDS analysis is that the coccoliths are both thin and small compared to the sampling area. The EDS point analysis counts electrons coming from a radius of 1 µm from where the point is set. The electrons may come from up to 2 µm below the surface. For most of the samples two points (or more) were measured on the coccoliths. The acquisition time was chosen to be until the graph remained constant, but in retrospect should have been held for a longer time to increase counting statistics.

When looking at the results in Chapter 4, it seems like the results are good. However, the acquisition time and number of counts was quite low. The number of counts should be more than 500, but in some of the samples the number was under that limit.

In addition, the emission energies for Mg and Na are quite close, so Na could have been counted as Mg: NaK emission (1.08 keV) and MgK emission (1.30 keV). Since there was a lot of NaCl in the samples, this might account for the high Mg-counts. It is difficult to know if the coccoliths actually contained as much Mg as it would seem from the EDS. For instance, the controls seem to only have Mg, and no Ca, which is inconsistent with the most articles on coccolithophores.

In addition there was no correlation with the Mg-concentration in the ESAW and the amount observed by the EDS.

In addition to this, we also considered spectroscopic techniques such atom abs or ICP-MS. These would have been rather good techniques to determine the composition of the coccoliths provided that the washing method had removed the organic material.

X-ray Diffraction analysis

XRD can give a very good idea of what your sample contains in terms of crystalline phases, and also in terms of extent of solution in solid soluble systems such as the $CaCO_3$ – $MgCO_3$ system. It can also be used to provide the composition of such solid soluble compounds even though they would be in a mixture with other crystalline or amorphous phases. The technique can not discriminate the origin between different crystallites of the same phase, which is why it is important to compare the results to the ESAW.

The pure calcite that was analyzed matched the PDF for calcite, proving that the system was well alligned. All of the analyzed cultures were compared to this standard. Some of the reflections were of particular interest: the highest intensity reflection (d_{104}) and one of the reflections at a higher angle (d_{211}). The (d_{104}) reflection is easiest to identify and the higher angle (d_{211}) reflection is most affected by variations in composition of the calcite phase.

If there was significant amounts of Mg in the $CaCO_3$, a shift in d_{211} would be expected. However, d_{211} did not shift at all in any of the samples. This can indicate that there is a pure calcite pahse in all of the samples. On the other hand, halite (NaCl), has a reflection at the

same angle as the d_{211} was expected to be for calcite. It is hard to prove that the calcite reflection d_{211} did not shift at all when there is a halite reflection there.

When looking at the other reflection of interest, d_{104}, there were many other reflections in the range between pure $CaCO_3$ and pure $MgCO_3$ that we were unable to identify as other crystalline materials. This can indicate that the structures consist of many different calcite phases with varying composition of Mg, i.e., that the Mg is not evenly distributed in the coccoliths.

All of these possible Mg-containing phases were used as input for calculating the Mg concentrations using Vegard's law. The analysis of the d-shift gives the impression that both *E. huxleyi* and *P. carterae* can take up Mg. The shift in refraction d_{104} in different phases gives high-Mg-phases ranging from 0.9-27% Mg in *E.huxleyi* and 1.4-27% Mg in *P. carterae*.

This looks like good results, but when these reflections are compared to the Mg-enriched ESAW, the same reflections are present. This means that for the Mg-enriched cultures it is impossible, with this method, to know if the Mg-phases are made by the coccolithophores. It is likely that it is not. However, the strongest calcite reflection appeared somewhat shifted, but this shift indicates somewhere between 0.9-1.5% Mg in the calcite structure. This is uncertain since the shift should also have been seen in the d_{211} reflection. In addition, the shift does not seem to change with a higher Mg-content. As mentioned above, there is a specific correlation between the shift of the (d_{104}) and (d_{211}) reflections where the intensity of the first is highest, and therefore most easy to observe. Unfortunately many of the diffractograms, especially from the first cultures, did not show any clear (d_{211}) reflection, most probably due to too low intensity. It was therefore not possible to verify and support the assumptions that the additional (d_{104}) reflections did indeed originate from additional Mg-containing calcite phases. Since no coccoliths were found in the SEM it might also mean that these coccoliths were destroyed by the preparation method.

For the cultures from the repeated experiments there were several additional reflections, and by shifting the calcite PDFs, all the reflections could be matched, but not by the same PDF. This can indicate that there are many phases that were unidentified, or that there are unidentified phases that do not match the calcite reflections. Since none of the shifted PDFs could match all the reflections, there is a possibility that the reflections did not come from calcite. In the litterature many calcifying species that can substitute Ca are described. For

coccolithophorids it seems that they may contain Mg, but in small amounts, 0.1-0.2 mmol/mol, in normal seawater[58]. Since the controls in this experiment seemed to have this shift in the d_{104} reflection as well, it is possible that this shift is mostly due to the seawater composition and the lack of proper cleaning methods.

XRD analysis of the repeated culture experiments showed several additional reflections, however, they could not all be matched by calcite with varying degree of Mg composition. This indicates that additional phases were present. These were checked against the known $CaCO_3$ phases vaterite, aragonite, and dolomite. However, no complete match could be obtained for these phses. Since this reflection also could correspond to different phases of magnesian calcite, that matched more, but not all, the other reflecitons, it can be considered more likely to be magnesian calcite. Since no shift was observed in the d_{211} the most likely conclusion is that there was no calcite. This is strange since coccoliths were observed in the SEM. One possibility is that coccoliths do not store well, and dissolve over time. In such a scenario, Ca and Mg could still be present in the ESAW, but give completely different phases. This hypothesis could also explain why coccoliths were not found in the generational experiment.

Considering the other cations, Fe, gave no coccoliths, and mostly resulted in a bloom. Mn-enriched seawater seemed to result in a higher Mg-uptake. A possible explanation for this is that even with 40-fold higher concentrations of Mn in ESAW, the normal values of Mg will be higher. It can also mean that Mg is more easily substituted than Mn.

Overall weaknesses

One of the major weaknesses of this study was the lack of doubles. Part of the reason for this is lack of time, and focus rather on having a wide variety of different ESAW concentrations. This means that this study should be repeated in order to give a more presise picture of the cation substitution in coccoliths.

Some of the trouble also seems to be what analytical methods to use, and uncertainties in these. Certainly, it would be better to use additional different methods, but rinsing away the seawater to check what is inside the coccoliths, and what is not, has been a major issue. This needs to be solved before moving on to even more precise analytical methods, such as Atomic absorption spectroscopy (AAS) and ICP-MS.

6 Conclusion

The objective of this thesis was to find out whether or not we can use algae for material production through substituting the cations.

Both the SEM analysis and XRD analysis, points in the direction that coccoliths contain dolomite/magnesian calcite, although, we cannot know for sure whether we have magnesian calcite/dolomite inside the coccolith, or on the outside of the coccolith. It is also uncertain how much we have of the different phases. However, the SEM analysis was run as a point analysis and showed high Mg-content in the coccolith, and not on the outside. However, the XRD analysis should have given a shift in both of the reflections $d_{104}$and d_{211}, which could not be found. This makes it likely that there the reflections did not come from calcite or magnesian calcite.

Looking at the results from the growth, it seems that these cations are not toxic. In *E. huxleyi* Mn-enriched ESAW seems to give as good growth even with low Ca-concentrations. It also seems that low Ca-concentrations give larger cells and low calcite production.

After these experiments it is not possible to conclude that these cations can substitute Ca in coccoliths, but it cannot be outruled either.

7 Future aspects

Since it is likely that *E. huxleyi* and *P. carterae* can substitute part of the Ca with Mg, it means that these coccolithophores, possibly also other species, can be used to produce functional materials such as cathode materials. This should be a good reason to investigate this possibility further.

In this regard, it is one thing in particular that needs to be solved: How do we separate the organic material from the coccoliths? This was one of the issues with this thesis. Just before the deadline, a paper about cleaning techniques was discovered. This paper was issued in 2001 by Stoll et al. The paper compares different cleaning techniques for coccoliths, and descirebes one technique that dissolves organic material for precise measurements of coccoliths with ICP-MS. The same paper also shows that coccolithophores can take up 6% more Mg for every 1 ºC rise in temperature[58].

Since the cleaning issue is already solved, it means that cation substitution can be studied with a more precice answer. As there might be differences between the species, it would be advantageous to study the substitution in different species, for instance *Coccolithus pelagiucus* or *Helicosphaera carteri*. It would also be good to try other possible cations such as Sr, since $SrCO_3$ is used in Cathode Ray Tubes, which has a wide range of applications in new technology.

This project did not intend to investigate how algae can be used to take up CO_2, at the same time as producing useful materials. It would, however, be a good project idea to try to combine these two assets: Making new materials and take up CO_2.

Studying biomineralization in general, offers some quite far fetched ideas, and it will be interesting to see where this knowledge will take us.

Literature

[1] Villars, P., Cenzual, K., *Pearson's crystal data: Crystal Structure Database for Inorganic Compounds*, ASM International®, Materials Park, Ohio, USA, **2009/10**.

[2] Ozaki, N., Sakuda, S., Nagasawa, H.,Isolation and Some Characterization of an Acidic Polysaccharide with Anti-calcification Activity from Coccoliths of a Marine Alga, Pleurochrysis carterae, *Bioscience, Biotechnology, and Biochemistry*, **2001**, *65*, 2330-2333.

[3] Didymus, J. M., Young, J. R., Mann, S.,Construction and Morphogenesis of the Chiral Ultrastructure of Coccoliths from the Marine Alga Emiliania huxleyi, *Proceedings of the Royal Society of London B: Biological Sciences*, **1994**, *258*, 237-245.

[4] Graham, L., Graham, J., Wilcox, L., Benjamin Cummings (Pearson), San Francisco, CA, **2009**.

[5] van der Wal, P., de Jong, E. W., Westbroek, P., de Bruijn, W. C., Mulder-Stapel, A. A.,Polysaccharide localization, coccolith formation, and golgi dynamics in the coccolithophorid Hymenomonas carterae, *Journal of Ultrastructure Research*, **1983**, *85*, 139-158.

[6] Wal, P., Vrind, J. P., Jong, E. W., Borman, A. H.,Incompleteness of the coccosphere as a possible stimulus for coccolith formation in *Pleurochrysis carterae* (Prymnesiophyceae), *Journal of Phycology*, **1987**, *23*, 218-221.

[7] Parke, M., Manton, I., Clarke, B.,Studies on marine flagellates II. Three new species of Chrysochromulina, *Journal of the Marine Biological Association of the United Kingdom*, **1955**, *34*, 579-609.

[8] Young, J. R., Davis, S. A., Bown, P. R., Mann, S.,Coccolith Ultrastructure and Biomineralisation, *Journal of Structural Biology*, **1999**, *126*, 195-215.

[9] Young, J. R., Henriksen, K.,Biomineralization within vesicles: the calcite of coccoliths, *Reviews in Mineralogy and Geochemistry*, **2003**, *54*, 189-215.

[10] Young, J. R., Didymus, J. M., Brown, P. R., Prins, B., Mann, S.,Crystal assembly and phylogenetic evolution in heterococcoliths, *Nature*, **1992**, *356*, 516-518.

[11] Mookherji, A., C. Mathur, S.,Magnetic Studies on Siderite (FeCO3), *Journal of the Physical Society of Japan*, **1965**, *20*, 1336-1339.

[12] Nam, K. T., Kim, D.-W., Yoo, P. J., Chiang, C.-Y., Meethong, N., Hammond, P. T., Chiang, Y.-M., Belcher, A. M.,Virus-Enabled Synthesis and Assembly of Nanowires for Lithium Ion Battery Electrodes, *Science*, **2006**, *312*, 885-888.

[13] Lee, S.-W., Mao, C., Flynn, C. E., Belcher, A. M.,Ordering of Quantum Dots Using Genetically Engineered Viruses, *Science*, **2002**, *296*, 892-895.

[14] Gorby, Y. A., Yanina, S., McLean, J. S., Rosso, K. M., Moyles, D., Dohnalkova, A., Beveridge, T. J., Chang, I. S., Kim, B. H., Kim, K. S., Culley, D. E., Reed, S. B., Romine, M. F., Saffarini, D. A., Hill, E. A., Shi, L., Elias, D. A., Kennedy, D. W., Pinchuk, G., Watanabe, K., Ishii, S. i., Logan, B., Nealson, K. H., Fredrickson, J. K.,Electrically conductive bacterial nanowires produced by Shewanella oneidensis strain MR-1 and other microorganisms, *Proceedings of the National Academy of Sciences*, **2006**, *103*, 11358-11363.

[15] Mao, C., Sun, W., Shen, Z., Seeman, N. C.,A nanomechanical device based on the B-Z transition of DNA, *Nature*, **1999**, *397*, 144-146.

[16] Weibel, D. B., Garstecki, P., Ryan, D., DiLuzio, W. R., Mayer, M., Seto, J. E., Whitesides, G. M.,Microoxen: Microorganisms to move microscale loads, *Proceedings of the National Academy of Sciences of the United States of America*, **2005**, *102*, 11963-11967.

[17] Bao, Z., Weatherspoon, M. R., Shian, S., Cai, Y., Graham, P. D., Allan, S. M., Ahmad, G., Dickerson, M. B., Church, B. C., Kang, Z., Abernathy Iii, H. W., Summers, C. J., Liu, M., Sandhage, K. H.,Chemical reduction of three-dimensional silica micro-assemblies into microporous silicon replicas, *Nature*, **2007**, *446*, 172-175.
[18] Chauton, M., Skolem, L. B., Olsen, L., Vullum, P., Walmsley, J., Vadstein, O.,Titanium uptake and incorporation into silica nanostructures by the diatom Pinnularia sp. (Bacillariophyceae), *Journal of Applied Phycology*, **2015**, *27*, 777-786.
[19] Davis, T. A., Volesky, B., Mucci, A.,A review of the biochemistry of heavy metal biosorption by brown algae, *Water Research*, **2003**, *37*, 4311-4330.
[20] Paasche, E.,A review of the coccolithophorid Emiliania huxleyi (Prymnesiophyceae), with particular reference to growth, coccolith formation, and calcification-photosynthesis interactions, *Phycologia*, **2001**, *40*, 503-529.
[21] Berges, J. A., Franklin, D. J., Harrison, P. J.,Evolution of an artificial seawater medium: Improvements in enriched seawater, artificial water over the last two decades, *Journal of Phycology*, **2001**, *37*, 1138-1145.
[22] Sakuma, H., Andersson, M. P., Bechgaard, K., Stipp, S. L. S.,Surface Tension Alteration on Calcite, Induced by Ion Substitution, *The Journal of Physical Chemistry C*, **2014**, *118*, 3078-3087.
[23] Temmam, M., Paquette, J., Vali, H.,Mn and Zn incorporation into calcite as a function of chloride aqueous concentration, *Geochimica et Cosmochimica Acta*, **2000**, *64*, 2417-2430.
[24] Goldsmith, J. R., Graf, D. L., Joensuu, O. I.,The occurrence of magnesian calcites in nature, *Geochimica et Cosmochimica Acta*, **1955**, *7*, 212-230.
[25] Staessen, J. A., Roels, H. A., Emelianov, D., Kuznetsova, T., Thijs, L., Vangronsveld, J., Fagard, R.,Environmental exposure to cadmium, forearm bone density, and risk of fractures: prospective population study, *The Lancet*, **1999**, *353*, 1140-1144.
[26] Hess, J., Bender, M. L., Schilling, J.-G.,Evolution of the Ratio of Strontium-87 to Strontium-86 in Seawater from Cretaceous to Present, *Science*, **1986**, *231*, 979-984.
[27] Vidyasagar, K., Gopalakrishnan, J., Rao, C. N. R.,A convenient route for the synthesis of complex metal oxides employing solid-solution precursors, *Inorganic Chemistry*, **1984**, *23*, 1206-1210.
[28] Borszcz, T., Kukliński, P., Taylor, P.,Patterns of magnesium content in Arctic bryozoan skeletons along a depth gradient, *Polar Biology*, **2013**, *36*, 193-200.
[29] Barrère, F., Mahmood, T. A., de Groot, K., van Blitterswijk, C. A.,Advanced biomaterials for skeletal tissue regeneration: Instructive and smart functions, *Materials Science and Engineering: R: Reports*, **2008**, *59*, 38-71.
[30] Boskey, A. L.,Will Biomimetics Provide New Answers for Old Problems of Calcified Tissues?, *Calcified Tissue International*, **1998**, *63*, 179-182.
[31] Presser, V., Schultheiß, S., Berthold, C., Nickel, K. G.,Sea Urchin Spines as a Model-System for Permeable, Light-Weight Ceramics with Graceful Failure Behavior. Part I. Mechanical Behavior of Sea Urchin Spines under Compression, *Journal of Bionic Engineering*, **2009**, *6*, 203-213.
[32] Brooks, R. R., *Plants that hyperaccumulate heavy metals: their role in phytoremediation, microbiology, archaeology, mineral exploration and phytomining*, CAB international, **1998**.
[33] Bazylinski, D. A., Frankel, R. B., Konhauser, K. O.,Modes of Biomineralization of Magnetite by Microbes, *Geomicrobiology Journal*, **2007**, *24*, 465-475.
[34] Weiner, S., Dove, P. M.,An overview of biomineralization processes and the problem of the vital effect, *Reviews in Mineralogy and Geochemistry*, **2003**, *54*, 1-29.

[35] Johnson, M. K., Rees, D. C., Adams, M. W.,Tungstoenzymes, *Chemical reviews*, **1996**, *96*, 2817-2840.
[36] Hille, R.,Molybdenum and tungsten in biology, *Trends in Biochemical Sciences*, **2002**, *27*, 360-367.
[37] McConnell, D.,Inorganic constituents in the shell of the living *Brachiopod lingula*, *Geological Society of America Bulletin*, **1963**, *74*, 363-364.
[38] Rehder, D.,Structure and function of vanadium compounds in living organisms, *Biometals*, **1992**, *5*, 3-12.
[39] Kokubu, N., Hidaka, T.,Tantalum and Niobium in Ascidians, *Nature*, **1965**, *205*, 1028-1029.
[40] Carlisle, D. B.,Niobium in Ascidians, *Nature*, **1958**, *181*, 933-933.
[41] Kobayashi, M., Shimizu, S.,Cobalt proteins, *European Journal of Biochemistry*, **1999**, *261*, 1-9.
[42] Lane, T. W., Morel, F. M. M.,A biological function for cadmium in marine diatoms, *Proceedings of the National Academy of Sciences*, **2000**, *97*, 4627-4631.
[43] Sani, R. K., Peyton, B. M., Dohnalkova, A.,Comparison of uranium(VI) removal by Shewanella oneidensis MR-1 in flow and batch reactors, *Water Research*, **2008**, *42*, 2993-3002.
[44] Rothschild, L. J., Mancinelli, R. L.,Life in extreme environments, *Nature*, **2001**, *409*, 1092-1101.
[45] Borowitzka, M. A., Larkum, A. W. D., Nockolds, C. E.,A scanning electron microscope study of the structure and organization of the calcium carbonate deposits of algae, *Phycologia*, **1974**, *13*, 195-203.
[46] Decho, A. W.,Overview of biopolymer-induced mineralization: What goes on in biofilms?, *Ecological Engineering*, **2010**, *36*, 137-144.
[47] www.glencoe.mheducation.com, Biology: The Dynamics of Life, California Edition, 25.01.2016, McGraw-Hill Global Education Holdings, LLC,
[48] Chave, K. E.,Aspects of the biogeochemistry of magnesium 1. Calcareous marine organisms, *The Journal of Geology*, **1954**, 266-283.
[49] Moberly, R.,Composition of Magnesian Calcites of Algae and Pelecypods by Electron Microprobe analysis, *Sedimentology*, **1968**, *11*, 61-82.
[50] Milliman, J., Gastner, M., Müller, J.,Utilization of magnesium in coralline algae, *Geological Society of America Bulletin*, **1971**, *82*, 573-580.
[51] Wasylenki, L. E., Dove, P. M., De Yoreo, J. J.,Effects of temperature and transport conditions on calcite growth in the presence of Mg2+: Implications for paleothermometry, *Geochimica et Cosmochimica Acta*, **2005**, *69*, 4227-4236.
[52] Pikey, O. H., Goodell, H. G.,Trace elements in recent mollusk shells, *Limnology and Oceanography*, **1963**, *8*, 137-148.
[53] Richardson, C. A., Chenery, S. R. N., Cook, J. M.,Assessing the history of trace metal (Cu, Zn, Pb) contamination in the North Sea through laser ablation‹ICP-MS of horse mussel Modiolus modiolus shells, *Marine Ecology Progress Series*, **2001**, *211*, 157-167.
[54] Likins, R. C., Berry, E. G., Posner, A. S.,Comparative fixation of calcium and strontium by snail shell *Annals of the New York Academy of Sciences*, **1963**, *109*, 269-277.
[55] Ji, L., Liu, J., Song, W., Li, S., Miao, D.,Effects of dietary Europium complex and Europium(III) on cultured pearl colour in the pearl oyster Pinctada martensii, *Aquaculture Research*, **2013**, *44*, 1300-1306.

[56] Zouboulis, A. I., Loukidou, M. X., Matis, K. A.,Biosorption of toxic metals from aqueous solutions by bacteria strains isolated from metal-polluted soils, *Process Biochemistry*, **2004**, *39*, 909-916.
[57] Herfort, L., Loste, E., Meldrum, F., Thake, B.,Structural and physiological effects of calcium and magnesium in Emiliania huxleyi (Lohmann) Hay and Mohler, *Journal of Structural Biology*, **2004**, *148*, 307-314.
[58] Stoll, H. M., Ruiz Encinar, J., Ignacio Garcia Alonso, J., Rosenthal, Y., Probert, I., Klaas, C.,A first look at paleotemperature prospects from Mg in coccolith carbonate: Cleaning techniques and culture measurements, *Geochemistry, Geophysics, Geosystems*, **2001**, *2*, n/a-n/a.
[59] Stoll, H. M., Ziveri, P., Geisen, M., Probert, I., Young, J. R.,Potential and limitations of Sr/Ca ratios in coccolith carbonate: new perspectives from cultures and monospecific samples from sediments, *Philosophical Transactions of the Royal Society of London A: Mathematical, Physical and Engineering Sciences*, **2002**, *360*, 719-747.
[60] Politi, Y., Batchelor, D. R., Zaslansky, P., Chmelka, B. F., Weaver, J. C., Sagi, I., Weiner, S., Addadi, L.,Role of Magnesium Ion in the Stabilization of Biogenic Amorphous Calcium Carbonate: A Structure−Function Investigation, *Chemistry of Materials*, **2010**, *22*, 161-166.
[61] Jordan, R. W., Kleijne, A., Heimdal, B. R., Green, J. C.,A Glossary of the Extant Haptophyta of the World, *Journal of the Marine Biological Association of the United Kingdom*, **1995**, *75*, 769-814.
[62] Corstjens, P. L. A. M., Van Der Kooij, A., Linschooten, C., Brouwers, G.-J., Westbroek, P., Jong, E. W. d. V.-d.,GPA, a calcium-binding protein in the coccolithophorid *Emiliania huxleyi* (*Prymniophyceae*), *Journal of Phycology*, **1998**, *34*, 622-630.
[63] Fagerbakke, K. M., Heldal, M., Norland, S., Heimdal, B. R., Båtvik, H.,*Emiliania huxleyi*: Chemical composition and size of coccoliths from enclosure experiments and a Norwegian fjord, *Sarsia*, **1994**, *79*, 349-355.
[64] van der Wal, P., de Bruijn, W. C., Westbroek, P.,Cytochemical and X-ray microanalysis studies of intracellular calcium pools in scale-bearing cells of the coccolithophoridEmiliania huxleyi, *Protoplasma*, **1985**, *124*, 1-9.
[65] Westbroek, P., Brown, C. W., Bleijswijk, J. v., Brownlee, C., Brummer, G. J., Conte, M., Egge, J., Fernández, E., Jordan, R., Knappertsbusch, M., Stefels, J., Veldhuis, M., van der Wal, P., Young, J.,A model system approach to biological climate forcing. The example of Emiliania huxleyi, *Global and Planetary Change*, **1993**, *8*, 27-46.
[66] Marsh, M. E.,Polyanion-mediated mineralization — assembly and reorganization of acidic polysaccharides in the Golgi system of a coccolithophorid alga during mineral deposition, *Protoplasma*, **1994**, *177*, 108-122.
[67] Marsh, M. E., Dickinson, D. P.,Polyanion-mediated mineralization — mineralization in coccolithophore (Pleurochrysis carterae) variants which do not express PS2, the most abundant and acidic mineral-associated polyanion in wild-type cells, *Protoplasma*, **1997**, *199*, 9-17.
[68] Marsh, M.,Coccolith crystals ofPleurochrysis carterae: Crystallographic faces, organization, and development, *Protoplasma*, **1999**, *207*, 54-66.
[69] www.skepticalscience.com, OA not OK part 13: Polymorphs - the son of Poseidon, 20.01.2016, Mackie, D.,
[70] http://www.webelements.com, Iron, 21.01.2016, Winter, M.,

[71] Bischoff, W. D., Bishop, F. C., Mackenzie, F. T.,Biogenically produced magnesian calcite; inhomogeneities in chemical and physical properties; comparison with synthetic phases, *American Mineralogist*, **1983**, *68*, 1183-1188.
[72] Zhang, F., Xu, H., Konishi, H., Roden, E. E.,A relationship between d104 value and composition in the calcite-disordered dolomite solid-solution series, *American Mineralogist*, **2010**, *95*, 1650-1656.
[73] http://www.webelements.com, Calcium, 20.01.2016, Winter, M.,
[74] http://www.webelements.com, Magnesium, 21.01.2016, Winter, M.,
[75] http://www.webelements.com, Manganese, 21.01.2016, Winter, M.,
[76] http://www.mindat.org/, Siderite, The Hudson Insitute of Mineralogy,
[77] Harrison, P. J., Berges, J. A.,Marine culture media, *Algal culturing techniques*, **2005**, 21-34.
[78] Winter, A., Siesser, W. G., *Coccolithophores*, Cambridge University Press, **2006**.
[79] Šupraha, L., Gerecht, A. C., Probert, I., Henderiks, J.,Eco-physiological adaptation shapes the response of calcifying algae to nutrient limitation, *Scientific Reports*, **2015**, *5*, 16499.
[80] Sorrosa, J., Satoh, M., Shiraiwa, Y.,Low Temperature Stimulates Cell Enlargement and Intracellular Calcification of Coccolithophorids, *Marine Biotechnology*, **2005**, *7*, 128-133.
[81] Cubillos, J., Wright, S., Nash, G., De Salas, M., Griffiths, B., Tilbrook, B., Poisson, A., Hallegraeff, G.,Calcification morphotypes of the coccolithophorid Emiliania huxleyi in the Southern Ocean: changes in 2001 to 2006 compared to historical data, *Marine Ecology Progress Series*, **2007**, *348*, 47-54.
[82] Paasche, E.,Reduced coccolith calcite production under light-limited growth: a comparative study of three clones of Emiliania huxleyi (Prymnesiophyceae), *Phycologia*, **1999**, *38*, 508-516.
[83] Nielsen, M. V.,Growth, dark respiration and photosynthetic parameters of the coccolithophorid Emiliania huxleyi (Prymnesiophyceae) acclimated to different day length-irradiance combinations1, *Journal of Phycology*, **1997**, *33*, 818-822.
[84] Brand, L. E., Guillard, R. R. L.,The effects of continuous light and light intensity on the reproduction rates of twenty-two species of marine phytoplankton, *Journal of Experimental Marine Biology and Ecology*, **1981**, *50*, 119-132.
[85] McIntyre, A., Bé, A. W. H.,Modern coccolithophoridae of the atlantic ocean—I. Placoliths and cyrtoliths, *Deep Sea Research and Oceanographic Abstracts*, **1967**, *14*, 561-597.
[86] Conte, M. H., Thompson, A., Lesley, D., Harris, R. P.,Genetic and Physiological Influences on the Alkenone/Alkenoate Versus Growth Temperature Relationship in Emiliania huxleyi and Gephyrocapsa Oceanica, *Geochimica et Cosmochimica Acta*, **1998**, *62*, 51-68.
[87] Marsh, M. E., Chang, D. K., King, G. C.,Isolation and characterization of a novel acidic polysaccharide containing tartrate and glyoxylate residues from the mineralized scales of a unicellular coccolithophorid alga Pleurochrysis carterae, *Journal of Biological Chemistry*, **1992**, *267*, 20507-20512.
[88] Moheimani, N., Borowitzka, M.,The long-term culture of the coccolithophore Pleurochrysis carterae (Haptophyta) in outdoor raceway ponds, *Journal of Applied Phycology*, **2006**, *18*, 703-712.
[89] http://www.marine.csiro.au/microalgae/, Methods, 21.01.2016, Australian National Algae Culture Collection, Jameson, I.,
[90] Takano, H., Jeon, J., Burgess, J. G., Manabe, E., Izumi, Y., Okazaki, M., Matsunaga, T.,Continuous production of extracellular ultrafine calcite particles by the marine

coccolithophorid alga Pleurochrysis carterae, *Applied Microbiology and Biotechnology*, **1994**, *40*, 946-950.
[91] www.seallabs.com, How SEM works, 21.01.2016, Seal Laboratories,
[92] www.iop.org, Episode 530: X-ray diffraction, 25.01.2016, Institute of Physics,
[93] www.ibgm.med.uva.es, CASY Cell Counter + Analyser System, 10.08.2015, Roche Innovatis AG,
[94] www.ninolab.dk, Reeady-to-use dilution liquid for cell cultures, 21.01.2016, Schärfe Systems,
[95] http://roscoff-culture-collection.org, RCC1402 - *Pleurochrysis carterae*, 27.01.2016, Roscoff Culture Collection,

List of figures

List of tables

Appendix A – Health, Environment, Safety

The SOP (Standard Operation Procedure) from the Department of Chemistry and the Department of Biosciences were followed during the project.

The most hazardous parts of the experiment where 1) making the ESAW using higher concentrations of chemicals and 2) to use Lugol to kill algae.

The chemicals were most dangerous as powders when they can be inhaled or by accident get into eyes or on the skin. The risk of poisoning was greatest while measuring and then later when the right amount was put into the salt water "bucket".

To prevent exposure a lab coat, gloves and goggles were used. The containers of the chemicals where covered when not in use. In case of exposure: change gloves, rinse the conflicted area. In case of inhalation: Get fresh air, contact physician if symptoms of poisoning occur.

When I used Lugol I also used a flow hood, in addition to previously mentioned measures.

Appendix B - Cell culturing

The pH-meter was used to measure the pH-of the seawater before and after the experiment. The pH-meter measures the activity of the H-ions in the solution. This is obtained by measuring the voltage between a glass-electrode and a reference electrode. Before each measurement, the probes are dipped into a solution with a known pH and calibrated. Temperature might influence the results.

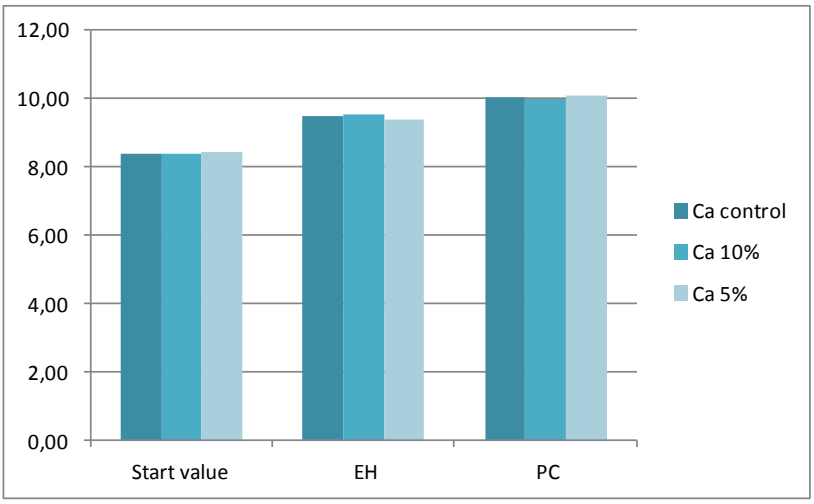

Figure 57: pH-changes in *Emiliania huxleyi* (EH) and *Pleurochrysis carterae* (PC) controls after 21 days in culture.

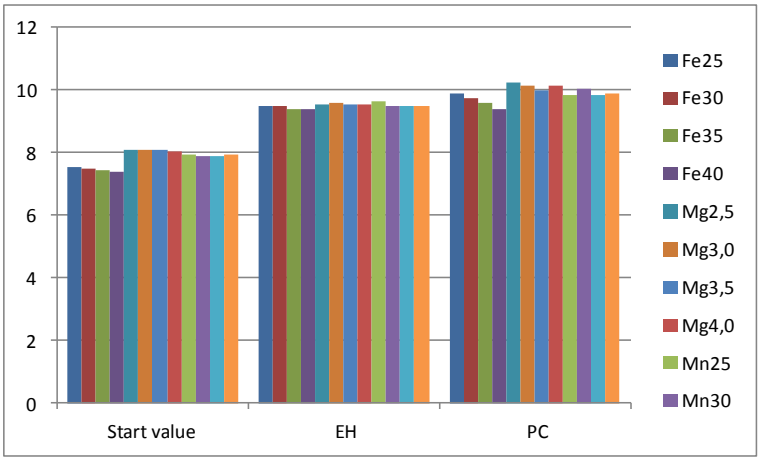

Figure 58: pH-change in *Emiliania huxleyi* (EH) and *Pleurochrysis carterae* (PC) after 21 days in culture, Ca 10%.

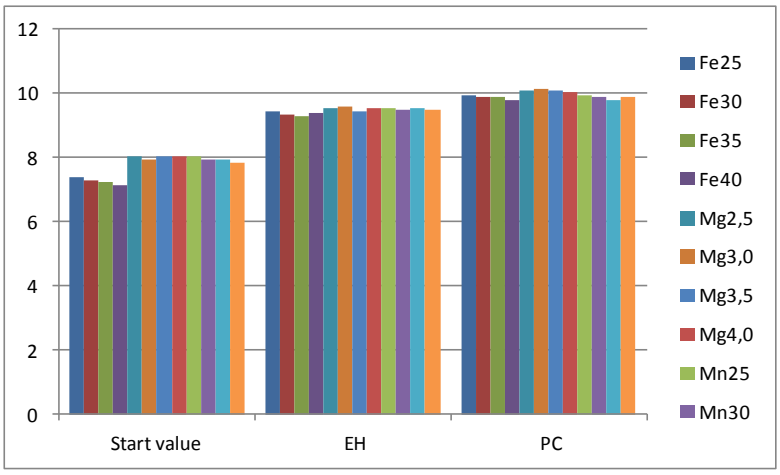

Figure 59: pH-change in *Emiliania huxleyi* (EH) and *Pleurochrysis carterae* (PC) after 21 days in culture. Ca 5%.

Table 21: Counted cells in *P. carterae*, from the repeated experiment.

P. carterae	ca normal	1 mL alger/4 mL	Day 3cells/mL	0,5 mL	Day 6 cells/mL	0,25 mL	Day 9 cells/mL	0,2 mL - 5 mL	Day 13	100uL-5mL	Day 17		Day 22		Day 22 x
PC Fe 25		1963	9815	3329	33290	3275	65500	5045	126125	1802	90100	4475	223750	4503	225150
PC Fe 30		1497	7485	3520	35200	2837	56740	4123	103075	1749	87450	4692	234600	4374	218700
PC Fe 35		1896	9480	4874	48740	2555	51100	4118	102950	2062	103100	4617	230850	4524	226200
PC Fe 40		2705	13525	5866	58660	2228	44560	3825	95625	2341	117050	4642	232100	4952	247600
											0		0		0
PC Mg 2.5		1724	8620	6155	61550	4139	82780	5222	130550	2005	100250	4589	229450	3757	187850
PC Mg 3.0		1561	7805	3467	34670	3844	76880	4915	122875	2056	102800	4106	205300	3847	192350
PC Mg 3.5		1344	6720	5276	52760	3622	72440	4655	116375	2730	136500	4034	201700	4431	221550
PC Mg 4.0		1324	6620	3367	33670	3682	73640	5079	126975	2286	114300	4128	206400	4258	212900
											0		0		0
PC Mn 25		2214	11070	7103	71030	2968	59360	4071	101775	2842	142100	3318	165900	4496	224800
PC Mn 30		2206	11030	5419	54190	3864	77280	4878	121950	3122	156100	3950	197500	4401	220050
PC Mn 35		2082	10410	8393	83930	3819	76380	4826	120650	3503	175150	4189	209450	4953	247650
PC Mn 40		1882	9410	7277	72770	3733	74660	5287	132175	3132	156600	3847	192350	4515	225750
	Ca 1/10										0		0		0
PC Fe 25		1506	7530	1221	12210	580	11600	1091	27275	4609	230450	4190	209500	4131	206550
PC Fe 30		1285	6425	1225	12250	504	10080	1145	28625	4736	236800	4248	212400	4096	204800
PC Fe 35		1090	5450	1440	14400	640	12800	1150	28750	4378	218900	4080	204000	3675	183750
PC Fe 40		1034	5170	628	6280	943	18860	1631	40775	4411	220550	4824	241200	4120	206000
											0		0		0
PC Mg 2.5		2724	13620	2302	23020	1039	20780	2353	58825	4689	234450	3817	190850	4561	228050
PC Mg 3.0		2422	12110	2080	20800	2757	55140	1688	42200	3860	193000	4119	205950	5333	266650
PC Mg 3.5		2267	11335	1907	19070	1623	32460	1879	46975	3792	189600	3413	170650	5425	271250
PC Mg 4.0		2005	10025	2018	20180	2264	45280	1744	43600	3779	188950	3782	189100	3820	191000
											0		0		0
PC Mn 25		3643	18215	2743	27430	2103	42060	3099	77475	2955	147750	3944	197200	3999	199950
PC Mn 30		2477	12385	2938	29380	2509	50180	3850	96250	3221	161050	4246	212300	4220	211000
PC Mn 35		2547	12735	3157	31570	2692	53840	4451	111275	3898	194900	4364	218200	4792	239600
PC Mn 40		2542	12710	3194	31940	3131	62620	4269	106725	3646	182300	3609	180450	4518	225900
	Ca 1/20										0		0		0
PC Fe 25		1435	7175	1190	11900	1486	29720	649	16225	2993	149650	1384	69200	2681	134050
PC Fe 30		1196	5980	750	7500	1254	25080	1490	37250	2013	100650	1303	65150	2744	137200
PC Fe 35		2012	10060	724	7240	1046	20920	815	20375	1347	67350	1456	72800	2853	142650
PC Fe 40		1483	7415	1277	12770	906	18120	1325	33125	1964	98200	2445	122250	2622	131100
											0		0		0
PC Mg 2.5		1326	6630	566	5660	947	18940	1730	43250	2213	110650	1356	67800	3457	172850
PC Mg 3.0		1364	6820	821	8210	1120	22400	2133	53325	2161	108050	1788	89400	3158	157900
PC Mg 3.5		1343	6715	1212	12120	1312	26240	1023	25575	2294	114700	1518	75900	2892	144600
PC Mg 4.0		1407	7035	3511	35110	1176	23520	1663	41575	2448	122400	1950	97500	2978	148900
											0		0		0
PC Mn 25		2040	10200	1635	16350	1638	32760	2265	56625	2502	125100	2660	133000	3026	151300
PC Mn 30		2152	10760	1804	18040	1288	25760	1886	47150	1766	88300	2309	115450	2646	132300
PC Mn 35		2111	10555	1907	19070	1336	26720	1841	46025	2372	118600	2604	130200	2498	124900
PC Mn 40		2547	12735	1294	12940	889	17780	1702	42550	2974	148700	2610	130500	2855	142750
											0		0		0
PC KONTROLL		1676	8380	3027	30270	1532	30640	2676	66900	2904	145200	3486	174300	4879	243950
PC Ca 1/10		2046	10230	2051	20510	1289	25780	2346	58650	2757	137850	2869	143450	2197	109850
PC Ca 1/20		2226	11130	1925	19250	1022	20440	917	22925	688	34400	3196	159800	1687	84350

Table 22: Counted cells in *Emiliania huxleyi*, from the repeated experiment.

Emiliania Huxley	ca normal	1 mL alger/4 mL (	Day 3cells/mL	0,5 mL	Day 6 cells/mL	0,25 mL	Day 9 cells	0,2 mL-5 mL	Day 13	100uL - 5 mL	Day 17	100uL-5mL	Day22	100uL-5mL ex	DAy22
EH fe 25		16410	82050	18969	189690	23182	463640	18708	467700	25758	1287900	16461	823050	10921	546050
EH fe 30		10685	53425	15064	150640	13684	273680	11778	294450	24333	1216650	17608	880400	19405	970250
EH fe 35		9795	48975	12020	120200	11346	226920	32289	807225	20137	1006850	20049	1002450	20164	1008200
EH fe 40		8677	43385	14480	144800	9715	194300	7935	198375	14683	734150	27019	1350950	22755	1137750
EH Mg 2.5		15208	76040	33169	331690	31690	633800	29941	748525	14790	739500	14926	746300	13148	657400
EH Mg 3.0		13803	69015	30508	305080	32331	646620	29954	748850	16068	803400	11954	597700	16507	825350
EH Mg 3.5		12463	62315	24120	241200	29484	589680	28258	706450	19261	963050	16665	833250	18130	906500
EH Mg 4.0		11110	55550	21805	218050	28000	560000	30033	750825	15591	779550	15440	772000	17832	891600
									0		0				
EH Mn 25		10811	54055	23349	233490	24055	481100	28943	723575	18651	932550	13204	660200	8715	435750
EH Mn 30		8746	43730	2202	22020	1149	22980	29278	731950	18555	927750	14853	742650	13267	663350
EH Mn 35		8156	40780	12871	128710	17752	355040	32746	818650	19625	981250	15417	770850	11332	566600
EH Mn 40		9078	45390	14271	142710	28865	577300	25494	637350	18812	940600	15614	780700	10678	533900
	Ca 1/10								0		0		0		0
EH fe 25		15451	77255	14033	140330	16369	327380	23404	585100	16035	801750	13824	691200	15574	778700
EH fe 30		12896	64480	12470	124700	12352	247040	16000	400000	17059	852950	13397	669850	14269	713450
EH fe 35		12497	62485	2369	23690	9821	196420	10404	260100	14069	703450	12269	613450	14609	730450
EH fe 40		14277	71385	10303	103030	9844	196880	9680	242000	9780	489000	12248	612400	14370	718500
									0		0		0		0
EH Mg 2.5		16946	84730	29156	291560	26240	524800	19169	479225	9675	483750	7822	391100	7863	393150
EH Mg 3.0		16298	81490	27632	276320	29004	580080	17089	427225	10890	544500	8496	424800	8573	428650
EH Mg 3.5		1251	6255	25163	251630	29723	594460	19591	489775	10850	542500	9970	498500	8771	438550
EH Mg 4.0		12765	63825	19106	191060	26154	523080	19197	479925	13580	679000	9604	480200	8837	441850
									0		0		0		0
EH Mn 25		12526	62630	22695	226950	29100	582000	25098	627450	22794	1139700	13173	658650	11857	592850
EH Mn 30		10165	50825	16834	168340	22326	446520	24786	619650	20508	1025400	15218	760900	11761	588050
EH Mn 35		11631	58155	14812	148120	21293	425860	26639	665975	23727	1186350	15674	783700	13851	692550
EH Mn 40		12191	60955	16080	160800	17874	357480	27073	676825	22621	1131050	15500	775000	15159	757950
	Ca 1/20								0		0		0		0
EH fe 25		13162	65810	14120	141200	12686	253720	20023	500575	18689	934450	14979	748950	11134	556700
EH fe 30		12228	61140	12173	121730	9583	191660	9533	238325	12163	608150	15235	761750	12735	636750
EH fe 35		10943	54715	10623	106230	9376	187520	10969	274225	12155	607750	16685	834250	14463	723150
EH fe 40		10516	52580	12954	129540	9125	182500	8571	214275	7279	363950	13102	655100	15015	750750
									0		0		0		0
EH Mg 2.5		4059	20295	27406	274060	42551	851020	18311	457775	9428	471400	8890	444500	6580	329000
EH Mg 3.0		15409	77045	25976	259760	35490	709800	14120	353000	8763	438150	16105	805250	5667	283350
EH Mg 3.5		13851	69255	24110	241100	24360	487200	16086	402150	11189	559450	7577	378850	7959	397950
EH Mg 4.0		13330	66650	14429	144290	20602	412040	18149	453725	10625	531250	12129	606450	7353	367650
									0		0		0		0
EH Mn 25		12628	63140	15308	153080	3722	74440	26828	670700	20071	1003550	14107	705350	13527	676350
EH Mn 30		12446	62230	13792	137920	3861	77220	24965	624125	16958	847900	13894	694700	12826	641300
EH Mn 35		1778	8890	10712	107120	17216	344320	26428	660700	13769	688450	13626	681300	13100	655000
EH Mn 40		12259	61295	16568	165680	12872	257440	25658	641450	18667	933350	15666	783300		0
									0		0		0		0
EH KONTROLL		11249	56245	16872	168720	19110	382200	25746	643650	15646	782300	12105	605250	8575	428750
EH Ca 1/10		11088	55440	16925	169250	14949	298980	24660	616500	11206	560300	7651	382550	4839	241950
EH Ca 1/20		8181	40905	17087	170870	15696	313920	17134	428350	5977	298850	6254	312700	4789	239450

Appendix C – Scanning Electron Microscope

After looking at the first generation of *E. huxleyi* in the SEM it was easy to see that something was amiss since no coccoliths were observed in any of the experiments.

The one culture which got coccoliths had one, Figure 60.

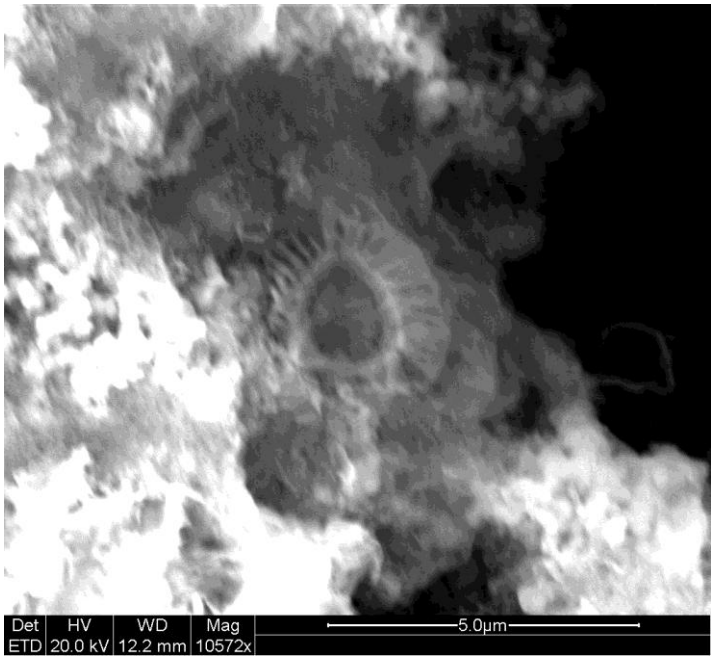

Figure 60: This is the only coccolith found in the first batch of *Emiliania huxleyi*. The coccolith was found in the ESAW Ca 100%-Fe25. The coccolith is partly hidden in something assumed to be organic material. ETD was used to take the picture.

When the ongoing samples were inspected, they still had coccoliths. This led me to believe that there was something wrong with the method. This is why the method was changed for the repeated experiment. Some coccoliths were also found for *P. carterae* and they seem slightly damaged, as shown in Figure 61.

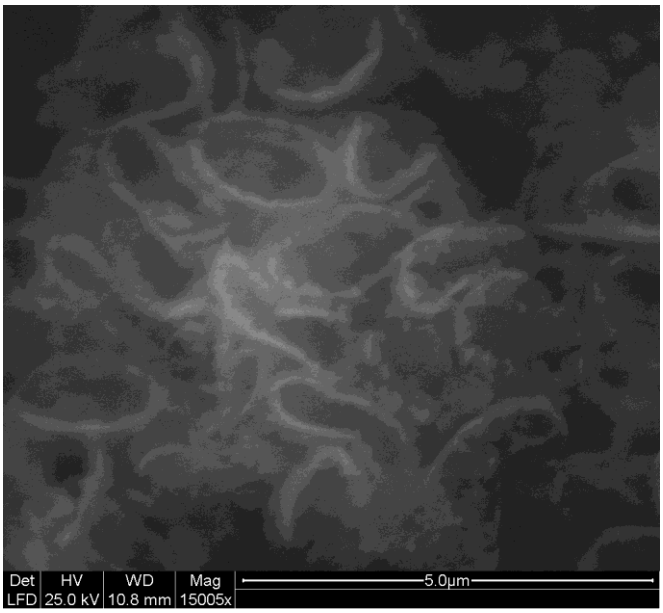

Figure 61: *Pleurochrysis carterae* coccoliths from the first experiment. The ESAW had Mn35, Ca 5%.

Appendix D – X-ray Diffraction

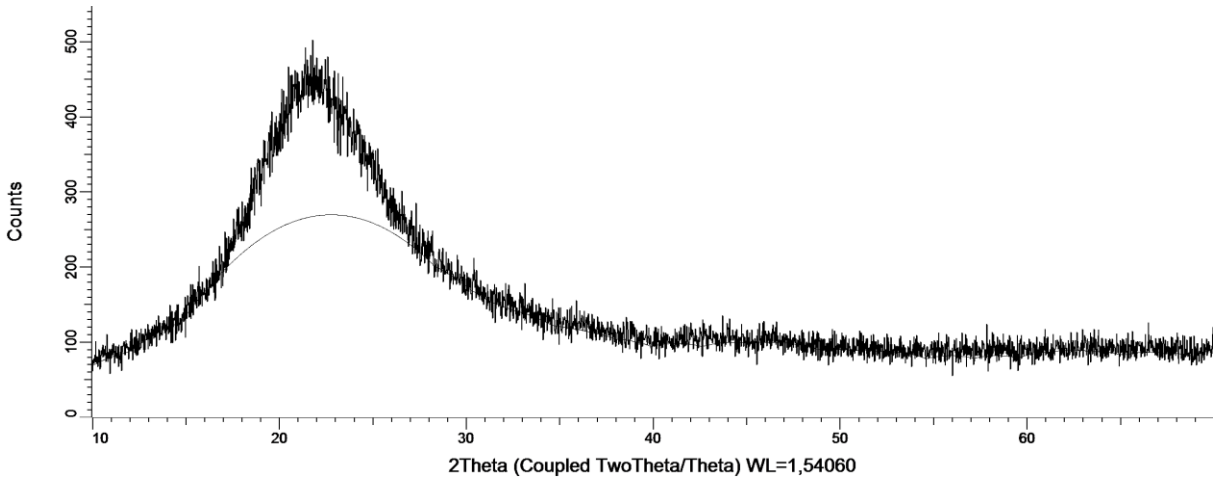

Figure 62: XRD scan of empty sample holder. There is quite a high background.

Table 23: Overview of all the reflections in all the samples from XRD

angle	Assumed material	Saltwater (Ca10)	EHCa100%	EH first-Ca	EH I Mg25	CaK	EH EH EH PC K-last	PC K	PC Mg25	CaK	PC PC PC	PC Mg25	Ca1/10	PC PC	PC	PC10	PC20	PC Fe25	EH10	EH20	PCMg25Ca	PC PCl	PC Mn30	PC	PCB3Mg25Ca20	PCE	PC EH	Mn30	CaK	EH	EH I	EH EH	CaCO3-pure	EH Mg40	EH EH	EHB2	Ca20	Mg35
10,50	unknown	x small																																			
11,65	unknown		x				x sm≤ x s x										x							x										x x x		
14,70	Fe2SO4	x small	x		x small		x s x s x s x		x small		x s x s x small											x small			x				x x x			x				
15,40	Jahnsite (CaMnMn)*		x				x								missi x		x		x	x	x small	x small															
16,30	unknown		x				x s x small				x small		x sn x s≤ x s≤ x															x x x			x					
17,40	unknown		x small								x small		x sn x s≤ x s small						x				x small			x small	x s≤ x	x x			x					
19,00	(possibly Jahnsite?)		x														x	x	x							x				x small		x small				
20,30	unknown		x		x small		x s x s x s x small								x	x	x		x	x	x	x				x		x x x			x				
20,26	C5H14BF4NO	x small																																			
21,74	Jahnsite or FeSO4	x small	x		x	x x x small	x						x sma x	x				x	x	x		x	x small				x small									
22,04	SrCl2	x small																																			
21,08	MnSO4	x small																																			
22,10	Dolomite?				x small		x s x s x s x small				x small		x small	x sma x sm≤ x				x sma x sma x		x	x	x small			x small		x sr x s x				x					
23,08	Calcite	x small	x		x D		xD xC xD x small						x sr x sr x sma x sm≤					x	x			x small			x small				x x			x					
23,50	Fe+3(OH)3		x		x	x x x	x small		x small D				x sr x s≤ x small D					x sr x sr x		x		x small	x sr x										x x	x		
23,75	unknown (H3(BO3) or x		x			x																	x small					x x x			x					
24,70	organic or CoSO4	x	x		xD	xC xD x			x small				x s x s x sr x		x x x x			x	x x x				x		x m		x sr x sr x s x			x					
25,09	Fe2(SO4)3 or Mg(CO3	x	x		x	x x x			x small				x x s x sr x		x x x x			x	x x x				x		x m			x small							
25,50	unknown	x															x																				
25,80	unknown																													x small		x small				
26,91	(possibly Jahnsite?)		x		x	x x x	x small						x sma x sm≤ x					x	x	x		x small			x		x x x			x small					
27,50	NaCl?	x	x		x	x x x			x small		x x x x		x x x x					x	x	x		x			x		x x x			x					
27,91	unknown or H3(BO3)																													x small							
28,42	Si	x	x		xD	xD xC xD x			x		x x x x small		x sn x sr x	x sma x sm≤ x				x sm≤ x					x		x small											
29,44	Cacite		x	x	x small D	x s x s x s x		x			x		x x x	x sma x				missi missi x					x	mi≤ x		x x				x si x		x small	x x x		
29,5-29,7	Calcite, magnesian		x						x		x x x						x sm≤ x									x										
30,50	Ca-Mn (kutnohorite) ? x		x			x											x	x small	x sm≤ x sma x small			x small						x si x sr x s x			x				
30,9-31,2	Dolomite or Jahnsite		x		x small		x s x s x s x		x		x x x				xD	xD	x sma x	x small	x	x	x small		x small				x small m		x small m			x				
31,40	Calcite	x																													x						
31,6-32	NaCl?		x		x	x x x			x		x x x x				x	x	x	x	x	x	x		x		x	x	x			x		x	x x		
32,90	unknown	x			x	x x x												x small																		
33,88	Fe2 (SO4) or NaCO3	x				x																								x small		x small				
34,00	MnSO4		x small		x	x x x small												x	x sm≤ x small																	
36,00	Calcite		x	x			(missing x								x	x	missi missi missing missing?																			
37,70	MnSO4 ?																													x small		x small				
38,50	K Br ?	x small	x		x small		x s x s x s x				x small				x sn x	x	x	x small	x sm≤ x sma x				x						x small		x small				
39,45	calcite	x small	x	x			x small x								x	x	missing?													x						
39,80	magnesian calcite														x	x																				
40,65	Kutnuhorite or vaterit	x small	x				x s x small											x																		
43,16	Calcite		x		x +shift		x small x								x	x														x						
44,80	Dolomite?							x																													
45,50	NaCl	x	x		x		x x x x		x		x x x x				x	x	x	x	x	x	x		x		x	x	x	x		x					
45,65-45,75	Jahnsite?		x																																	
47,10	Calcite		x		NO TOP?		x s x								x	x		x small			x small		x s x small						x						
47,33	Si or magnesian calcite		x					x							x	x	x				x small															
47,50	Calcite														x	sr x small															x					
48,00	Magnesian calcite or Fe+3(OH)3		x		x small		x s x s x small												x sm≤ x small			x small													
48,52	Calcite of NaHCO3	x small	x	x			x	x							x	x		x			x small		x s x small						x	x sr x s x	x				
48,85	Magnesian calcite		x				x small																													
49,25	magnesian calcite or vaterite		x		x small		x s x s x s x small												x small																	
50,3-50,4	Jahnsite		x															x			x small (not aligned)															
50,55-50,85	(Dolomite or Siderite(	x small	x												x	x	x ?				x	x x x		x		x small				x			x			
51,45	Dolomite	x small	x		x small		x s x s x s x small									x small	x		x	x	x x					x				x					
53,8-54	(seve Magnesite Mg(Co3) or NaCl		x													x small						x									x small					
55,65	unknown						x									x small	x																			
56,50	NaCl or CaCO3		x		(small pea x		x x x x		x sma x D				xD xD xD x		x	x x x			x	x sm≤ x	x		x		x		x		x	x x x		x			
57,40	CaCO3		x	x												x x																x				
58,08	CaCO3																															x				
60,67	CaCo3																															x				
61,00	CaCO3																															x				
61,37	CaCO3																															x				
63,05	CaCO3																															x				
64,64	Calcite or Dolomite		x																													x				
65,60	CaCO3																															x				
66,25	NaCl, Magnesite, Mag	x			x		x x x x		x		x x x x				x	x	x	x	x	x	x		x		x		x		x	x x x					
69,17	Calvite																															x					